5-2016

Modulation of cardiac Kv currents by Kvbeta2 and pyridine nucleotides.

Peter Joseph Kilfoil
University of Louisville

MODULATION OF CARDIAC Kv CURRENTS BY Kvβ2 AND PYRIDINE
NUCLEOTIDES

By

Peter Joseph Kilfoil
B.E., Vanderbilt University, 2001
M.S., University of Kentucky, 2007

A Dissertation
Submitted to the Faculty of the
University of Louisville School of Medicine
in Partial Fulfillment of the Requirements
for the Degree of

Doctor of Philosophy
In Biochemistry and Molecular Biology

Department of Biochemistry and Molecular Genetics
University of Louisville
Louisville, KY

May 2016

MODULATION OF CARDIAC Kv CURRENTS BY Kvβ2 AND PYRIDINE

NUCLEOTIDES

By

Peter Joseph Kilfoil
B.E., Vanderbilt University, 2001
M.S., University of Kentucky, 2007

A Dissertation Approved on

April 6, 2016

by the following Dissertation Committee

_____
Dissertation Director
Dr. Aruni Bhatnagar

_____
Dr. Ronald Gregg

_____
Dr. Daniel Conklin

_____
Dr. Barbara Clark

_____
Dr. Alan Cheng

DEDICATION

This dissertation is dedicated to my beloved wife Carrie and son Rowan.

ACKNOWLEDGMENTS

ABSTRACT

MODULATION OF CARDIAC Kv CURRENTS BY Kvβ2 AND PYRIDINE

NUCLEOTIDES

Peter Joseph Kilfoil

April 6, 2016

Myocardial voltage-gated potassium (Kv) channels regulate the resting membrane potential and the repolarization phase of the action potential. Members of the Kv1 and Kv4 family associate with ancillary subunits, such as the Kvβ proteins, that modify channel kinetics, gating and trafficking. Previous investigation into the function of cardiac β subunits demonstrated that Kvβ1 regulates I_{to} and $I_{K,slow}$ currents in the heart, but the role of Kvβ2 in the myocardium remains unknown. In heterologous expression systems, Kvβ2 increases surface expression of Kv1 channels, shifts the activation potential of Kv1 channels to more polarized voltages, and increases the inactivation of Kv1 channels. Accordingly, the electrophysiological phenotype in Kvβ2$^{-/-}$ mice was examined to uncover its role.

To investigate the effects of the loss of Kvβ2 on cardiac repolarization, we performed whole-cell electrophysiology on primary cardiac myocytes. We found Kv current density was reduced and action potential duration prolonged in

myocytes lacking Kvβ2. To isolate the molecular interactions by which Kvβ2 was affecting Kv currents, we show that Kvβ2 co-immunoprecipitates with Kv1.4 and Kv1.5 in heart lysates. To measure if surface expression of these Kv channels was reduced with the loss of Kvβ2, we performed immunofluorescent confocal microscopy of isolated cardiac myocytes.   We found that the surface expression of Kv1.5 was reduced in Kvβ2$^{-/-}$ myocytes.   We also performed a membrane fractionation technique to demonstrate that the proportion of total cellular Kv1.5 at the membrane was reduced in Kvβ2$^{-/-}$.   Together, these findings support our hypothesis that Kvβ2 plays a role in the generation of functional Kv currents in the myocardium by interacting with members of the Kv family.

The pyridine nucleotides, NAD[P](H), are ubiquitous cofactors utilized as electron donors and acceptors by over 250 cellular oxidoreductases. Work out of our laboratory has shown that the Kvβ proteins are functional enzymes of the aldo-keto reductase family, that utilize NAD[P]H to catalyze the reduction of substrates. Furthermore, follow up work has shown that the redox status of bound pyridine nucleotide (PN) modifies the gating of Kvα-Kvβ channel complexes in heterologous expression systems. To examine a physiological role for PN in cardiac repolarization, whole-cell and single channel cardiac myocyte currents were recorded under the exposure to various PN redox states. We found that the inactivation rates and open probabilities of Kv currents in isolated myocytes are sensitive to the redox status of PN, and that surface action potentials in an isolated heart model are prolonged by treatment with factors that increase intracellular NADH concentration.

TABLE OF CONTENTS

LIST OF FIGURES

LIST OF TABLES

LIST OF SCHEMES

CHAPTER I

BACKGROUND

The ability to maintain and utilize ionic gradients across a semipermeable membrane is one of the defining characteristics of life on this planet. It has been long believed that life on Earth originated in the sea as single-celled microorganisms that have acquired increasing complexity over the ages. In time, the protocell somehow acquired the ability to maintain a high K^+/low Na^+ cytoplasm while bathed in the high Na^+ of the oceans. It should be noted that an alternative theory, in which the primordial cell developed terrestrially, has recently been proposed.[1] In this new paradigm, evidence is presented supporting the argument that the birthplace of the first cell was in vapor-rich vents in inland geothermal systems. There are two main driving evidences behind this hypothesis. First, the protocell would not have yet acquired the molecular machinery (i.e. active transport via energy dependent transmembrane pumps) to maintain a high intracellular K^+ concentration in low $[K^+]$ seawater, implying that, initially, these cells' cytoplasm was of similar composition to that of the aqueous environment from which they arose. Second, cells across all three domains, archaea, bacteria, and eukarya, utilize trace elements such as zinc, manganese and phosphate in a variety of conserved cellular processes. Seawater is low in Mn^{2+} and Zn^{2+}, the latter being found at concentrations in the picomolar to femtomolar range.[2] Analysis of the

composition of geothermal pools shows these inorganics to more closely match that of the cytoplasm.[1]

While the origin of the primordial cell may be debated, it is evident that the increasing complexity of life has mirrored its ability to asymmetrically distribute inorganic ions (and later, organic molecules) across its semipermeable membranes, and more importantly, to utilize this gradient as a form of potential energy. The evolution of selectively permeable ion channels and transporters is key to higher forms of life.

In the animal kingdom, maintenance of the steady-state ratio of K^+/Na^+ across the cell membrane via the sodium-potassium-ATPase accounts for up to 4% of total energy expenditure in the myocardium[3] and up to 20% in neurons.[4] Furthermore, myocardial Ca^{2+}-ATPase (SERCA) utilizes up to 30% of cellular energy reserves.[5] The appropriation of energy to maintaining various ionic gradients underscores their critical importance.

Eurkaryotic cells have the capacity to synthesize ATP by utilizing a proton gradient generated across the inner mitochondrial membrane, i.e. aerobic respiration. One of the key evolutionary differences separating prokarya from eukarya is the presence of membrane-enclosed organelles, such as the mitochondria, and subsequently the ability to increase the efficiency of ATP conversion from energetic substrates.

Aside from the universally conserved usage of the mitochondrial proton gradient to produce cellular energy (ATP), various specialized cell types utilize the electrochemical gradient generated by other asymmetrical ionic distributions to

2

perform unique functions. Most cells maintain a negative cytoplasmic resting membrane potential relative to their surroundings, which is generated by three main processes: the Gibbs-Donnan equilibrium, the activity of the Na-K-ATPase pump, and the summation of chord conductances of ions to which the membrane is permeable, i.e. Na^+, K^+, and Cl^-.

The Gibbs-Donnan equilibrium states that the majority of intracellular membrane-impermeant ions have a negative charge at physiological pH, such as proteins, organic polyphosphates, amino acids and nucleic acids. Since these species cannot reach a chemical equilibrium across the membrane, they impart a net negative charge to the cytoplasm. These anions contribute approximately -10 mV to the resting membrane potential relative to the extracellular fluid.

Excitable cells, such as neurons and myocytes, maintain a much more hyperpolarized resting membrane potential than other cell types, typically in the range of -40 to -90 mV. The majority of this potential results from gradients of various inorganic ion concentrations across the plasma membrane. Cytoplasmic concentrations of K^+ (~150 mM), Na^+ (~10 mM), and Cl^- (5 mM) differ considerably from those typically found in the extracellular solution, K^+ (5mM), Na^+ (145 mM), Cl^- (120 mM). The equilibrium potentials for each ion can be calculated using the Nerst equation:

$$E_{in}\text{-}E_{out} = \text{-} RT * 2.303 \log ([X]_{in} / [X]_{out}) / zF$$

where $[X]_{in}$ and $[X]_{out}$ are the concentrations of ion X across a membrane, R is the ideal gas constant, T is the temperature in Kelvin, F is Faraday's constant and z is the ion valence. The equilibrium potential for Cl^- (E_{Cl}) in skeletal muscle is

approximately -90 mV, near this tissue's resting membrane potential, so the net movement of Cl^- at resting membrane potential is near zero. E_K in skeletal muscle is about -100 mV, resulting in a small net movement of K^+ ions out of the cell. E_{Na} is approximately +65 mV, thus both the electrical and concentration forces on Na^+ drive it into the cell.

As described supra vide, a significant portion of a cell's energy is expended by the Na-K-ATPase to maintain Na^+ and K^+ gradients against their electrochemical equilibria. This pump moves 3 Na^+ ions out of the cell for every 2 K^+ that moves in, causing a net positive charge to exit the cell, and is thus termed "electrogenic". In itself, this net movement of positive charge out of the cell is responsible for ~-5 mV of a neuron's or skeletal and cardiac muscles' resting membrane potential. In other cell types, such as smooth muscle, it may contribute over -20 mV to the transmembrane voltage difference. While its direct effect on membrane potential is not insignificant, its true indispensible function is the maintenance of the K^+/Na^+ gradient utilized by voltage-gated channels.

By far the greatest contribution to membrane potential in excitable cells is the utilization of passive diffusion of Na^+ and K^+ down their electrochemical gradients though variably conductive pores. The conductance of a membrane to an ion can be described as the sum of the conductance of various ion channels to which that ion is permeant. This relationship is described by the chord conductance equation:

$$E_m = (g_K * E_k)/(g_K + g_{Na} + g_{Cl}) + (g_{Na} * E_{Na})/(g_K + g_{Na} + g_{Cl}) + (g_{Cl} * E_{Cl}/(g_K + g_{Na} + g_{Cl})$$

Where g is the conductance of the membrane to the noted ion and E is the equilibrium potential to the noted ion and E_m is the equilibrium potential of the membrane. As a membrane becomes more permeant to a particular ion, the membrane potential is driven toward the equilibrium potential of that ion. In the cardiac myocyte and neuron, the relative steady-state gK^+ is high, thus the resting membrane potential is near the equilibrium potential for K^+. During the action potential, the relative gNa^+ increases drastically and Na+ rushes into the cell, causing rapid depolarization to near E_{Na} of approximately +65 mV. Membrane potential is then restituted as gNa^+ rapidly falls and gK^+ increases, driving the cell back toward the E_K of about -90 mV. It is the finely tuned activity of multiple families of voltage-gated ion channels that both maintain and make use of this form of potential energy to accomplish a wide range of functions in various electrically active cell types.

The action potential

An action potential is a rapid depolarization in membrane potential followed by a return to resting membrane potential. The shape, duration and size of action potentials differ considerably between excitable tissues, reflective of the diverse populations of voltage-gated ion channels functionally expressed on a tissue and cell type-specific basis. While virtually all mammalian cell types express some combination of voltage-gated ion channels, only cells in the nervous system, muscle (skeletal and cardiac) and some neuroendocrine cells exhibit classical action potential firing patterns. These tissues exhibit what can be considered the

evolutionarily conserved purpose of the action potential: finely tuned management of intracellular calcium levels through the activation of voltage-dependent calcium channels. Calcium is unique when compared to other ions in that its transmembrane concentration gradient is very large; basal cytosolic calcium concentration in most cells is on the order of 10^{-8} to 10^{-7} M, compared to 10^{-3} M in extracellular fluids. Comparatively, intracellular and extracellular concentrations of both Na^+ and K^+ differ by 1 to 2 orders of magnitude.

Cells expend a great deal of energy to maintain nanomolar $[Ca^{2+}]_i$, by actively transporting it out of the cell or into dedicated internal stores such as the sarcoplasmic reticulum. This finely tuned management is necessary because calcium acts as a second messenger, coupling electrical activities with many cellular events. Disruption of calcium homeostasis has detrimental effects on cell physiology, and prolonged elevation of intracellular calcium levels is common to both pathological (necrotic) and programmed (apoptotic) cell death, as well as contractile dysfunction in muscle.

In neurons, calcium entry through voltage-gated Ca^{2+} channels initiates synaptic transmission. In this process, calcium-sensitive synaptotagmins in the presynaptic terminal are activated by the transient rise in calcium concentration. These secretory proteins transduce the chemical Ca^{2+} signal to the exocytotic machinery, causing neurotransmitter release. The synaptotagmins are common to most other Ca^{2+}-regulated exocytotic processes, including hormone release from endocrine and neuroendocrine cells.

In muscle cells, calcium acts as a second messenger transducing cellular depolarization with contraction, a process known as excitation-contraction coupling. Activation of sarcolemmal voltage-gated Ca^{2+} channels by depolarization results in the entry of calcium ions that further promote Ca^{2+} release through the ryanodine receptor from the sarcosplasmic reticulum. The excitation-contraction signaling terminates on the myofilament apparatus; calcium binds to one of 4 high affinity sites on troponin C, causing a conformational change that displaces tropomyosin from its actin binding sites. This allows crossbridging between the actin and myosin filaments, resulting in the power stroke that is the functional hallmark of muscle tissue.

Restitution of nanomolar cytosolic calcium levels is accomplished through active transport out of the cell through the plasma membrane Ca^{2+}-ATPase (PMCA) and the Na^+-Ca^{2+} exchanger (NCX) and into internal stores through the sarcoplasmic reticulum ATPase (SERCA). In the mammalian myocardium, Ca^{2+} extrusion is dominated by SERCA (70-90%) and NCX (10-30%).[6]

In order to turn off the stimuli of the excitation-contraction and exocytotic pathways, i.e. calcium entry through voltage-gated Ca^{2+} channels, the cell must repolarize to membrane potentials at which the open probability of these channels is negligible. The preponderance of this repolarization is accomplished by the activation of the voltage-gated K^+ channels.

Voltage-gated K^+ channels

The voltage-gated K+ channel (Kv) family represents one of the most diverse families of ion channels. The products of these gene families have 6 transmembrane spanning domains (S1-S6) and assemble tetramerically through association of an N-terminal tetramerization (T1) domain to form a central ion-conducting pore. Over 40 mammalian Kv channel α-subunits encoded by 11 gene families (Kv1-Kv11) have been identified to date. These proteins form channels that vary widely in their gating properties, kinetics, and pharmacology. Even within gene families, different genes may encode for alpha subunits with vastly different properties (i.e. Kv1.4 and Kv1.5 generate rapidly-inactivating A-type currents and non-inactivating delayed rectifier currents, respectively). Their functional diversity is further underscored by the fact that different alpha subunits of the same family may heterotetramerize in vivo, such as Kv1.2/Kv1.5 in vascular smooth muscle[7] and Kv1.3/Kv1.5 in T-lymphocytes.[8] This produces functional channels with gating and pharmacological properties intermediate to that of homotetramers formed from their individual components. Furthermore, the gating and pharmacology of Kv channels is altered by ancillary beta subunits, which include Kcne, KChIP, and Kvβ family proteins. The result is an impressive functional diversity that matches repolarization dynamics to a cell's requirements. The critical role of ancillary Kv channel subunits is demonstrated by the fact that mutations in these proteins have been linked to a various pathologies in both humans and animals, including cardiac arrhythmias, hypertension, epilepsy and learning deficits.[9][10]

Not unexpectedly, mutations in Kv alpha subunits are also associated with a wide range of diseases. Mutations in Kv1 family members cause ataxia,[11]

epilepsy,[12] atrial arrhythmias,[13-15] and olfactory deficits.[16] Mutations in the Kv2 family have been linked to reduced left ventricular mass[17] and infantile epilepsy.[18] Kv3 mutations are associated with spinocerebellar ataxia and cognitive defects[19] and antibiotic-induced cardiac arrhythmia.[20] A truncation in Kv4.2 has been linked to temporal lobe epilepsy.[21] Genome wide association studies (GWAS) will undoubtedly uncover more genetic variants responsible for channelopathies afflicting various tissues and organs.

Kv channel structure and function

The first mammalian Kv structure resolved with x-ray crystolography brought great insight into the structure-function relationship of this channel family.[22] In this work, Kv1.2 from *Rattus norvegicus* was determined to a resolution of 2.9 Å, elucidating the structures and mechanisms responsible for voltage sensing and electromechanical coupling involved in the opening of the ion-conducting central pore. This study built upon structural descriptions of the prokaryotic K^+ channels KcsA and KvAP, which elucidated the amino acid bases for the K^+ selectivity filter (transmembrane segments S5 and S6), voltage sensing (transmembrane segments S1-S4) and central pore formation.[23, 24] These works confirmed the tetrameric association of α-subunits, arranged in four-fold symmetry around the central axis forming the conduction pore (Figure 1.1).

The selectivity filter is lined with carbonyl groups along a 12 Å segment of the S6 along the central pore. These electronegative carbonyls coordinate with the cation and allow for the dehydration of K^+ ions as they enter the central pore.

In the aqueous environment of the central pore, the K^+ ion is resolvated and expelled into the extracellular space by electrostatic forces. A consensus sequence (Thr-Val-Gly-Try/Phe-Gly) in the selectivity filter is highly conserved throughout evolution and is present in almost all K^+ channels. The atomic radius of Na^+ (0.96 Å) is smaller than that of K^+ (1.33 Å), and thus cannot fully coordinate with the carbonyls of the selectivity filter, resulting in a 10^4-fold preference for the passage of K^+ over Na^+.

The defining characteristic of Kv channels is their ability to sense and respond to changes in the transmembrane potential by altering their conductance. This process is dependent on four key arginine residues located on the S4 TM segment, loosely attached to the perimeter of the pore. Upon changes in membrane transmembrane potential, the positively charged sidechains of these 4 arginine residues from each of the 4 tetramerically arranged α-subunits transfer a total of 12-14 positive elemental charges across the membrane electric field from inside to outside. The movement of these residues is transduced through the S4-S5 linker helix to constrict or dilate the S6 helix that forms the inner part of the pore, thus allowing the voltage sensor to perform mechanical work on the pore.[25] This process comprises the activation gating of the voltage-gated ion channel, allowing for the conductance of K^+ ions down their electrochemical gradient as the S6 region causes pore dilation (open state). Membrane repolarization removes the electrical field effect on the voltage sensing domains, causing them to return to their initial position. This movement is transduced via the same S4-S5 linker

helix to the S6 helix lining the pore returning it to its original constricted (closed) state in a process known as deactivation.

In addition to activation and deactivation gating, voltage-gated ion channels can occupy a third gating state: the inactivated state. Inactivation of a channel occurs when it enters into a stable, non-conducting conformational state from an activated state following membrane depolarization. When in the inactivated state, a channel cannot conduct ions even if the transmembrane potential is favorable. Inactivation of an ion channel is accomplished through two mechanisms: C-type inactivation and N-type inactivation (Figure 1.2). The C-type inactivation property was initially discovered when it was found that some voltage-gated channels displayed inactivation kinetics that were dependent upon splice variations in the C-terminus.[9] This mode of inactivation was also found to be independent of N-terminal deletion. C-type inactivation, which typically occurs on a slow time scale (10^{-1}-10^{0} s), involves extracellular conformational changes in the channel that result in the occlusion of the outer mouth of the ion-conducting central pore.[26] Like activation, the return to the active channel state is voltage dependent. This indicates that C-type inactivation is coupled to movement of the voltage sensing S4 domain during its initial response to membrane depolarization. Recovery from inactivation occurs as the membrane is repolarized and the S4 domain returns to its original location, transducing a mechanical signal to open the pore mouth. C-type inactivation has been observed in all members of the Kv1 family. It also occurs in the related Kv4 and hERG (human ether-a-go-go related gene) family channels,

but with much faster recovery from inactivation kinetics, indicating a different molecular mechanism.[27]

N-type inactivation, also known as ball and chain inactivation and fast inactivation, occurs with much more rapid kinetics (10^{-3} to 10^{-2} s) (Figure 1.3). Channels that display N-type inactivation contain an N-terminal domain of approximately 20 amino acids that are critical to this mechanism. This N-terminus "ball" is followed by 60 amino acids in the "chain" domain. Mutagenesis experiments on the N-terminus of the Kv1 drosophila homolog *ShakerB* demonstrated that the charge of the ball domain is critical to inactivation; increasing the positive charge in this region increases the rate of inactivation and conversely, decreasing the positive charge slows the rate of inactivation.[28] Upon channel activation and pore opening, a negatively charged surface on the pore mouth is exposed. This region electrostatically interacts with the positively charged residues in the N-terminus (the inactivation particle), rapidly occluding the conduction pore and placing the channel in an inactivated state. Recovery from N-type inactivation to the closed but non-inactivated state requires the removal of the N-terminus inactivation particle from the pore. The time course of recovery from inactivation is voltage dependent and sensitive to extracellular [K^+], which indicates a mechanism in which a K^+ ion displaces or destabilizes the interaction between the pore and the inactivation particle.[29]

A Kv channel's activation, inactivation, and recovery from activation kinetics are important in determining its contribution to cellular repolarization. A rapidly activating and rapidly inactivating current such as the A-type currents generated

by Kv1.4 and Kv4.2 have a transient contribution to a cell's repolarization, providing brief bursts of current early in the action potential that is not sustained. In the heart and neuron, these A-type currents are prominent and responsible for the early phase of repolarization. Slowly activating but rapidly inactivating currents, such as those generated by hERG in the heart, provide repolarization capacity only later in the action potential. Rapidly activating slowly inactivating currents, such as the cardiac I_{kur} (ultrarapid delayed rectifier potassium current), provide sustained repolarization capacity throughout the duration of the action potential. Recovery from inactivation kinetics also dictates a channel's contribution to repolarization on a use-dependent basis. High-frequency action potential firing, as seen in the central nervous system, require rapid Kv channel recovery from inactivation to ensure their availability to participate in a series of repolarizing events.[30] Conversely, prolonged Kv recovery from inactivation contributes to frequency dependent increases in excitability and changes in action potential shape. This phenomena is well documented in the heart; the rate dependence of action potential duration and refractoriness in the ventricular endocardium differs from that of the epicardium.[31] At the molecular level, the transient outward current, I_{to}, which dominates the early phase of cardiomyocyte repolarization, is generated by two different ion channels, Kv1.4 and Kv4.2. These channels have significantly different rates of recovery from inactivation; Kv1.4 recovery occurs on the order of seconds[32] while Kv4.2 recovers in milliseconds.[33] Thus, the currents encoded by these channels are known as $I_{to,slow}$ and $I_{to,fast}$, respectively. The assymetrical distribution of these channels across the transmural gradient of the ventricular wall

is responsible for regional differences in repolarization and believed to be a mechanism by which to prevent re-entrant arrhythmias.[34, 35]

Kv channel ancillary subunits

When expressed in heterologous expression systems *in vitro*, Kvα- subunits form functional channels on their own. *In vivo*, Kv channels are found to be coassembled with ancillary subunits in heteromultimeric protein complexes that modulate their gating kinetics (activation, inactivation, recovery from inactivation), pharmacology, and trafficking. Mutations in these subunits are associated with multiple pathologies in both human and animals, including hypertension, epilepsy, arrythmogenesis, hypothyroidism and periodic paralysis,[10] which underscores their physiological importance.

Four families of ancillary subunits are associated in vivo with members of the Kv superfamily: KChIPs (Kv channel interacting proteins), KCNE (i.e. mink, minimal potassium channel subunit), DPPLs (dipeptidyl aminopeptidase-like proteins), and the Kvβs. These subunits may associate with only one Kv subfamily, as demonstrated in KChIP preference for Kv4 channels, or with multiple Kv subfamilies, as with Kvβ proteins' interaction with Kv1 and Kv4 members. Furthermore, their structures and mechanisms of physical interaction with the halochannel are distinct. This is clearly demonstrated in the case of Kv4, which may associate in vivo with KChIP, DPPL, and Kvβ proteins simultaneously. Members of the same subunit family may have different or opposing effects on channel gating or trafficking. Much of the information on subunit modulation of

14

channel function has been garnered through in vitro experiments and is described at the single cell level.   Animal models harboring subunit point and deletion mutations have also given insight into the function of these proteins.

KChIPs

The K^+ channel interacting proteins (KChIPs) associate with the cytosolic domain of Kv4 channels. Kv4 channels are highly expressed in the ventricular myocardium, where they generate the cardiac transient outward current $I_{to,fast}$ [36] and in dendrites of central neurons, where they generate the A-type current.[37] The association of various KChIPs with Kv4 produce channel complexes exhibiting a wide range of activation, inactivation and recovery from inactivation kinetics.[38] Alternative splicing of the products of the four known KChIP genes (KChIP1-4) makes it the most diverse family of Kv channel subunits.

The binding of KChIPs to the Kv4 N-terminus alters both the voltage-dependence and time course of the Kv4 current in a manner that is dependent on both KChIP subunit and Kv4 isoform composition. Different KChIPs also have profound and differential effects on current density, presumably through altering surface expression. For example, KChIP1 increases the rate of Kv4.1 inactivation but causes a 4-fold decrease in the rate of Kv4.2 inactivation.[39] KChIP1 depolarizes the voltage dependence of activation ($V_{1,2-act}$) of Kv4.1 by approximately 10 mV but hyperpolarizes the Kv4.2 $V_{1,2-act}$ by up to -40 mV. Coexpression of KChIP1 with Kv4.2 causes a 15-fold decrease in expression whereas coexpression of KChIP2 with Kv4.2 causes a 55-fold increase in surface

expression.[40] Clearly, the association of KChIPs with different Kv4 members produce channel complexes exhibiting a profound range of electrophysiological signatures.

DPPLs

The dipeptidyl aminopeptidase-like proteins (DPPLs) modify the effects of KChIPs on Kv channels. Heterologous expression of Kv4 with various KChIPs did not fully reconstitute the kinetics of A-type currents recorded from primary neurons, despite strong evidence that they originated from Kv4.2. Indeed, coimmunoprecipitation of Kv4 in rat brain membranes revealed an association with DPPX, a protein of then unknown function.[41] Co-expression of this protein with Kv4.2 in Xenopus oocytes caused a large increase in current density by facilitating trafficking and surface expression. It also accelerated the rate of inactivation and recovery from inactivation. When the Kv4.2/KChIP2/DPPX complex was expressed, current properties better matched the A-type kinetics found in neurons and the I_{to} kinetics in the heart.[42]

KCNEs

The KCNE gene family encodes single-pass integral membrane proteins that associated with members of the Kv7 family (KCNQ) early in their maturation and assist in their trafficking and alter their gating. KCNE1 interacts with Kv7.1 to slow its time course of activation, right-shift its current-voltage relationship, reduce inactivation and increase single channel conductance[43] and increase its surface

expression.[44] Together, Kv7.1 and KCNE1 form the slow delayed rectifier potassium current I_{ks}, a prominent delayed rectifying current in the heart.[45] Of the 4 families of ancillary Kv subunits, KCNE probably has the most critical function in the heart; mutations in KCNE1 are associated with the life threatening long QT syndrome.[46] Mutations in KCNE2-5 are also associated with other ventricular and atrial arrhythmias.[10] Interestingly, KCNE proteins display promiscuous binding to many members of the Kv superfamily, including Kv1, Kv2, Kv3, Kv4, and Kv11 (hERG).[44] The interaction with hERG, which generates the delayed rectifier potassium current I_{Kr}, is of particular importance to the proper functioning of the heart. hERG plays a critical role in cardiac repolarization due to multiple known mutations in this gene linked to arrhythmias[47] and the variety of drugs known to interact with the hERG channel to cause QT interval prolongation.[48]

The Kvβ subunits

Structure of the Kvβ proteins

The Kvβ protein was first discovered in rat brain membranes by chromatography when it co-eluted from a dendrotoxin 1 (DTX-1) affinity column.[49] The purified proteins were run on a gel and silver stained, showing 3 bands. One band at 76-80 kDa, corresponded to the column target, the DTX-1-sensitive alpha subunit, which was known to be a member of the Kv1 channel family. Two other bands at 35 kDa (determined to be a degradation product) and 38 kDa of unknown origin were also revealed. The molecular weights of these proteins closely matched that of the products of the Drosophila A-type K^+ channel, which seemed

17

to contain peptides of 70 and 35 kDa, and was cloned a year earlier.[50] Together these studies gave the first evidences of the heteromultimeric $\alpha_4\beta_4$ composition that functional Kv channels assume in vivo.

The concept of auxiliary subunits modulating the electrophysiological properties of ion channels had already been described for Na^+ [51] and Ca^{2+} channels,[52] and established a precedent for the functionality of the newly discovered Kv β-subunit. Furthermore, cloned DTX-1-sensitive channels were known to be responsible for the synaptic A-type current in rat brain neurons, yet expression of these and other related Kv1 clones in *Xenopus* oocytes produced current with strikingly different inactivation characteristics.[9, 53]

Rettig and Pongs[54] were the first to demonstrate that *Xenopus* oocyte co-expression of a β-subunit (Kvβ1) with members of the Kv1 family converted the non-inactivating Kv1 current into a rapidly inactivating current, quantitatively similar to the neuronal A-type current (Figure 1.4). In this study, Kvβ1 and Kvβ2 cDNA were cloned from the rat brain and their protein products compared; alignment showed a C-terminal sequence that was 85% identical and an N-terminal domain of 79 amino acids that were present in Kvβ1 but not Kvβ2. Hydropathy analysis and N-glycosylation patters indicated that the Kvβ proteins were cytosolic. Alignment of the Kvβ1 N-terminus with the N-termini of rapidly inactivating Kv1.4 and Kv3.4 demonstrated high homology in the "ball" region. Electrophysiological assays demonstrated that Kvβ1 imparted rapid inactivation to the non-inactivating RCK1 (Kv1.1). Furthermore, coexpression of Kvβ1 with an N-terminal truncation mutant of Kv1.4 lacking its ball and chain region restored rapid inactivation

properties to the channel complex, which indicated that the Kvβ1 proteins can provide the inactivating ball in a manner analogous to the N-type inactivation of Kv1.4. Consistent with this model, Kvβ2, which has a shorter N-terminal domain, is not found to induce N-type inactivation in delayed rectifying channels, although when assembled with Kv1.5, Kvβ2 causes a -10 mV shift in the activation threshold and accelerates channel activation. Kvβ2 also has been shown to modestly accelerate inactivation of Kv1.4 currents.[55] Kvβ3, which possesses an inactivating ball region with 90% sequence identity to that of Kvβ1 has been subsequently found to impart rapid inactivation to slowly inactivating Kv1.5 channels.[56]

Follow up studies investigated the nature of the association of the Kvβ subunits with various members of the Kv family. It was found that Kvβ1 and Kvβ2 expressed in COS-1 cells associated with all known members of the Kv1 family with similar affinities but not with the Kv2 or Kv3 families.[57] Kvβ1 and Kvβ2 also coimmunoprecipitated with Kv4.2. The non-covalent nature of the α-β interaction was confirmed by noting the detergent sensitivity of the immunoprecipitation process, yet interaction was strong enough to withstand high salt treatment.[58] Interestingly, the interaction between Kvβ and Kv1 (dissociated by 0.2% SDS) is more detergent sensitive than that between Kvβ and Kv4 (not dissociated by <0.6% SDS).[57] In Kv1 channels, the N-terminal contains a hydrophilic NAB (N-terminal A and B box) region that is necessary for α-subunit tetramierization.[59] This domain, the T1 tetramerization domain, also contains a structural motif FYE/QLGE/DEAM/L in Kv1.5[60] that is necessary for Kvβ1-mediated inactivation of the channel.[61] NAB domains within the Kv1-Kv4 families share about 40% amino

19

acid identity[59, 62]; α-subunits of these different families do not tetramerize. NAB domains share about 70% within subfamilies, which is enough to allow for heterotetramerization. The Kv4 α-subunits homology in this region with Kv1 is insufficient for Kvβ interaction; they associate with Kvβ by a distinct mechanism that is C-terminus but not N-terminus dependent.[63] Thus, Kvβ utilize distinct molecular mechanisms to interface with these two families of Kv channels.

Phosphorylation

The primary structures of Kvβ suggest the presence of 15 consensus phosphorylation sites: 1 for PKA, 10 for PKC, and 4 for casein kinase II.[64] Protein kinase A phosphorylation of N-terminus serine 24 in Kvβ1.3 has been demonstrated to decrease its inactivation effect on Kv1.5 and thus to increase outward current.[65] The effect of this phosphorylation event is unsurprising given its location—addition of negative charge at or near the inactivation ball inhibits its interaction with the open pore of the Kvα. PKC-dependent phosphorylation of Kvβ1.2 using phorbol 12-myristate 13-acetate (PMA) decreases the current conducted by Kv1.5/Kvβ1.2 complexes by depolarizing the voltage dependence of activation.[66]

Aside from the effects of on channel complex gating, phosphorylation also regulates export from the endoplasmic reticulum and cell surface trafficking.[67] The association of Kvα and Kvβ subunits occurs during translation in the ER, with maturation of the complex into its $\alpha_4\beta_4$ form completing before ER export.[68, 69] The Kvβ proteins are known to increase surface expression of Kv1 channels (described

in more detail below). The positive membrane trafficking effect on Kv1.2 by Kvβ2 is dependent on phosphorylation of α-subunit at Ser 440 and Ser 441.[70] Phosphorylation of Kvβ2 at Ser 9 and Ser 41 was also shown to be critical to the increase in Kv1.2 at the cell membrane. Cycline-dependent kinase (Cdk) phosphorylation of Kvβ2 at Ser9 and Ser 31 regulates axonal targeting of Kv1 channels in the hippocampus.[71] These neurons have a highly localized distribution of Kv1.1 and Kv1.2 channels at the juxtaparonode, which is lost both by genetic knockout of Kvβ2 or Ser/Ala mutations at the phosphorylation sites. The mechanism of this effect occurs through the microtubule plus end-tracking protein (EB1) domain of Kvβ2, phosphorylation at S9 and S31 by Cdk2 and Cdk5 disrupts its binding to EB1, promoting its dissociation from microtubules and insertion into the membrane. *In vivo*, Kvβ2 is found in complex with the atypical protein kinase C zeta (PKC-ζ), connected by the scaffolding proteins PKC-ξ interacting proteins 1 and 2 (ZIP1 and ZIP2).[72] The purpose of PKC-ξ phosphorylation is not fully elucidated, but inhibition of PKC-ξ activity may play a role in the ceramide-dependent inhibition of Kv currents in pulmonary artery smooth muscle.[73]

The Kvβ proteins are functional enzymes

Three human Kvβ genes undergo alternative splicing to form a total of 6 Kvβ proteins (amino acid length): Kvβ1.1 (401), Kvβ1.2 (408), Kvβ1.3 (419), Kvβ2.1 (367), Kvβ2.2 (353) and Kvβ3 (404). The Kvβ proteins are members of the aldo-keto reductase (AKR) superfamily that includes 15 individual families of oxidoreductases involved in carbonyl metabolism. Members of individual families

share at least 40% sequence homology with each other and <40% homology with other AKRs. All AKRs share a $(\beta/\alpha)_8$ triosephosphateisomerase-barrel structural fold in which the active site is located at the C-terminus. These proteins do not contain a Rossmann fold, but they bind pyridine nucleotides with high affinity via unique AKR nucleotide binding domains (discussed below).

The AKR nature of Kvβ proteins was first identified by the significant homology between the amino acid sequence of the Shaker β-subunit and proteins of the AKR superfamily.[74] Amino acid alignments also showed that the AKR residues involved in cofactor binding are conserved in the Shaker β-subunit.[75] In accordance with these predictions, our lab found that purified Kvβ proteins bind to pyridine nucleotides with high affinity (Kd values between 0.1 and 6 μmol/L).[76] In vitro these proteins bind NADP(H) with higher affinity than NAD(H). However, the nature of the cofactor bound to Kvβ in vivo is unclear, because NAD(H) levels in excitable tissues are 2- to 7-fold higher than that of NADP(H); therefore, it is possible that the lower affinity of Kvβ for NAD(H) is offset by higher NAD(H) levels in the cell. Hence, the extent and the nature of the nucleotide bound to Kvβ in vivo may depend on the prevailing concentration of all 4 nucleotides in a cell. We believe that this might allow the Kvβ to respond to a wide range of metabolic conditions by being sensitive to changes in both NADP(H) and NAD(H) levels.

To examine the functional effects of pyridine nucleotide binding, our group previously studied Kvβ1.3-mediated inactivation of Kv1.5 expressed in COS-7 cells (Figure 1.5).[77] Our lab found that oxidized nucleotides (NAD[P]$^+$) prevent inactivation, whereas reduced nucleotides have no effect. These findings have

been corroborated and expanded by subsequent investigations, which have shown that NAD(P)$^+$ removes the inactivation of Kv1.1 by Kvβ1[78] and Kv1.5 inactivation by Kvβ3.[79] NAD(P)$^+$ also has been shown to prevent the Kvβ2-mediated hyperpolarizing shift in Kv1.5 activation[79] and the acceleration of Kv1.4 current inactivation.[80] The results of whole-cell patch-clamp have been substantiated by excised inside-out single-channel experiments in which it was found that the mean open time and the open probability of Kv1.5+Kvβ1.3[77] and Kv1.1+Kvβ1[78] currents are increased by adding NAD$^+$ to the perfusate. The specificity of these interactions has been established by site-directed mutagenesis studies, which indicate that active site mutations that prevent nucleotide binding abolish the effects of NAD(P)$^+$ on current inactivation.[81] Additional mutagenesis and domain-deletion experiments have shown that oxidized nucleotides promote the binding of Kvβ N-terminus to the core of the protein and thereby remove inactivation by preventing the N-terminus from blocking the channel.[82] This interaction also may be regulated by the cytosolic C-terminus of the membrane-spanning channel protein. For instance, it has been reported that deletion of Kv1.5 C-terminus prevents NAD(P)$^+$-mediated removal of inactivation by Kvβ3.[79] Moreover, even though NAD(P)H does not affect Kv1.5 inactivation by Kvβ1.3,[77] it accelerates Kv1.5 inactivation by Kvβ3[79]. Collectively, these observations indicate that pyridine nucleotides bind directly to the Kvβ active site and that NAD(P)$^+$ binding induces a specific conformational change that prevents Kvβ-induced inactivation, whereas NADP(H) binding preserves or promotes inactivation.

Kv1 currents in the myocardium and the cardiac action potential

The coordinated contraction and relaxation of cardiac muscle is necessary for the efficient pumping of blood. Synchronized contraction requires the rapid electrical activation of cardiac myocytes throughout the entire heart. This is accomplished through very low resistance connections, the gap junction proteins, which connect adjacent myocytes at the intercalated disk. These proteins form physical connections between cells that freely allow the passage of ions and other small molecules. The electrical syncytium formed by these cytoplasmic connections allows the depolarizing wave to be rapidly transmitted across the heart.

Action potential morphology differs considerably between species, but the mechanisms of depolarization and propagation are highly conserved; in all mammalian hearts, cardiac action potential upstroke (depolarization) is accomplished by the activation and subsequent inactivation of voltage-gated Na^+ channels. The substantial interspecies variation is attributed primarily to heterogeneous expression of Kv and L-type Ca^{2+} channels, which is reflected in the time course of myocardial repolarization (Figure 1.6).

Repolarizing K^+ currents can be broadly segregated into two categories, the transient outward currents, I_{to}, and the outwardly rectifying currents, I_K.[36] Within each category, multiple subclasses exist, which display distinct kinetic and pharmacological properties. In the mouse heart, two transient outward currents

can be distinguished, $I_{to,fast}$ and $I_{to,slow}$, which vary in their recovery from inactivation and pharmacological properties. The expression of these two currents also differs spatially; while $I_{to,fast}$ can be recorded from all areas of the ventricular myocardium, including the interventricular septum, $I_{to,slow}$ expression is restricted to the septum.[83] Outwardly rectifying currents in the mouse myocardium are described by three currents with various kinetics, $I_{K,slow1}$, $I_{K,slow2}$, and $I_{sustained}$ (or I_{ss}).[83, 84] No regionally distinct expression profile has been determined for these outward rectifiers. Inwardly rectifying K^+ currents of the K_{IR} class also play a role in human but not mouse cardiac repolarization and set the resting membrane potential of the cardiac myocyte in both species.[36]

The molecular identities of mouse cardiac Kv currents

The transient outward current I_{to}

Kv1.4 was the first gene cloned from the mammalian heart that encoded a rapidly inactivating K^+ current.[85] The cDNA for this gene, called RHK1 at the time, was isolated from a rat heart library and revealed a deduced amino acid sequence displaying characteristics of the *Shaker* voltage-gated K^+ channels recently cloned from Drosophila: six segments corresponding to transmembrane domains, a domain homologous to the S4 voltage-sensor domain and a leucine zipper domain found between S4 and S5. Southern blot analysis demonstrated expression of this gene was restricted to the brain and heart, with an absence in smooth and skeletal muscle. Expression of the cloned gene in *Xenopus* oocytes generated an A-type rapidly inactivating current with activation and inactivation time courses and

voltage dependences that were grossly similar to the I_{to} current recorded from rat cardiac myocytes. The time course of recovery from inactivation for the cloned RHK1 gene differed substantially from that of I_{to}. With the limited but growing understanding of the effects of ancillary Kv subunits, it was reasonably speculated that the oocyte expression system might have lacked a protein responsible for modifying the recovery rate of the channel.

Shortly thereafter, Tamkum et al. cloned another set of K^+ channel genes from rat heart and aorta cDNA libraries.[86] Five channels were cloned, four of which (RK1-RK4) were identical or similar to other Kv1 genes identified previously. The fifth, RK5, encoded a unique channel with a sequence homology to the Drosophila *Shal* family (now known to be homologous to the mammalian Kv4 family), and stood as the first report of *Shal* family channel expression in a mammalian tissue. cDNAs of this gene were expressed in *Xenopus* oocytes in subsequent work for electrophysiological characterization.[87, 88] These studies showed that rat *Shal* gave rise to rapidly activating and rapidly inactivating voltage-gated K^+ channels with voltage dependences of activation and inactivation similar to both neuronal A-type K^+ currents and cardiac I_{to}. Slight differences in pharmacology and inactivation time course between the RK5/*Shal*4 and native I_{to} currents have since been attributed to differential KChIP subunit expression in the heart and brain.[10]

Ensuing studies combining molecular and electrophysiological approaches to elucidated the contributions of *Shaker* RCK4 and *Shal* RK5 in generation of cardiac I_{to}. Early studies demonstrated that the kinetics of I_{to} varied across the ventricular wall and in different regions of the heart. This was examined eloquently

26

by Backx et al., who demonstrated regionally restricted Kv1.4 and Kv4.2 protein expression and a transmurally graded protein expression of Kv4.2 in the rodent heart.[89] The later finding was subsequently explained by differential transmural KChiP expression by the transcription factor Irx5.[90]

Many evidences by several groups support that the cardiac transient outward current is actually two regionally-restricted currents, $I_{to,fast}$ ($I_{to,f}$) and $I_{to,slow}$ ($I_{to,s}$), attributable to Kv4 and Kv1.4 respectively. In addition to their spatial distribution, the two transient outward currents in the mouse myocardium can be distinguished readily based on their pharmacology and rates of recovery from inactivation matching their molecular correlates.[91] The $I_{to,f}$ current displays a rapid recovery from steady state inactivation (on the order of 10s through hundreds of milliseconds) and is sensitive to the giant crab spider toxin *Heteropoda* toxin at nanomolar concentrations. Pharmacolicial isolation of $I_{to,f}$ using Heteropoda toxin (HpTx2) demonstrates that this current displays A-type rapid inactivation and activation at relatively polarized membrane potentials.[83] Together, these provided more evidence that Kv4.2 is the molecular correlate of the $I_{to,f}$ current in mice. This finding was further substantiated by Marban et al., who suppressed rat ventricular I_{to} using viral infection of a dominant-negative truncated Kv4.2 construct.[92] Follow up studies indicated that in larger animals, including humans and dog, $I_{to,f}$ is encoded by the closely related Kv4.3.[93] The $I_{to,f}$ current is highly conserved in the mammalian heart, having been well characterized in human, dog, cat, rat and mouse ventricular myocytes.[94] The $I_{to,slow}$ current is predominantly found in the

septum of mice and atrium of humans, which mirrors the protein expression of Kv1.4.[89, 95]

Although the physiological importance of cardiac Kv1.4 is not as defined as it is for Kv4.2, the relationship between the two appears to be of importance in disease. Many experimental and genetic models of heart failure and hypertrophy cause a decrease in ventricular I_{to} current density.[96] In humans, Kv4.3 is downregulated in heart failure.[97] In diabetic animals, Kv4.2 message and protein is reduced while Kv1.4 transcript and protein is increased, mimicking the changes in I_{to} kinetics in diabetes.[98-101] This so called "isoform switching" between Kv4.2 and Kv1.4 in the diabetic heart is being investigated as a possible contribution to increased incidence of ventricular arrhythmias in diabetic patients.

The outwardly rectifying currents $I_{K,slow1}$ and $I_{K,slow2}$

Whereas the mouse and human generate their transient outward currents through Kv4.2/Kv4.3 and Kv1.4 channels, their generation of delayed rectifying currents occurs through distinct molecular mechanisms. The human ventricular delayed rectifying currents are distinguishable as three components, I_{Kur} ($I_{K(ultrarapid)}$), I_{Kr} ($I_{K(rapid)}$), and I_{Ks} ($I_{K(slow)}$), which are categorized based on the their rate of activation.[36] The inactivation of these currents is slow enough such that they play a significant role in repolarization throughout phase 3 of the human action potential (Figure 1.2). I_{Kr} and I_{Ks} can be detected in human myocytes isolated from the ventricles while I_{Kur} is a completely atrial current in humans. The α-subunits responsible for generating these currents has been established after years of

intensive research. The molecular correlate of I_{Kr} is hERG (also known as Kv11.1), the product of the gene KCNH2. The I_{Ks} current is generated by the KVLQT1 channel (also known as Kv7.1), the product of human KCNQ1. The I_{Kur} current is generated by Kv1.5, the product of the *Shaker*-related gene KCNA5. These channels are of immense clinical importance as mutations in and inadvertent pharmacological interactions with these channels are responsible for a multitude of channelopathies, including Long QT syndrome, Short QT syndrome, Familial Atrial Fibrillation, *torsades de pointes*, and idiopathic lone atrial fibrillation.[36]

While hERG and KVLQT1 are not expressed in the mouse heart, Kv1.5 is a predominant current in the mouse ventricle.[102] Initial investigations into mouse ventricular Kv currents demonstrated a very slowly inactivating component, termed $I_{K,slow}$, played a significant role in myocyte repolarization. Pharmacological approaches at characterizing the channel responsible for this current revealed two distinct components. One component was sensitive to micromolar concentrations of 4-aminopyridine (4-AP), strongly indicative of Kv1-family contribution. The second component was 4-AP insensitive but sensitive to tetraethylammonium (TEA), suggesting Kv2 family involvement. Transgenic mice were also generated to further identify the channels involved in the $I_{K,slow}$ current. The targeted genetic replacement of Kv1.5 with a truncated Kv1.1 to created a functional Kv1.5 knockout mouse removed the 4-AP sensitive component of $I_{K,slow}$ and increased the incidence of spontaneous and triggered arrhythmias and caused QT prolongation.[102] A functional Kv2.1 knockout mouse was generated using a

dominant negative mutant, Kv2.1-N216, which eliminated the TEA-sensitive component of $I_{K,slow}$ and increased action potential duration.[103]

The properties of mouse $I_{K,slow1}$ are indistinguishable from the I_{Kur} found in atrial myocytes from larger animals, including human,[83, 104, 105] and it is now accepted that Kv1.5 encodes the human atrial I_{Kur}. Indeed, Kv1.5 has become a target in the development of drugs to treat atrial arrhythmias.[106, 107] Perhaps not unexpectedly, many of the anti-arrhythmic compounds develop against Kv1.5 have had off target affects on other ion channels,[108] underscoring the structural and pharmacological similarities of the multiple Kv-family channels that play a role in cardiac repolarization. The development of Kv1.5-specific anti-arrhythmic agents remain a major focus of the pharmaceutical industry.[107] Furthermore, the critical role of Kv1.5 in human atrial function is demonstrated in its remodeling in patients with chronic atrial fibrillation where its protein abundance is reduced by up to 60%.[13, 109]
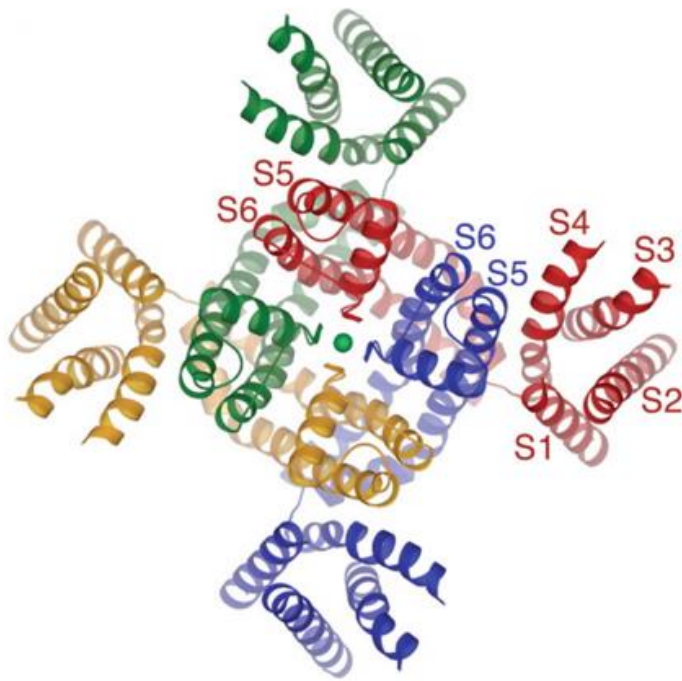
Figure 1.1: Overall structure of the Kv1.2 tetramer. viewed from the extracellular solution, shown as ribbons. Each of the four subunits is colored uniquely. The transmembrane helices S1 to S6 are labeled for the subunit colored in red. Each S4 helix (red, for example) is nearest the S5 helix of a neighboring subunit (blue, for example). Adapted from Long SB et al. Science 2005; 309:903-908
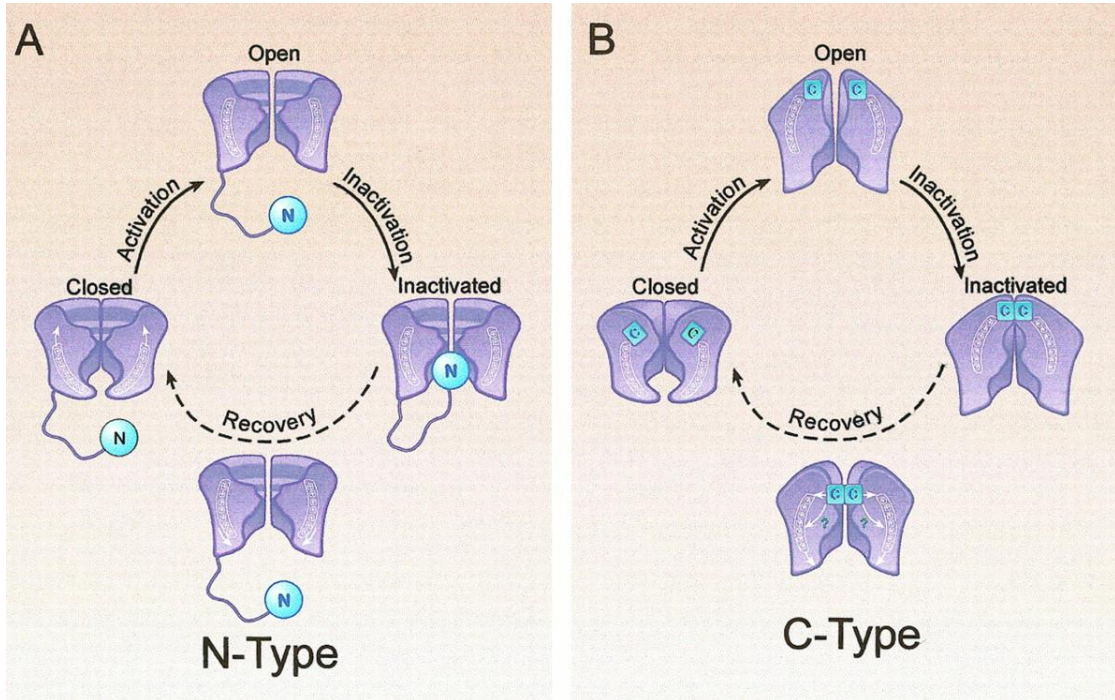
Figure 1.2: Models of N-type and C-type inactivation of K$^+$ channels. A) N-type inactivation is dependent on an N-terminal inactivation "ball" domain B) C-type inactivation involves the closure of the extracellular mouth of the channel. Adapted from Rasmusson RL et al. Circ Res. 1998;82:739-750
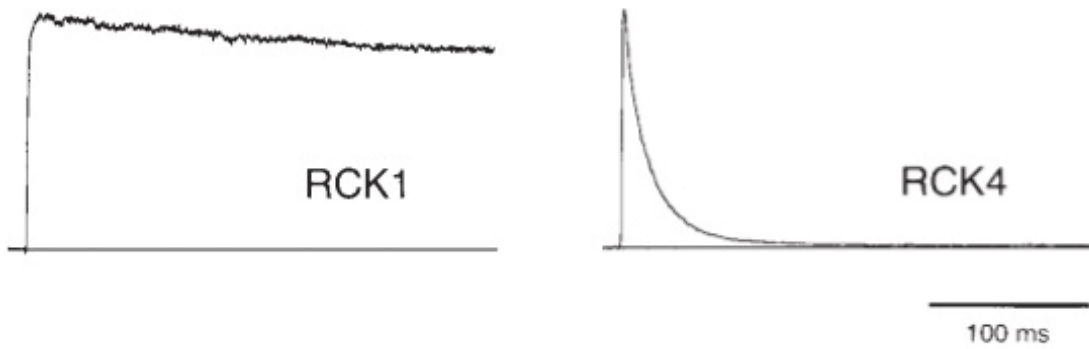
Figure 1.3: C-type and N-type inactivating currents. Outward currents elicited by a +50 mV depolarizing pulse from a holding potential of -100mV. Left: RCK1 (Kv1.1) lacks an N-terminal inactivation domain and inactivates by a slow C-type mechanism. Right: RCK4 (Kv1.4) has an N-terminal "ball" domain and rapidly inactivates upon channel opening. Adapted from Rettig et al. Nature. 1994 May 26; 369(6478):289-94
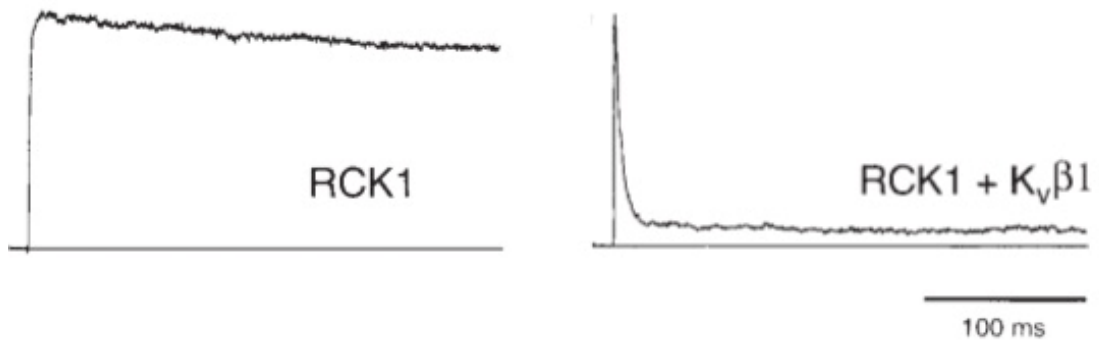
Figure 1.4: Kvβ1 imparts rapid N-type inactivation. Coexpression of Kvβ1 converts the slowly inactivating RCK1 (Kv1.1) into a rapidly inactivating channel complex. Adapted from Rettig et al. Nature. 1994 May 26; 369(6478):289-94.
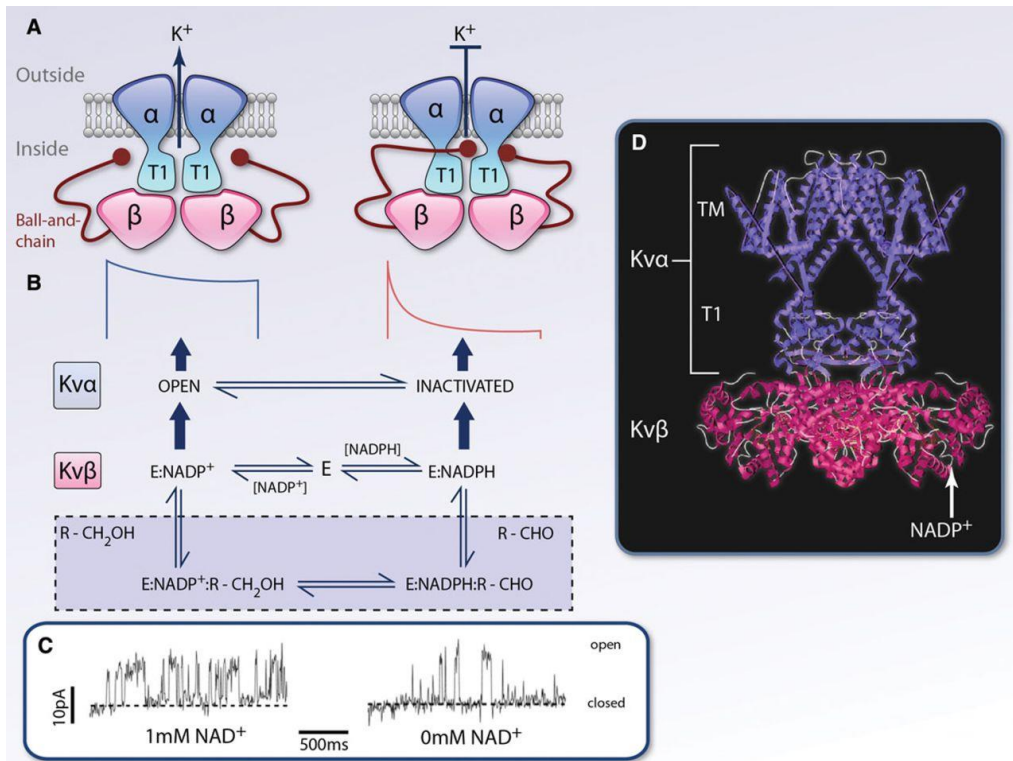
Figure 1.5: Model of physiological regulation of voltage-gated potassium (Kv) channel by pyridine nucleotides. A, Composite representation of the Kvα–Kvβ complex. The membrane-spanning domains of Kvα are shown in blue. The T1 domain, which docks with Kvβ, is shown in light blue. The N-terminus of Kvβ forms the inactivating ball and chain assembly. In the NADPH-bound state of the Kvβ subunit, the N-terminal domain of Kvβ inactivates the channel by plugging the internal opening of the ion-permeation pathway, resulting in N-type inactivation (**right**). Binding of NADP+ to Kvβ prevents inactivation. For clarity, only 2 of the 4 subunits of Kvα and β are shown. **B**, Schematic showing the regulation of channel function by NADPH. The noninactivated (open) state of the channel is stabilized by NADP+, whereas NADPH binding induces inactivation. The transition between the inactivated and noninactivated state of the channel is mediated either by pyridine nucleotide exchange or by catalytic turnover involving the substrate-dependent conversion of NADPH to NADP+. **C**, Effect of NAD+ on single channel Kv activity in inside-out patches recorded in COS-7 cells expressing Kvα1.5 and Kvβ1.3 before and after exposure to 1 mmol/L NAD+. Currents recorded in response to a +50-mV depolarizing pulse. Reprinted with permission from *Am J Physiol Cell Physiol*, Tipparaju et al.[42]**D**, Stereoview of a ribbon representation showing the side view of the channel complex containing the transmembrane (TM) domain, the T1 scaffolding, and the auxiliary β-subunits. The NADP+ cofactor bound to each β-subunit is shown as indicated.[36] (Illustration: Ben Smith.) Adapted from Kilfoil PJ et al Circ Res. 2013;112:721-741
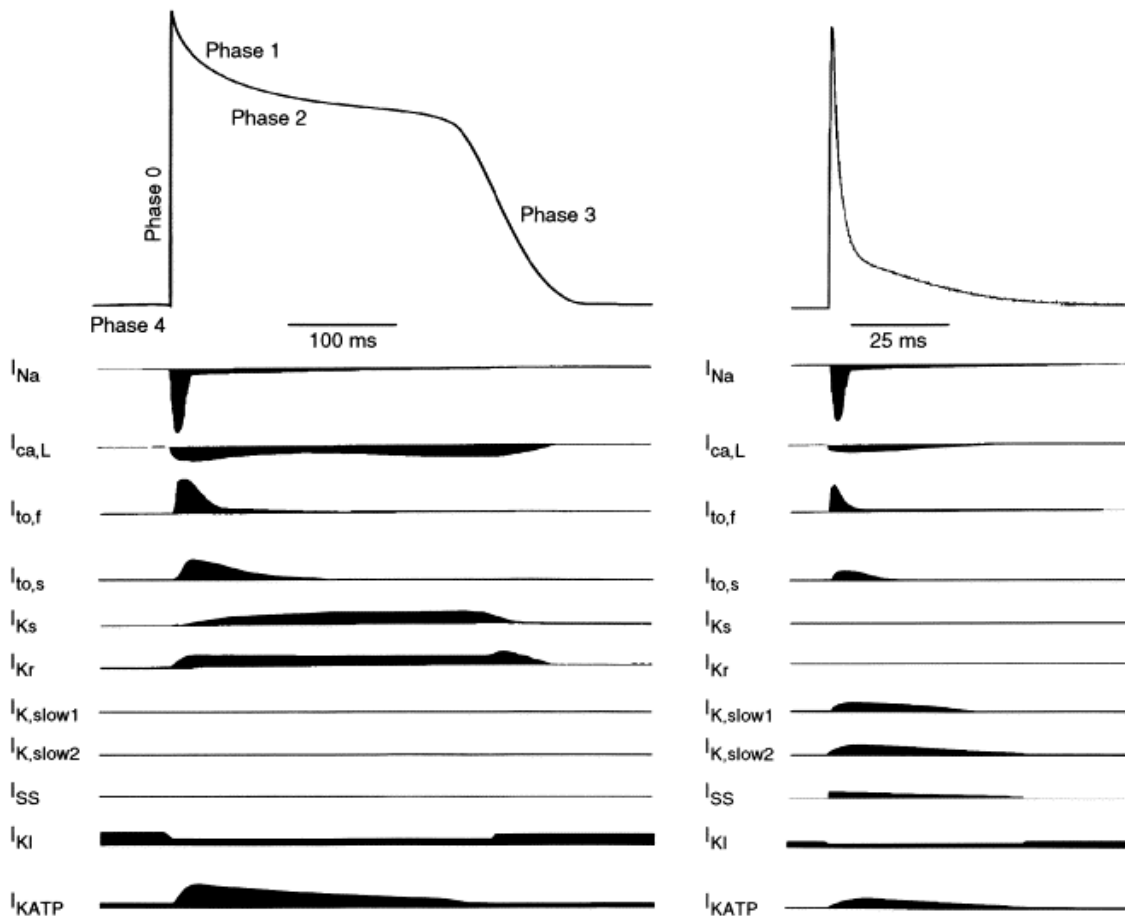
Figure 1.6: Action potentials and underlying ionic currents. Adult human (left) and mouse (right) ventricular myocytes have diverse outward K+ currents while inward Na+ and Ca2+ currents are similar. The diversity of K+ currents results in distinct action potential repolarization shapes in human and mouse ventricular cells. Adapted from Nerbonne JM Trends Cardiovasc Med. 2004 Apr;14(3):83-93.

CHAPTER II

DETAILED MATERIALS AND METHODS

Immunoprecipitations and Western Blot Analysis

Western blot analyses were performed on fractionated protein lysates prepared from whole heart, isolated ventricular cardiomyocytes, and whole brain tissue from adult (12 to 22 week) Kvβ2 WT and Kvβ2$^{-/-}$ mice to examine Kv1.4, Kv1.5, Kv4.2, Kvβ1 and Kvβ2 expression patterns. All antibodies used in this study are commercially available, have been previously tested for specificity and cross-reactivity and have been shown to be subunit specific. For Western blot analyses, proteins were fractionated on SDS-PAGE gels (any-kD or 7.5%, BioRad), transferred to PVDF membranes followed by overnight incubation at 4°C with a (polyclonal or monoclonal) anti-Kvβ2 (K17/70, Neuromab, Davis, CA), anti-Kv1.4 (K13/31, Neuromab), or anti-Kv1.5 (APC-004, Alomone, Jeruselum, Israel) antibody. Following thorough washing, the membranes were incubated with horseradish peroxidase-conjugated anti-mouse or anti-rabbit secondary antibodies. The membranes were again thoroughly washed to remove excess substrate and then bound antibodies were detected using luminescent horseradish peroxidase substrate (Pierce ECL/ECL Plus, Thermoscientific) and scanned on Typhoon.

For immunoprecipitations, 50 μL protein G-coated magnetic beads (Dynabeads Protein G, 10003D, Life Technologies) were incubated with rocking overnight at 4°C with 10 μg of anti-Kvβ2 (K17/70), Kv1.4 (K13/31), Kv1.5 (APC-004) or Kv4.2 (K57/1) antibody in 200 μL PBS plus 0.01% TWEEN-20 (to prevent bead aggregation). To decrease the signal from antibody heavy and light chains on Western blot, the antibodies were then cross-linked to the beads. This was achieved by first washing the beads twice each with 1 mL of sodium borate (50 mM, pH 9.0) followed by 30 min incubation by rocking at room temperature with 1 mL of 25 mM dimethyl pimelimidate made fresh in 50 mM sodium borate. After removing the supernatant, the beads were resuspended in 1 mL of ethanolamine and incubated by rocking for 2 hours at room temperature. The beads were then washed gently with 1 mL PBS plus 0.01% TWEEN-20 three times. Once cross-linking was complete, lysates were incubated with the beads by rocking overnight at 4°C. The supernatant was removed and saved. The beads were resuspended in 1:5 SDS loading buffer with 150 mM DTT in PBS plus 0.01% TWEEN-20 and then heated at 70°C for 10 min. The supernatant was then removed and boiled at 100°C for 10 min. The eluted sample was then fractionated and immunoblotted as described above.

Differential centrifugation was used to prepare membrane-enriched fractions from heart lysates. In this procedure, hearts were homogenized in chilled glass in cold lysis buffer containing (in mM): mannitol 225, sucrose 75, EGTA 0.1, Tris-HCl 30, pH 7.4. Protease and phosphatase inhibitor cocktails (Sigma) were added at a 1:100 concentration. The lysate was centrifuged at 3000 RPM for 10 min to

remove cellular debris and unbroken cells. The supernatant was removed and set aside on ice while the pellet was resuspended in lysis buffer and again homogenized. The 3000RPM spin was repeated on this lysate and the supernatants were pooled. The collected supernatants were then centrifuged at 124,000g for 1 hour at 4° C. The supernatant was removed and the pellet was resuspended in 200 µL of buffer containing (in mM): Tris 50, EDTA 1 and 2% sarkosyl. The pellet was pipetted and the solution sonicated 5 times for 30 seconds until completely dissolved. Protein content was then measured by Lowry's method and separated by SDS PAGE.

Electrophysiological Recordings

Cardiomyocytes isolated from the mouse ventricles were used for electrophysiological recordings. Whole-cell voltage-clamp and current-clamp experiments were performed within 12 hours of cell isolation at the temperatures noted using an Axopatch 200B patch-clamp amplifier (Axon Instruments, Foster City, CA). For voltage-clamp experiments, cells were patched using borosilicate glass pipettes (1B150F-4 and TW150F-4, World Precision Instruments, Sarasota, FL) pulled using a Sutter P-87 (Sutter Instrument, Novato, CA) to a resistance of 2-4 MΩ when filled with a pipette solution containing (in mM): K-aspartate 100, KCl 30, $MgCl_2$ 1, HEPES 5, EGTA 5, Mg-ATP 5, NaCl 5, pH adjusted to 7.2 with KOH. For current clamp experiments, pipette resistance was 7-10 MΩ when filled with the same solution. Cardiomyocytes were placed in a 0.25mL recording chamber (RC-26, Warner Instruments, Hamden, CT) and perfused with an external solution

containing (in mM): NaCl 135, MgCl2 1.1, $CaCl_2$ 1.8, KCl 5.4, HEPES 10, glucose 5.5, pH 7.4 adjusted with NaOH. $CdCl_2$ (0.3 mM) was added to the bath solution for voltage-clamp experiments. In experiments done at near physiological temperature, perfusate heating was controlled using an inline heater (64-0103, Warner Instruments) and heated magnetic platform (PM-1, Warner Instruments), controlled by a bipolar dual automatic temperature controller (TC-344B, Warner Instruments). Only quiescent, single, rod-shaped cardiomyocytes with clear striations were selected for recording. In voltage-clamp experiments, cells were held at -80 mV and depolarized for 5 sec to potentials from -100 mV to +50 mV in 10 mV steps at 0.05 Hz. In some experiments, cells were depolarized to a single potential of +50 mV from the same holding of -80 mV. All voltage clamp protocols were preceded by a 50 ms inactivating prepulse to -40 mV to eliminate Na^+ currents.[110] Whole-cell series resistances and capacitances were electronically compensated at least 80% to minimize voltage error. Action potentials were evoked by the injection of a small, short lasting current (0.8-2 nA, 1-2 ms) at 1.0 Hz. Cells were paced for 30 seconds to reach steady state and the final 5 action potentials were averaged for analysis.

Analysis of electrophysiological recordings

Voltage-clamp data were analyzed using Clampfit 9 (Axon Instruments). Peak currents were defined as the maximal K^+ current reached over the period of depolarization. The amplitudes and inactivation time constants of outward currents were best-fit using tri-exponential curve fitting, which was performed in Clampfit

using the Levenberg-Merquot (SP) iterative technique. Only fittings with a correlation ≥ 0.98 were used in analysis. Peak and component amplitudes were normalized by cell capacitance and expressed in pA/pF. Cell membrane capacitance were calculated immediately upon reaching whole-cell configuration by Clampfit through integration of the transient seen in response to a +10 mV voltage step from holding. Action potentials were analyzed using a custom written Visual Basic program in Microsoft Excel to calculate resting membrane potential, action potential amplitude, dV/dt_{maz}, and action potential durations at 20% (APD20), 50% (APD50) and 90% (APD90) repolarization. Action potentials recorded after 30 sec pacing at 1 Hz were used for comparison.

Mice

Male $Kv\beta2^{-/-}$ mice as well as strain-matched WT mice were bred in house and maintained on a mixed C56BL/6 x 129/SvEv background. The $Kv\beta2^{-/-}$ mice were originally obtained from Dr. Geoffrey Murphy of the University of Michigan Department of Physiology and The Molecular & Behavioral Neurosciences Institute. All procedures were approved by the University of Louisville Institutional Animal Care and Use Committee, IACUC number 14047.

Isolation of adult mouse cardiac myocytes

Male mice 12-24 weeks of age were used for cardiac myocyte isolation. Twenty minutes prior to anesthetization, an intraperitoneal injection of heparin sodium salt (>350 USP units, H3149, Sigma Aldrich) was administered to prevent

blood clotting in the coronary vasculature upon excision of the heart. Mice were anesthetized by an intraperitoneal injection of sodium pentobarbital (160mg/kg) and placed in a supine position with limbs restrained by tape. Upon positive confirmation of full anesthesia by paw pinch, the heart was rapidly and gently removed by thoracotomy and placed in a 70mm petri dish containing ice-cold (~1°C) calcium-free phosphate buffer solution (Gibco, ThermoFisher Scientific). Any non-cardiac tissue attached to the heart was rapidly removed while the heart was submerged in PBS, and the aorta was identified. Using microfine foreceps, the aorta was lifted onto a 22-gauge cannula attached to a modified Langendorff system and the heart was secured to the cannula using #4-0 surgical suture. The heart was perfused in retrograde Langendorff mode with buffers maintained at 37°C using a water-jacketed heat exchanger (Radnotti LLC, Monrovia CA) and negative feedback heated water bath and pump. Upon canulation, the heart was perfused with Tyrode's solution containing (in mM) $NaHCO_3$ 18, NaCl 126, KCl 4.4, $MgCl_2$ 1, HEPES 4, glucose 11, BDM 10, Taurine 30, pH 7.4) under a constant pressure of 70mm Hg. The perfusion of this first calcium-free buffer serves the purpose of removing all blood from the coronary vasculature as well as causing the dissociation of gap junctions which aids in myocyte isolation. Perfusion of calcium-free Tyrode's solution was no longer than 5 min to avoid a decline in myocyte health due to the "calcium paradox", [111, 112] a phenomenon wherein reintroduction to physiological Ca^{2+} levels (1-3 mM) following perfusion of Ca^{2+}-free buffer causes rapid deterioration of cell quality and myocyte hypercontracture due to Ca^{2+} influx.

42

After 5 minutes, the perfusion solution was exchanged with an enzyme solution consisting of the above Tyrode's solution with the addition of Liberase TH 280µg/mL, CaCl2 25µM, endotoxin-free BSA 0.1%, DNAse (Roche) 15µg/mL, protease type XIV (Sigma Aldrich) 16.8µg/mL, pH 7.4 with NaOH. The heart was digested for approximately 8-10 minutes and then inspected visually for proper digestion. The ventricles were then cut off the cannula and the heart was placed in a 35 mm dish containing mincing solution at 37°C comprised of the above enzyme solution with the addition of BSA 9mg/mL. In this buffer, any remaining vasculature or nonventricular tissues were quickly dissected away and the heart was minced using fine tip forceps until most large pieces of tissue were gone. The tissue and cells were then gently triturated by aspirating the solution with a serological pipette several times. The cell-containing solution was passed through a 100-mesh stainless steel filter to remove any underdigested tissue. The filtered solution containing dissociated cardiac myocytes were then purified of damaged or calcium intolerant cells by reintroducing calcium in 5 steps of increasing concentration. Cardiac myocytes were allowed 10 minutes to pellet in 5 tubes containing 50 µM, 75 µM, 125 µM, 275 µM and 525 µM $CaCl_2$. Following this final stage, a small aliquot (10 µL) of suspended cells was transferred to a hemocytometer for counting and inspection of isolation quality. Using this protocol, over $1 * 10^6$ cardiac myocytes (>90 % rod shaped with long aspect ratio) are routinely obtained.

For electrophysiological experiments, the cardiac myocytes were then suspended in a cold (4°C), high K^+ solution containing (in mM): K^+-glutamate 100,

KCl 25, KH$_2$PO$_4$ 10, MgSO$_4$ 1, glucose 22, EGTA 0.5, HEPES 5, pH 7.2 with KOH. Cells were stored in the refrigerator until study, at which time a small aliquot of suspended cells was transferred into the bath of the patch clamp microscope.

For immunofluorescence imaging studies, the cardiac myocytes were fixed as follows. Cells were allowed to pellet in a 15 mL test tube and any remaining buffer was aspirated. The pellet was then resuspended in 2 mL of calcium-free PBS 4°C. Cold paraformaldehyde (4% in PBS) was then slowly added to the suspension for a final concentration of 3% PFA and allowed to incubate for 15 min total. The first 10 minutes of fixation was performed with gentle rocking, and during the final 5 minutes the tube was placed upright to allow the cells to pellet. The fixed cardiac myocytes were washed 3 with 15 mL of cold PBS, allowing 15 minutes during each wash to allow the cells to pellet at the bottom of the tube. Following the final wash step, the cells were suspended in 2 mL of PBS and stored at 4°C for up to 3 months.

For protein and mRNA analysis, the pellet of cells was flash frozen in liquid N$_2$ and stored at -80°C for later use.

Cell Immunofluorescence

For immunofluorescent studies, 3000-5000 fixed cardiac myocytes were diluted into approximately 100µL and adhered to poly-L-lysine-coated coverslips using a Cytospin 4 Cytocentrifuge (Thermo Scientific) at 300 RPM. This produced an even distribution of cells without significant cell overlap and no disruption in morphology.

Cells were permeabilized by incubating in PBS containing 0.1% Triton X-100 for 10 minutes. The permeabilized myocytes were then washed in PBS three times for 5 min. Blocking was performed by incubating the cells in 1% BSA, 22.5 mg/mL glycine in PBS T (PBS + 0.1% Tween 20) for 30 minutes.

Primary antibody incubation dilutions were determined empirically for each antibody. Primary antibodies were diluted in 1% BSA in PBST and incubated for either 1 hour at room temperature or overnight at 4°C in a humidified chamber. Following primary antibody incubation, the cells were washed in PBS 3 times for 5 minutes.

Secondary antibodies, anti-rabbit or anti-mouse Alexa 647 (ThermoFisher Scientific) were diluted in 1% BSA at a concentration of 1:2500. Cells were incubated in the secondary antibody for 45 minutes at room temperature in an opaque box. Cells were then washed again in PBS 3 times for 5 minutes. Coverslips were then quickly dunked into a beaker containing deionized water, as we have found this minimizes the presence of any salt crystals formed by evaporation. Cells were counterstained with ProLong Antifade reagent containing 4,6-diamidino-2-phenylindole (DAPI, ThermoFisher Scientific), covered with a 12 mm coverslip and sealed using clear nail polish. Cells were stored in a slide box at 4°C until analyzed. Fluorescence was observed using a Nikon A1 confocal microscope equipped with a 405 nm laser (for DAPI) and a 632 nm laser (for Alexa 647).

Echocardiography

Transthoracic echocardiography was performed using the Vevo 770 echocardiography platform. Mice were anesthetized using 2% isoflurane initially, and were maintained under anesthesia for the remainder of the experiment using 1.5% isoflurane. Body temperature was maintained at 37°C using an electronic rectal thermometer interfaced to a servo-controlled heating lamp. Electrocardiograms were recorded using leads attached to each limb. Mice were placed supine on an examination board and depilatory cream was used to remove all hair on chest. Two-dimensional imaging of the parasternal long axis was performed using a 707-B 30 MHz scan head at 100 frames per second. Short axis images were also recorded by rotating the scan head. Two-dimensional images were obtained every millimeter between the papillary muscles and the apex. M-mode images were constructed from 2-D images and were used to measure heart rate (HR), left ventricular inner diameter during diastole and systole (LVIDd and LVIDs, respectively). These measures were used to calculate fractional shortening (FS) using the equation: FS= [(LVIDd-LVIDs)/LVIDd] x 100%. Ventricular volumetric indices (diastolic and systolic volumes) were calculated using Simpson's rule of integration on the serially acquired short-axis images. These were used to calculate stroke volume (SV) as SV=diastolic volume – systolic volume. Ejection fraction (EF) was calculated as EF= (stroke volume/diastolic volume) 100%. Cardiac output (CO) was calculated as: CO= SV * HR.

Cardiac histology

Hearts were rapidly excised and mounted on a 22-gauge blunted needle cannula as with the cardiac myocyte isolation protocol and were retrogradely perfused with room temperature PBS for 3 minutes followed by 4% PFA in PBS for 15 minutes. Hearts were then removed from the cannula, dissected of any non-myocardial tissues, and sectioned in either the coronal, sagittal or axial axes using a Zivic Mouse Heart Slicer (Zivic Instruments, Pittsburgh, PA) and incubated overnight in 4% PFA. The next morning, the heart sections were transferred to a beaker containing 70% ethanol for short-term storage. Heart sections were then processed and embedded in paraffin blocks for long term storage.   Paraffin-embedded tissue sections were sliced at 4 μm and stained with H&E. Images of mid-heart cross sections were made using a digital camera mounted to an Olympus microscope.

Quantitative RT-PCR

RNA was extracted from heart samples using the RNeasy mini kit (Qiagen). RNA concentration and purity was measured using the Nanodrop 1000A Spectrophotometer (Thermo Scientific). The cDNA library was prepared using a Bio-Rad mycycler Thermocycler at 42°C for 60 min and 94°C for 5 min. When not used immediately, cDNA samples were stored at -20°C. Total cDNA were diluted 20-fold using RNAse free water prior to use. RT-qPCR was done using iTax Universal SYBR Green Supermix (Bio-Rad) on the Applied Biosystems 7900 HT Real-Time PCR system. Primers for Kvα, Kvβ, and mGAPDH (internal control) were added to wells of a 384-well plate appropriately. cDNAs for each RNA

sample were run in triplicate. The RQ of each Kv channel subunit in each sample were calculated using the $2^{-\Delta\Delta Ct}$ method by normalization to the internal standard mGAPDH. Specific amplification was confirmed by visualizing melting curves for each sample for the presence of a single sharp peak.

Statistics

Data are reported as mean ± SEM. Data were analyzed using GraphPad Prism and Microsoft Excel with paired or unpaired t-test with Bonferroni correction or ANOVA. For paired experiments where treatment values were normalized to initial values, the Wilcoxon matched pairs nonparametric test was used. P-values <0.05 were considered to be significant.

CHAPTER III

Kvβ2 MODULATES CARDIAC Kv CURRENTS AND REPOLARIZATION

Introduction

The voltage-gated potassium (Kv) channels are widely expressed throughout excitable tissues and are the primary mediators of repolarization in neurons and the cardiac myocyte. In the heart, Kv channels regulate the resting membrane potential, the frequency of pacemaker and the shape and duration of the action potential.[106] As a superfamily consisting of over 40 different members, they form one of the most diverse ion channel families both in form and function. Their functional diversity is further expanded through the interaction with ancillary subunits, such as the Kvβ proteins. These cytoplasmic subunits, which bind to the intracellular domain of Kv1 and Kv4 family channels, can have profound effects on channel trafficking and membrane expression,[63, 68, 113] subcellular localization,[71, 114] and channel gating and kinetics.[54, 56, 115, 116]

Much of the information regarding the electrophysiological and catalytic functions of the Kvβ proteins has been gained through the use of heterologous expression systems. While much of both *in vivo* and primary cell characterization have been performed in the central nervous system, some descriptions of the physiological function of Kvβ proteins in other tissues and organs do exist. The loss of Kvβ1 in the heart has been demonstrated to alter the cardiac Kv currents

49

$I_{to,f}$ and $I_{k,slow}$.[117] Furthermore, antisense knock down of Kvβ2 has been demonstrated to reduce Kv conductance, hyperpolarize the conductance-voltage relationship ($V_{1/2\text{-act}}$, the voltage at which half the channels in a cell are in an activated state), increase the time course of current activation (τ_{act}, a measure of the rate of current change) and increase action potential duration in *Xenopus* myocytes.[118] Kvβ2^{-/-} mice also have a strong strain-dependent neurological phenotype. In mice on a C57BL/6 background, loss of Kvβ2 leads to deficits in memory and learning and causes occasional seizures.[119]

Therefore, we designed the present study to address our hypothesis that Kvβ2 plays a role in ventricular repolarization through a contribution to the generation of cardiac Kv currents by its interaction with one or more unknown members of the Kv family. To this end, we used an approach that included single cell patch clamp and organ-level (Langendorff perfused heart) electrophysiology, protein measurement by Western blotting, co-immunoprecipitation, and cellular immunofluorescence. We also assayed cardiac function using echocardiography to determine if contractile function of the heart was altered. Together, we aimed to determine the cardiac phenotype of mice bearing a targeted disruption of the Kvβ2 gene (Kvβ2^{-/-}) vs. their WT littermates.

Results

Kvβ2 expression in the mouse ventricle

Western blotting of whole-heart lysates was performed to confirm the presence of Kvβ2 protein in mouse ventricular lysates (Figure 3.1). We also

performed immunoblotting to determine if the loss of Kvβ2 impacts the protein expression of Kvα and Kvβ subunits previously described to interact with Kvβ2 in other cell types (Figure 3.1). Using whole-cell ventricular lysates, protein levels of Kv1.4, Kv1.5, and Kv4.2 were not significantly altered in ventricles from Kvβ2^{-/-} mice (Figure 3.2). To confirm cardiac myocyte expression of Kvβ2, isolated cardiac myocytes were fixed with paraformaldehyde, permeabilized and stained with a monoclonal anti-Kvβ2 antibody and anti-mouse Alexa 647 secondary antibody. Cells were viewed under confocal microscopy and it was shown that the greatest fluorescent intensity was localized to the sarcolemma (Figure 3.3).

Kvβ2 interacts with Kv1.4 and Kv1.5 in the mouse heart

Biochemical and electrophysiological work using expression systems has previously established that Kvβ2 interacts with most members of the Kv1[10] and Kv4[57, 63, 120] families both physically and functionally. In the brain, Kvβ2 has been shown to associate with Kv1.1, Kv1.2, Kv1.4, Kv1.6[121] and Kv4.3,[63] with Kv1.3 in lymphocytes[122] and Kv1.5 in pancreatic islets.[123] Previous work demonstrated that Kvβ1 directly interacts with Kv4.2 and Kv4.3, but not Kv1.4 or Kv1.5 in the mouse heart.[117]

To determine the *in vivo* binding partners of Kvβ2 in the mouse heart, a co-immunoprecipitation approach using magnetic bead-bound monocolonal anti-Kvβ2 antibody was utilized. Western blot analysis of ventricular lysates showed that Kv1.4 and Kv1.5 coimmunoprecipitate with Kvβ2. (Figure 3.4). No positive

co-immunoprecipitation was observed in lysates prepared from Kvβ2$^{-/-}$ hearts, supporting the specificity of the interaction.

Loss of Kvβ2 decreases surface expression of Kv1.5 in ventricular cardiac myocytes

In heterologous systems, co-expression of Kvβ proteins increases the membrane expression of Kv1 and Kv4 channels.[10, 124] To determine the effect of Kvβ2 on surface expression of Kv1.4, Kv1.5 and Kv4.2 channels, we compared the abundance of these Kv channels on the surface of ventricular cardiac myocytes isolated from WT and Kvβ2$^{-/-}$ mice. To this end, two techniques were utilized: sarcolemmal membrane fractionation using differential centrifugation and confocal microscopy of fixed isolated cardiac myocytes.

Whereas the total Kv1.5 protein in Kvβ2$^{-/-}$ ventricles was slightly greater than in WT (Figure 3.1), the ratio of Kv1.5 in the membrane-enriched fraction to that in supernatant was significantly reduced in Kvβ2$^{-/-}$ ventricular lysates (Figure 3.5); this result suggests a role for Kvβ2 in moving Kv1.5 to the sarcolemma. The efficacy of the membrane separation protocol was confirmed by comparing pan-cadherin detection in the membrane (M) and cytosolic (S) fractions (Figure 3.5), suggesting that all sarcolemmal protein was contained in the membrane-enriched fraction. Furthermore, in accordance with findings in the literature, the membrane bound Kv1.5 was found as a single band, whereas Kv1.5 from whole cell preparations typically runs at two bands of distinct molecular weights. In support of this finding, isolated cardiac myocytes were fixed and stained with anti-Kv1.5

antibody and visualized under confocal microscopy. Surface fluorescence of Kv1.5 was reduced in Kvβ2$^{-/-}$ cardiac myocytes compared to WT controls (Figure 3.6).   Together, these findings indicate a role for Kvβ2 in the surface expression of Kv1.5 channels in the heart.

Loss of Kvβ2 reduces outward Kv current in ventricular cardiac myocytes

To investigate whether Kv currents in cardiac myocytes were altered due to loss of Kvβ2, whole-cell voltage clamp (Figure 3.7) was used to compare the magnitude and time course of currents elicited in response to 5s, +50mV depolarizing pulses. Triexponential fitting was used to dissect currents into three components based upon inactivation time constants.[105]   Peak current density (I_{peak}) was reduced in Kvβ2$^{-/-}$ (p < 0.05, Figure 3.8 A-C). The magnitude of current associated with the most rapidly inactivating exponential component, previously described to be attributed to I_{to}, was reduced from 30.0+/- 4.6 pA/pF in WT to 15.8 +/- 2.0 pA/pF in Kvβ2$^{-/-}$ (p<0.01 Figure 3.8 D). The magnitude of intermediate and slowly inactivating currents were reduced but did not reach statistical significance (p=0.13 and p=0.054, respectively, Figure 3.8 E,F). The inactivation time constant values associated with each exponential term were not different between groups (Table 1).

Reduced Kv current magnitude results in delayed action potential repolarization

As Kv currents are the driving force for cardiac myocyte repolarization, we tested whether the reduced Kv current densities observed in voltage-clamp conditions manifested in prolonged action potential durations. Action potential repolarization was quantified as the time required for a cell to return to 20, 50, and 90% of its resting membrane potential (APD20, APD50, and APD90). Repolarization was slowed significantly at each APD, indicating a significant repolarization deficit in Kvβ2^{-/-} myocytes (Figure 3.9 B). Other action potential parameters including upstroke velocity (dV/dt$_{max}$), resting membrane potential (RMP), and action potential amplitude (APA) were unchanged, confirming that the changes caused by loss of Kvβ2 are specific to repolarization and not due to broad electrophysiological instability or cell health (Figure 3.10). We found that action potential duration was similarly prolonged by a partial blockade of Kv1.5 with the Kv channel blocker 4-aminopyridine. At the concentration used (100 µM), we expected approximately 30% inhibition of Kv1.5 (IC50 270 µM)[10], similar to the reduction in peak Kv current observed under voltage clamp. Prolongation of action potentials by 4-AP was qualitatively similar to that observed in the Kvβ2^{-/-} cells (Figure 3.9 C).

To further confirm a repolarization deficit in the Kvβ2^{-/-} heart, we perfomed a second series of experiments using the *ex vivo* Langendorff perfused heart model. Monophasic action potentials were recorded from the epicardial surface of the left ventricle during spontaneous beating (Figure 3.11 A-C). In agreement with the transmembrane action potentials recorded from single isolated cardiac

myocytes, action potentials were significantly prolonged at 20, 50, and 90% repolarization (Figure 3.11 D-F).

Baseline cardiac function is unchanged in Kvβ2$^{-/-}$ hearts

To examine if the prolonged cardiac repolarization seen in Kvβ2$^{-/-}$ manifested in changes in contractile function, we performed transthoracic echocardiography. All functional cardiac parameters, including stroke volume, ejection fraction and cardiac output were unchanged (Figure 3.12).   We did find through necropsy study that Kvβ2$^{-/-}$ mice have smaller hearts than age- and sex-matched WT mice. The heart weight to tibia length ratio in Kvβ2$^{-/-}$ is significantly lower in Kvβ2$^{-/-}$ compared to age-matched WT (6.2 ± 0.1 mg/mm vs 7.4 ± 0.3 mg/mm respectively, $p < 0.002$, Figure 3.13 A). This difference resulted from differential development in the left ventricle (Figure 3.13 B) as right ventricular development (Figure 3.13 C) was not different between groups. Some hearts were sectioned in the transverse plane and stained with hematoxylin and eosin to compare gross anatomy and to visualize left ventricular development (Figure 3.13 D). This difference does not arise from changes in cardiac myocyte size, which was not different between groups as measured either by microscopy or cellular capacitance during electrophysiological experiments (Figure 3.14).

Discussion

The results of this study show that Kvβ2 plays a role in repolarization in the heart through enhancement of Kv current density. We found that Kvβ2 protein is

expressed in the heart, specifically in the cardiac myocyte. We found that Kvβ2 physically associates with Kv1.4 and Kv1.5 *in vivo*, and plays a role in the functional expression of Kv currents through enhanced Kv current density. The significant reduction in peak current density in response to depolarization appears to be driven by a reduction in I_{to}, as the triexponential fitting model employed showed the largest reduction in the magnitude in the most rapidly inactivating component of the outward current. This is evidence to suggest a functional interaction of Kvβ2 with Kv4.2 or Kv1.4, channels it is known to both associate with and promote the surface trafficking of. We attempted to co-immunoprecipitate Kv4.2 using the method that showed positive interaction with Kv1.4 and Kv1.5, but were not able to detect this protein in the immunoprecipitated material. This is not definitive evidence for a lack of interaction of Kv4.2 with Kvβ2 in the heart, but it suggests that the reduction in Kv current may be occurring by another mechanism. One interpretation of our results is that the observed reduction in surface expression of Kv1.5 in the Kvβ2$^{-/-}$ could be participating in the reduction of peak current. Kv1.5, the molecular correlate of the human I_{kur} current is very rapidly activating; under voltage clamp conditions when the cell is depolarized to +50 mV, it almost instantaneously activates and contributes to the peak current density. This however does not explain a contribution to the rapidly inactivating component of the outward current. The most plausible explanation for the reduced rapidly inactivating current aside from an interaction of Kvβ2 with Kv4.2, which was not detected by Co-IP, is that Kvβ2 is interacting with Kv1.4 in the WT heart. Indeed, we found positive co-immunoprecipitation with Kv1.4. The magnitude of the current

with an intermediate inactivation rate, $I_{K,slow1}$ was reduced but not to a statistically significant level. This could be a result of a limitation in the fitting algorithm used. Recent work published since the time of these experiments supports the notion that 5 sec depolarizations are not adequately long enough to fully resolve the three components of the murine Kv currents, I_{to}, $I_{K,slow1}$ and $I_{K,slow2}$ and that depolarizations lasting as long as 20 seconds may be required to accurately separate the magnitudes of each Kv current.[125] (Liu J 189) Nevertheless, we interpret the findings of significantly reduced Kv current density, positive co-immunoprecipitation with Kv1.4 and Kv1.5, and reduced trafficking of Kv1.5 to the sarcolemma as strong evidences of a critical role of Kvβ2 in the generation of repolarizing currents in the mouse heart.

The impact of the observed reduction in Kv current is clear; in both single cell current-clamp and monophasic action potential recordings, Kvβ2 hearts have a significantly reduced repolarization capacity. Action potential durations are prolonged at all levels of repolarization, strongly indicating an effect on the rapidly activating components of the total cardiac Kv current, I_{to} and $I_{K,slow1}$. This is supportive of voltage clamp results and the observed interactions with Kv1.4 and Kv1.5, components of I_{to} and $I_{K,slow1}$, respectively. Further work is warranted to confirm whether Kvβ2 is interacting with Kv4.2 in the mouse heart.

In addition to the effects that Kvβ2 appears to have on the functional expression of Kv channels, that is the enhancement of Kv channel abundance at the sarcolemma, the results can also be interpreted as evidence that the loss of Kvβ2 may affect the gating of Kv1.4 and Kv1.5 in the heart. While the voltage

57

clamp results do not show any significant differences in inactivation rates of the three Kv component currents, we did not specifically address changes in their voltage dependence of activation, $V_{1/2\text{-act}}$. Accurately measuring the $V_{1/2\text{-act}}$ of a singly expressed channel in a heterologous system is straightforward, doing so in a primary cell that contains many different currents is not. We have not yet addressed this experimentally, in part due to the fact that the pharmacology of Kv1.5 inhibitors is lacking. The Kv1.5 blockers commercially available are chemical blockers that are not as highly specific as peptide inhibitors (i.e. spider toxins like HpTx) available for other channels. Inhibition of $I_{K,slow1}$/Kv1.5 with channel blockers such as 4-AP and Psora-4 likely would not allow for the very precise inhibition necessary to allow for measurement of activation kinetics. One potential compound to address this question does exist, diphenyl phosphine oxide (DPO-1), which blocks Kv1.5 in the sub micromolar range with an 8-fold specificity over I_{to}. This may be addressed in future experiments as we further characterize the mechanism by which Kvβ2 modulates cardiac Kv currents.
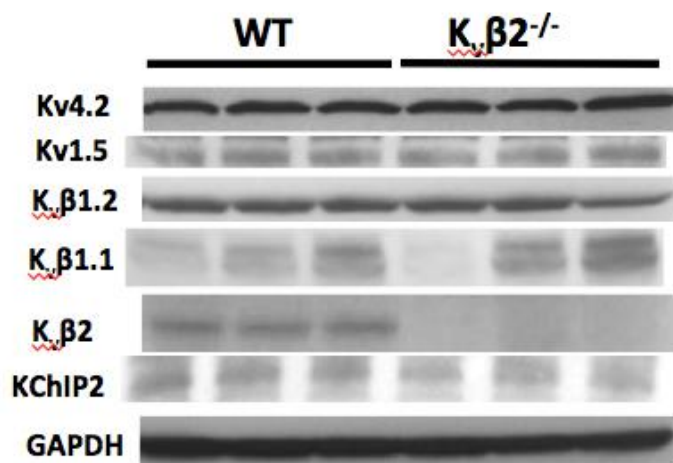
Figure 3.1: Expression of Kvα and Kvβ proteins in the mouse ventricle.
Whole heart lysates were separated by SDS PAGE and incubated with anti-Kv4.2, Kv1.5, Kvβ1.1, Kvβ1.2, Kvβ2 and KChIP2 antibodies.. Kvβ2 protein is expressed in WT (lanes 1-3) but not Kvβ2$^{-/-}$ (lanes 4-6) hearts.
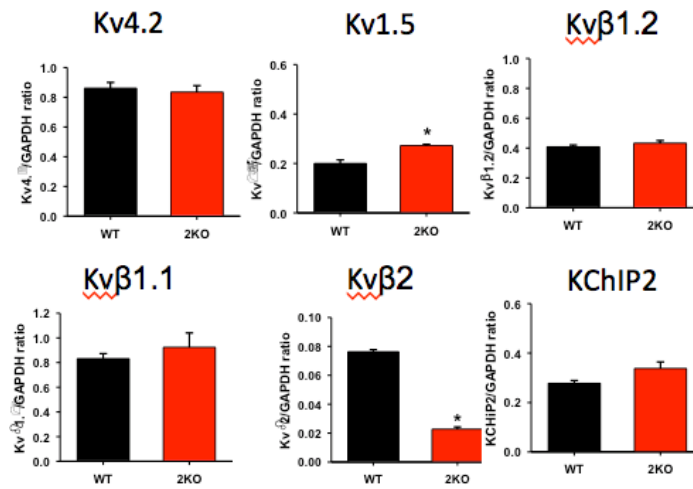
Figure 3.2: Quantification of Western immunoblots. Western blots from Figure 3.1 were quantified using ImageJ. . Detection of Kv1.5 was slightly increased ($p < 0.05$). n=3 WT and 3 Kvβ2$^{-/-}$ hearts.
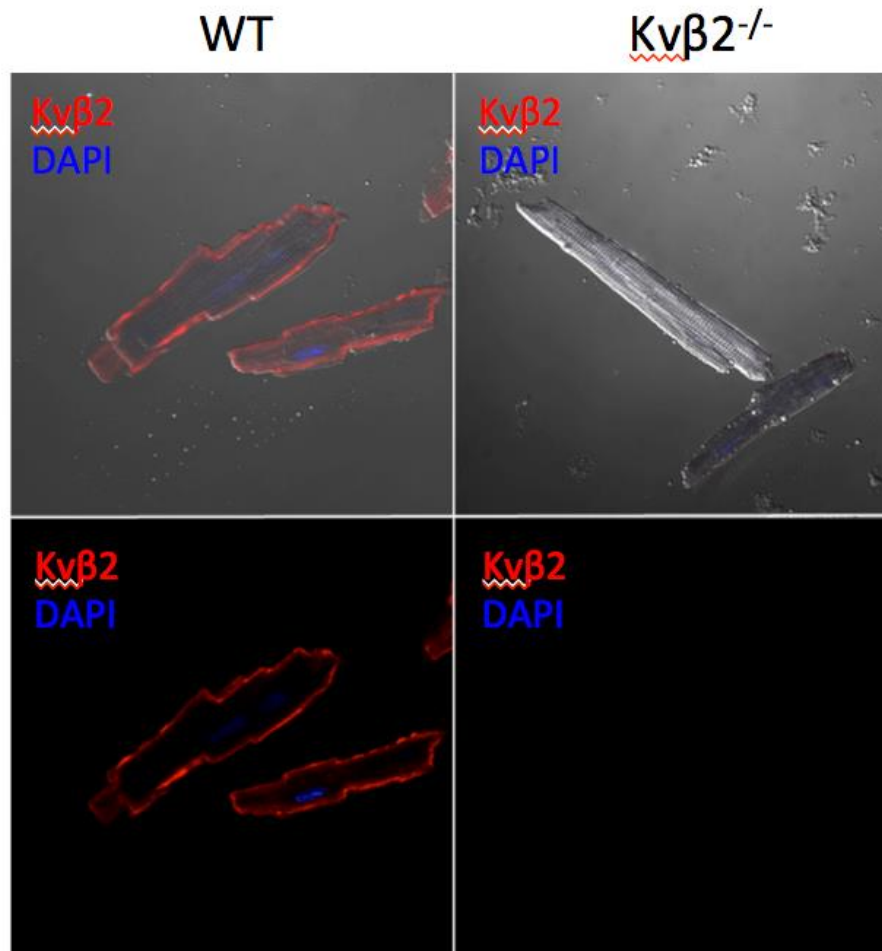
Figure 3.3: Cellular localization of Kvβ2 by immunofluorescence. Confocal microscopic images showing fixed isolated cardiac myocytes from WT (left) and Kvβ2$^{-/-}$ (right) mice stained with anti-Kvβ2 primary antibody (1:100) and Alexa647 secondary antibody. Red: anti-Kvβ2. Blue: DAPI.
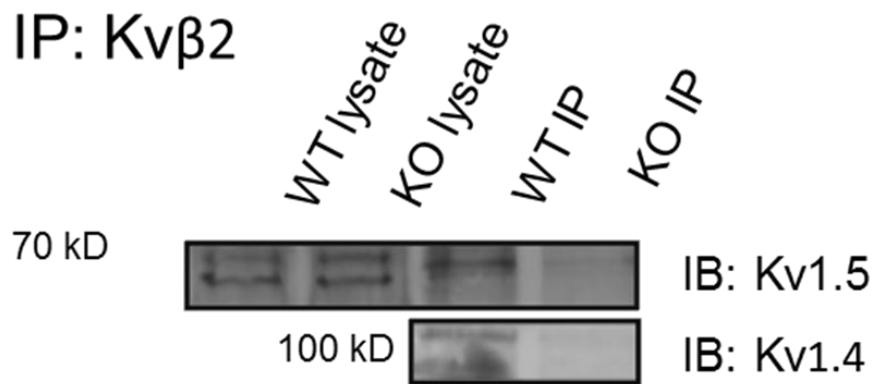
Figure 3.4: Immunoprecipitation of Kv1.4 and Kv1.5 by Kvβ2. Lysates prepared from isolated adult ventricles were immunoprecipitated (IP) using monoclonal anti-Kvβ2, antibody. Lysates before IP were also blotted with the same antibodies. Both Kv1.4 and Kv1.5 co-immunoprecipitate with Kvβ2 and are not detected in immunoprecipitation with Kvβ2[/-] ventricular lysates.
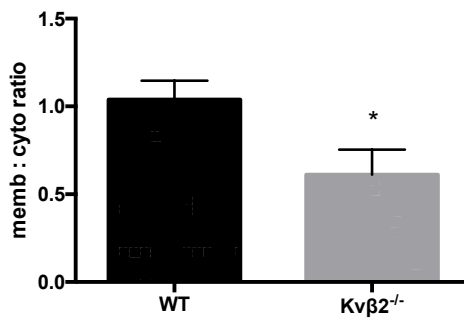
Figure 3.5: Ratio of Kv1.5 in the sarcolemma to cytosol. **Top:** A membrane preparation protocol was used to separate and enrich plasma membrane proteins. The efficacy of the separation was confirmed by blotting for pan-cadherin, a protein exclusively found in the sarcolemma. **Center:** For each heart (4WT and 6KO), two lanes were loaded, one with the membrane fraction (left) and cytosolic fraction (right). The band intensity of each pair was compared to find a membrane:cytosolic Kv1.5 ratio for that heart. Note: membrane bound Kv1.5 appears as a single band, cytosolic Kv1.5 appears as a double band, both bands were included. **Bottom:** Quantification of the group means, membrane:cytosolic ratio was significantly reduced in Kvβ2$^{-/-}$ (p<0.05).
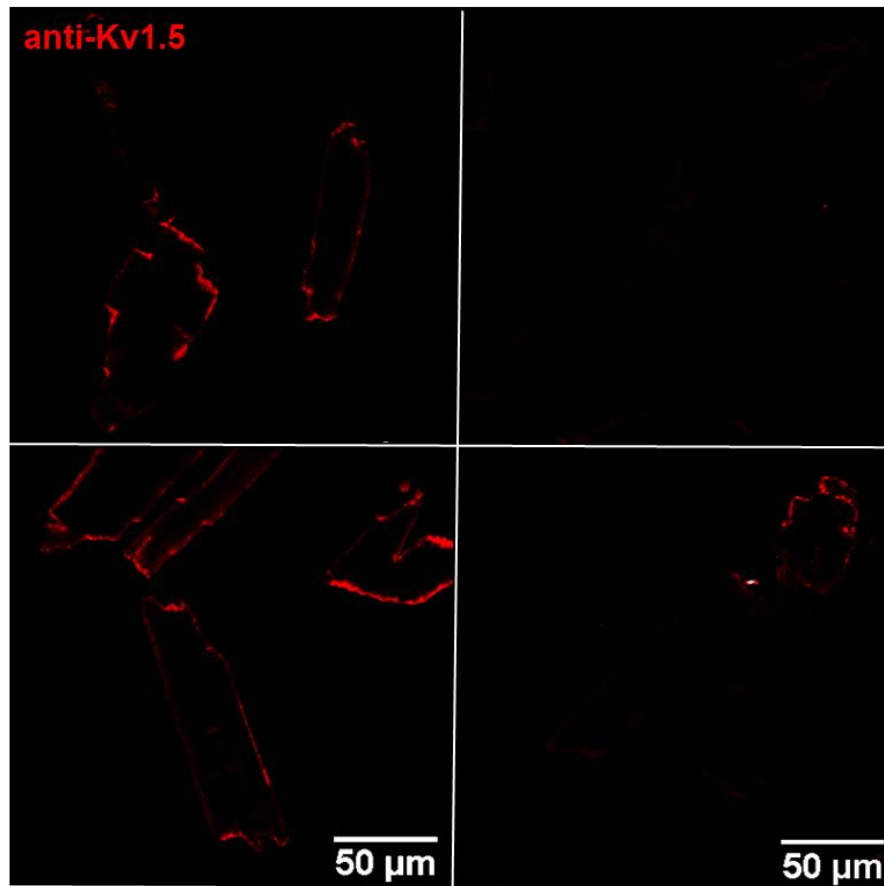
Figure 3.6: Cellular localization of Kv1.5. Isolated cardiac myocytes were stained with an extracelluar epitope anti-Kv1.5 antibody with secondary Alexa647 staining and viewed under confocal microscopy. Relative to WT, Kvβ2$^{-/-}$ showed reduced surface Kv1.5 reactivity. Result is representative of 3 experiments.
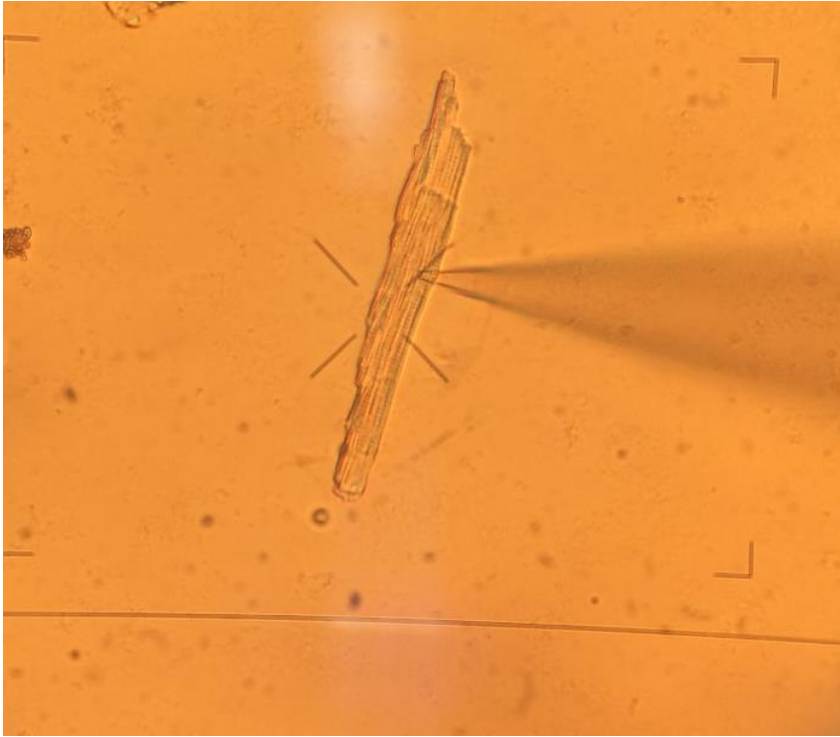
Figure 3.7: Isolated ventricular cardiac myocyte being recorded under whole-cell voltage-clamp configuration. $R_{pipette}$=2.5 MΩ
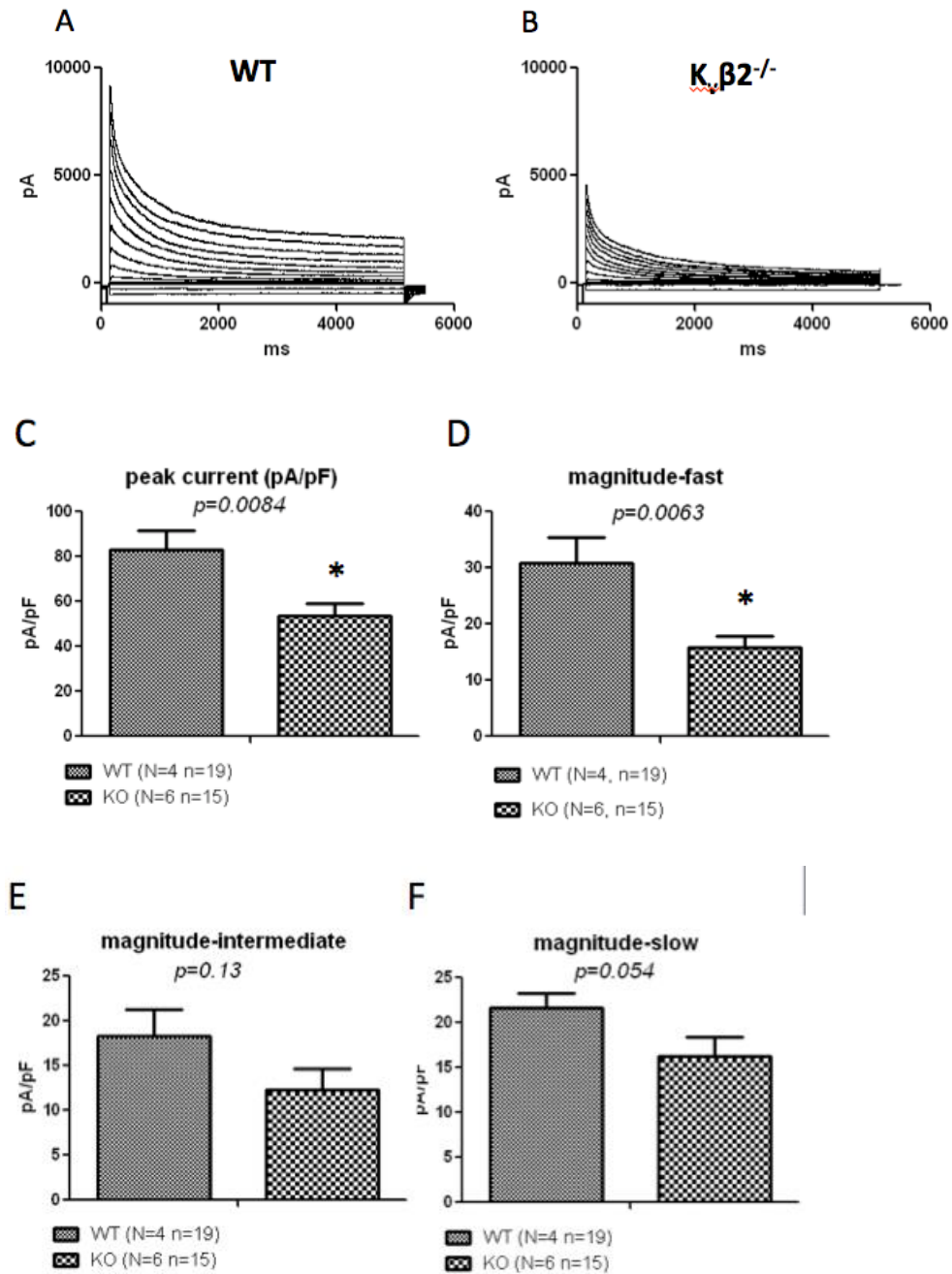
Figure 3.8: Kv currents in isolated cardiac myocytes. Representative outward current traces recorded from WT (A) and Kvβ2^{-/-} (B) ventricular cardiac myocytes in response to a family of 5s depolarizing pulses from -90 to +60 mV (Δ=10mV) from a holding potential of -80mV. Peak outward current density in response to +50 mV was significantly reduced (C). Tri-exponential fitting of current responses to a 5s 50mV depolarizing pulse was used to deconvolve individual currents based on inactivation rates (D-F). The magnitude of the rapidly inactivating current was significantly reduced by loss of Kvβ2. (*: $p<0.01$). N=# mice, n= # cells recorded.

Table 1: Cardiomyocyte Kv currents in WT and Kvβ2^{-/-}

	I_{to} (pA/pF)	τ (ms)	$I_{k, slow1}$ (pA/pF)	τ (ms)	$I_{k,slow2}$ (pA/pF)	τ (ms)	I_{ss} (pA/pF)
WT (n=19)	30.9 ± 4.6	60.0 ± 1.6	18.3 ± 3.1	429.2 ± 35.8	21.6 ± 1.7	2526.8 ± 177.2	8.8 ± 1.3
KO (n=15)	15.8 ± 2.0	63.8 ± 2.7	12.3 ± 2.3	467.3 ± 27.3	16.3 ± 2.1	2923.2 ± 274.7	8.1 ± 1.0
p<	0.01	ns	0.12	ns	0.055	ns	ns

T=21-23°C
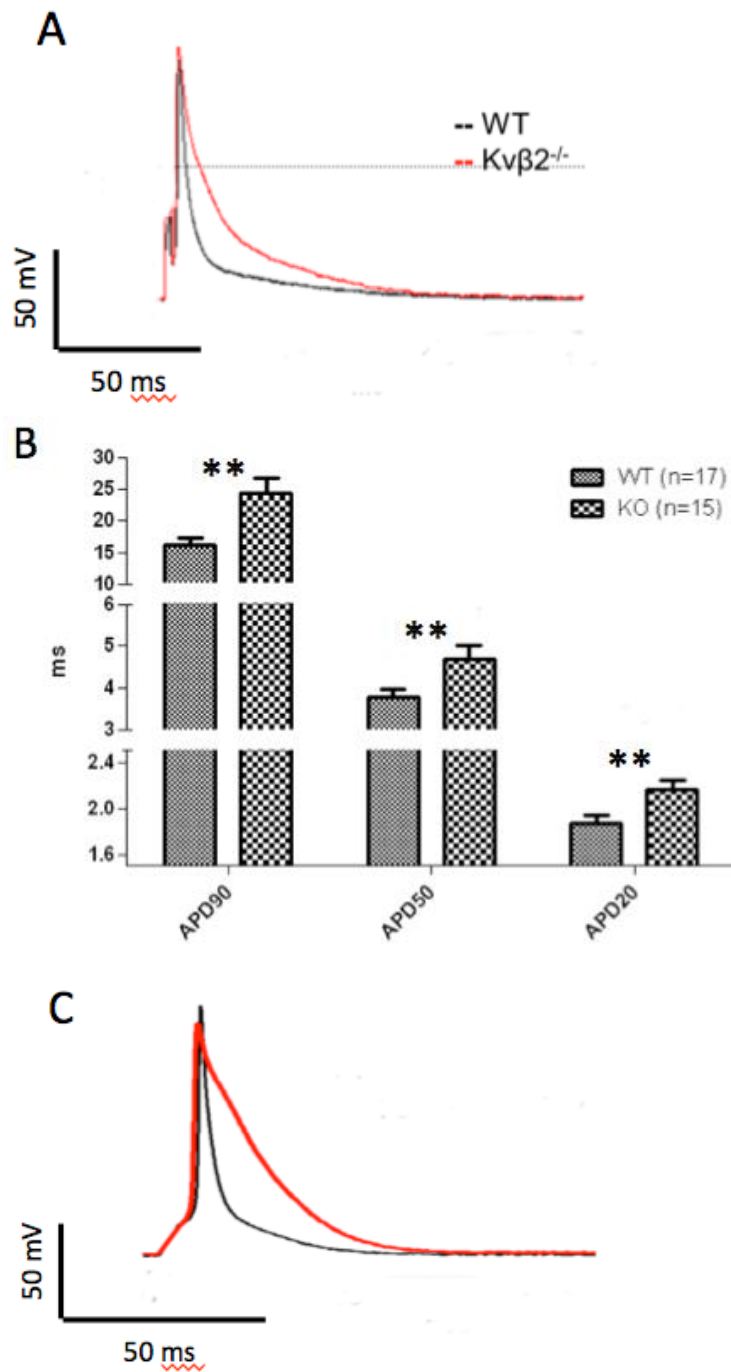
Figure 3.9: Action potentials in ventricular cardiac myocytes. A. Representative action potentials recorded from ventricular cardiomyocytes isolated from WT and Kvβ2$^{-/-}$ mice. B. Transmembrane action potentials of right ventricular cardiac myocytes were prologned at APD20, APD50, and APD90. C. Partial blockade of Kv1 currents using 4-AP (100 uM) similarly prolonged action potential durations in WT cardiomyocytes. **: $p<0.01$
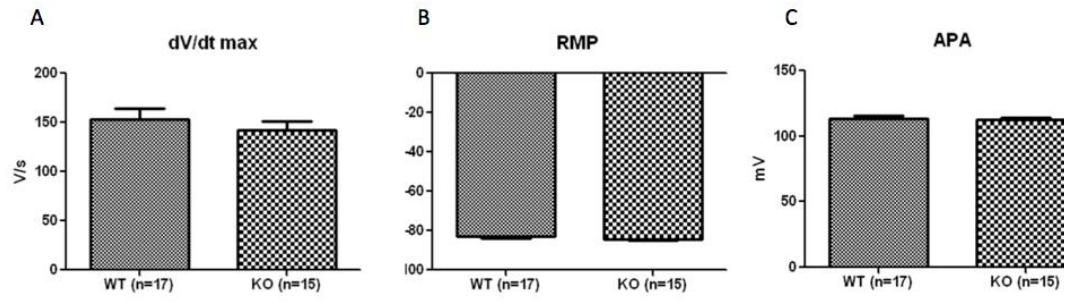
Figure 3.10 Non-repolarization indices of electrophysiological function. Non-repolarization indexes of cardiomyocyte function in Kvβ2$^{-/-}$ cells, including A. dV/dt$_{max}$, B. Resting membrane potential, and C. Action potential amplitude.
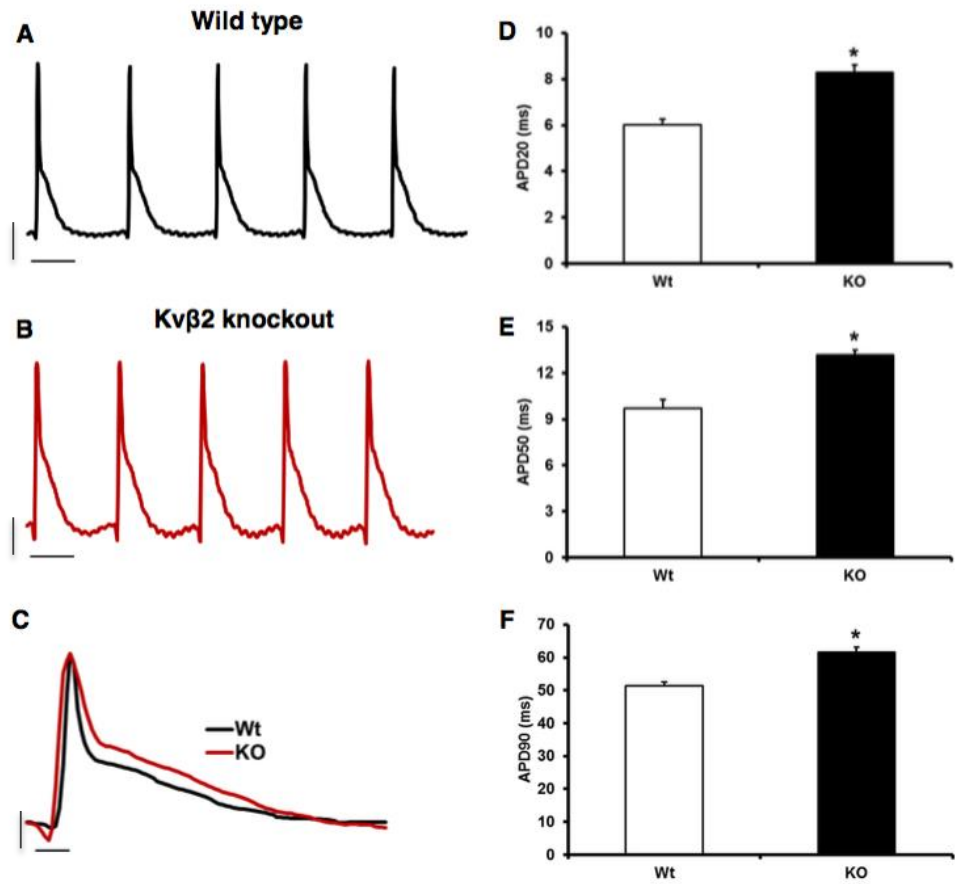
Figure 3.11: Surface action potentials. Monophasic action potentials were recorded from electrodes placed on the left ventricular epicardial surface of Langendorff perfused hearts. Representative action potentials recorded from WT (A) and Kvβ2$^{-/-}$ (B), overlayed (C). B. Action potential durations at APD20 (D), APD50 (E), and APD90 (F) were significantly prolonged in Kvβ2$^{-/-}$. n=5 mice WT and 6 mice Kvβ2$^{-/-}$ *: p<0.05. Horizontal cale bar = 10ms. Vertical scale bar = 20 mV. These experiments were performed in collaboration with Dr. Srinivas Tipparaju and Dr. Kalyan Chapalamadugu at the University of South Florida Department of Pharmaceutical Sciences.
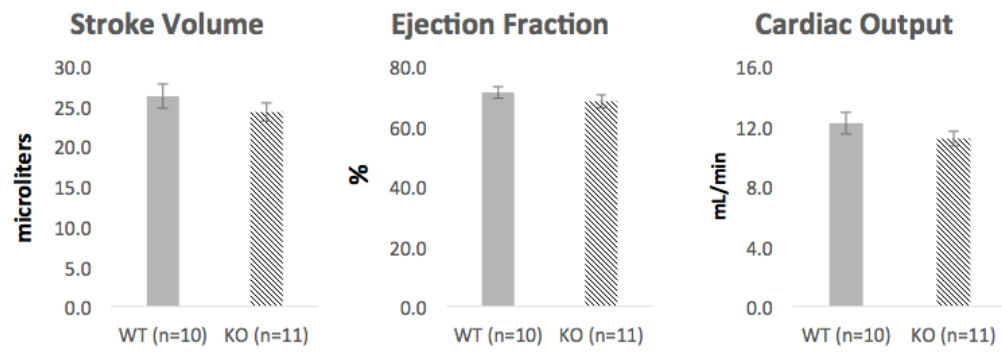
Figure 3.12: Baseline cardiac function. Echocardiography was used to measure stroke volume, ejection fraction and cardiac output. These functional values were similar between WT and Kvβ2$^{-/-}$ mice.
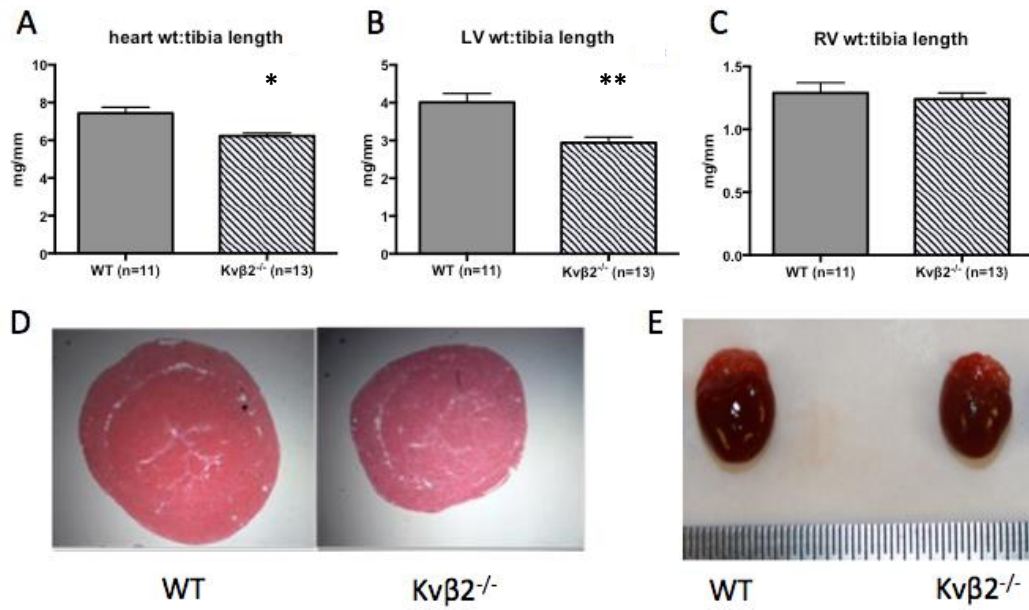
Figure 3.13: Cardiac anatomy. A. Heart weight normalized to tibia length in WT and Kvβ2$^{-/-}$ mice. B. Left ventricular weight normalized to tibia length in WT and Kvβ2$^{-/-}$ animals. C. Right ventricular mass was not reduced. D. Transverse sections of hearts were stained with H&E stained transverse sections of hearts from WT and Kvβ2$^{-/-}$ animals. E. Hearts excised from mice prior to dissection. **: $p<0.001$, *: $p<0.01$.
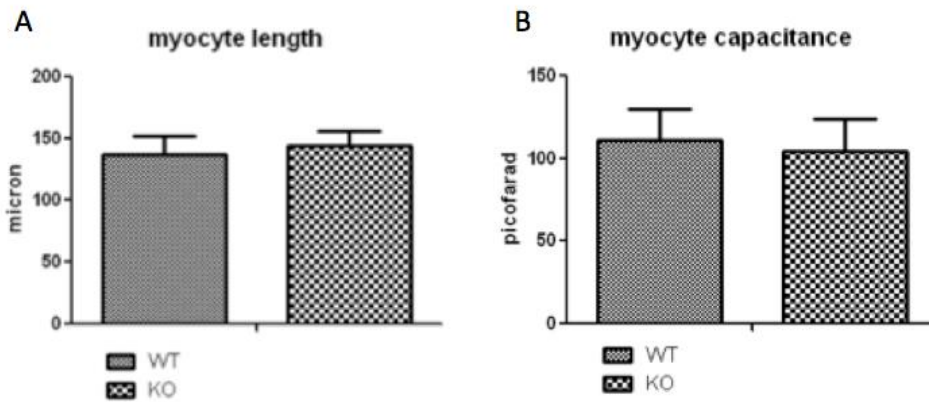
Figure 3.14: Cardiac myocyte size in WT and Kvβ2$^{-/-}$ mice. A. Cardiomyocyte length was measured under microscopy. B. Cardiomyocyte size was measured using capacitance during voltage-clamp experiments. Over 50 cells from each genotype were measured by both methods.

CHAPTER IV

REGULATION OF CARDIAC Kv CURRENTS AND REPOLARIZATION BY

PYRIDINE NUCLEOTIDES

<u>Introduction</u>

Faced with a limited oxygen supply during ischemia, the oxidation of NADH

by the mitochondrial electron transport chain complexes is inhibited, causing a rise

in cytosolic NADH levels. As a ubiquitous electron shuttling cofactor, changes in

the NAD^+/NADH ratio have widespread effects on the cell, including altering the

activity of various enzymes involved in intermediate metabolism. In the healthy

heart, the ratio of NAD+/NADH remain generally constant as they are constantly

recycled through various metabolic enzymes.   In the ischemic heart, this

equilibrium is disturbed by the lack of oxygen, and the reduced NAD^+ reserve is

reflected in the inhibition of various dehydrogenases involved in energy

metabolism.[126] The accumulation of glycolytic byproducts NADH, lactate, and H^+

may result in irreversible damage to the myocardium during ischemia.[127]

The redox status of the pyridine nucleotide bound to Kvβ is known to alter

the electrophysiological phenotype of the Kv channel complex (*vide supra*).

Nucleotides in the reduced state, NAD(P)H, allow the rapid inactivation of the Kv

channel by allowing free movement of the N-terminal inactivation domain of Kvβ1

and Kvβ3 containing complexes. Conversely, a bound nucleotide in the oxidized

74

state, NAD(P)$^+$, inhibits N-type inactivation by restraining the N-terminus of Kvβ1 and Kvβ3, preventing its access to the pore.[82] Furthermore, in the presence of a bound oxidized nucleotide, the hyperpolarizing effect of Kvβ2 on Kv1.5 is lost, and the channel complex displays a $V_{1/2-act}$ not significantly different than that of Kv1.5 alone, an effect that is likely conserved for all Kv1.5-Kvβ interactions.[79] We therefore propose that Kvβ channel complexes may provide a mechanism linking cardiac metabolism with repolarization, which may be of particular importance during myocardial ischemia.

The Kvβ proteins are members of the aldo-keto reductase (AKR) superfamily[119, 128] and are functional oxidoreductases that utilize pyridine nucleotides, NAD[P](H), for the reduction of a wide range of carbonyl substrates.[80, 129, 130] Accordingly, the Kvβ proteins bind pyridine nucleotides with high affinity, with K_d values in the low micromolar range.[76, 81]

The redox status of the bound pyridine nucleotide confers profound electro-physiological effects on the Kvα-Kvβ channel complex (Figure 1.5). Studies in heterologous expression systems have demonstrated that oxidized nucleotides, NAD[P]$^+$, prevent Kvβ1.3-mediated inactivation of Kv1.5.[77] These studies have been expanded to include other Kvα-Kvβ arrangments,[78-80] further elucidating how Kvβ-mediated modulation of Kv1 gating is dependent on the reduction state of the bound pyridine nucleotide. The Kvβ2 protein product is shorter than Kvβ1 and Kvβ3, lacking the N-terminal domain responsible for rapidly inactivating Kv1 channels. NAD(P)$^+$ has been shown to prevent the Kvβ2-mediated

hyperpolarizing shift in Kv1.5 activation voltage[79] and acceleration of Kv1.4 inactivation rate.[80]

We therefore designed experiments to test our hypothesis that the cytosolic redox ratio of pyridine nucleotide affects cardiomyocyte excitability through the modulation of outward Kv currents. We tested this using whole-cell voltage clamp, perforated-patch current clamp, excised-patch single channel patch clamp electrophysiology and Langendorff monophasic action potential recordings.

Results

Cardiac Kv current are differentially altered by pyridine nucleotide redox ratios

In heterologous systems, the coexpression of Kv1 and Kvβ subunits generate Kv currents whose inactivation rates are modulated by pyridine nucleotides.[54, 77, 80] To explore whether native cardiac Kv currents are sensitive to such changes, ventricular cardiac myocytes were patched in whole-cell configuration using pipette solutions chosen to represent normoxic and hypoxic cytosolic conditions (Figure 4.1).   Upon reaching whole-cell configuration, series resistance was compensated > 80% and pipette solution was allowed 5 min to dialyze with the cytoplasm before running voltage clamp protocols.   Outward currents were elicited with a +50 mV, 5 sec depolarization and fit triexponentially offline. We found that the inactivation rate of Kv currents was significantly accelerated under hypoxic compared to normoxic pipette conditions. The time constants associated with the intermediately and slowly inactivating Kv currents,

76

$I_{K,slow1}$ and $I_{K,slow2}$ were reduced in cardiac myocytes patched with hypoxic internal solution than normoxic internal solution (Figure 4.1). A comparison of all calculated values is found in Table 2. Most notably, the intermediate tau value, attributable to the cardiac current $I_{k, slow1}$, was reduced from 189 +/- 6 ms to 145 +/- 11 ms in myocytes patched with pipette solution containing high NADH (Figure 4.1). It has been previously proposed that the $I_{k,slow1}$ current is encoded by Kv1.5, which above we demonstrate to associate with Kvβ2.

Langendorff perfusion with lactate increases cellular NADH concentration and slows cardiac repolarization

We utilized a model developed by Dudley et al[131] to manipulate cytosolic NADH/NAD$^+$ ratios. In these experiments, sodium lactate and sodium pyruvate were added to the perfusion buffer to drive the lactate dehydrogenase reaction in the desired direction (Scheme 4.1). In a preliminary experiment, hearts from both WT and Kvβ2$^{-/-}$ were perfused with Tyrode's buffer containing 20 mM lactate for 20 minutes and then frozen for measurement of cellular NADH content. It was found that in both genotypes lactate perfusion significantly increased NADH levels (Figure 4.2).

In electrophysiological experiments, Langendorff hearts were allowed to beat spontaneously during perfusion and monophasic action potentials were recorded from the left ventricular epicardial surface. It was found that action potential durations were prolonged following 20 minutes of perfusion with lactate 20 mM as compared to each heart's control values. Action potential duration was

increased significantly at 20%, 50%, and 90% repolarization in WT hearts, $p < 0.05$, (Figure 4.3 A,B). Action potential durations were not different from control values in Kvβ2$^{-/-}$ hearts (Figure 4.3 C, D). In a separate series of experiments, surface action potentials were recorded from WT hearts perfused with 20 mM lactate for 20 min followed by 20 mM pyruvate for 20 min. In these experiments, pyruvate perfusion caused APD90 to shorten toward their control values, presumably by restoring intracellular NAD$^+$ levels (Figure 4.4).

Action potentials recorded in perforated patch mode are prolonged by lactate perfusion

We used current clamp to measure single cell action potentials in WT cardiac myocytes perfused with 10 mM lactate in Tyrode's perfusion buffer. The perforated patch configuration using Amphotericin B (250 µg/ml) was utilized because the pores formed by this perforating agent are sufficiently small to prevent the passage of any molecule larger than monovalent ions. This allowed lactate to drive an intracellular increase in NADH without it dialyzing out of the cell into the pipette as it would in the whole-cell configuration. Action potentials were elicited via small current injections of 0.8-1.0 nA lasting 2 ms at a frequency of 1 Hz. Action potential durations following approximately 8 minutes of lactate superfusion were normalized to control values in the same cell. We found that APD50 was significantly increased during this treatment while APD20 and APD90 trended toward prolongation as well (Figure 4.5 B). Action potential amplitude, resting

membrane potential and upstroke velocity, dV/dt were not affected by the treatment with lactate (Figure 4.5 C).

Single channel Kv activity was altered by perfusion with 1 mM NADH

To directly test the effect of NADH on Kv channel activity, single channel activity was measured in inside-out patches pulled from freshly isolated cardiac myocytes. Upon successfully obtaining an inside-out configuration, the membrane patch was perfused for at least 4 minutes with a minimal buffer containing 140 mM KCl, 10 mM HEPES and 1 mM HEDTA. Pipette internal solution was symmetrical. The minimal composition of the buffer eliminated contamination with other cationic currents.   Chloride channel activity was ruled out based on single channel conductance values.   Patches were subjected to 4.5 s, +30 mV pulses at a frequency of 0.05 Hz. Single channel activity was quantified as the percentage of time the patch stayed in the open and closed states during each sweep. In one representative experiment, the probability of the channel in the closed state increased 10-fold upon addition of 1 mM NADH to the perfusate (Figure 4.6 A, B). A marked increase in channel closure was seen almost immediately upon perfusion of NADH (Figure 4.6 C).

Discussion

We have demonstrated by multiple electrophysiological modalities that cardiac Kv conductance can be modulated by altering the pyridine nucleotide redox status in the cardiac myocyte. There are multiple reports in the literature, by

our group and others, who have clearly demonstrated a direct effect of pyridine nucleotides on Kv channel activity in heterologous expression systems (vide supra). To the best of our knowledge, the experiments herein described constitute the first demonstration of endogenous Kv channel modulation by pyridine nucleotides in a primary cell (cardiac myocyte) and tissue (the perfused heart).

In the classical biochemistry perspective, the pyridine nucleotides act as electron carriers, supporting oxidation-reduction reactions involved in a variety of anabolic and catabolic cellular processes. In addition to their role in support of metabolic oxidoreductase reactions, new roles for these cofactors have emerged with recent research. The pyridine nucleotides are now known to play roles in regulation of cell signaling, gene transcriptional regulation, free radical production, the thioredoxin and glutathione pathways and as ligands for ion channels.[126, 128, 132, 133] In the case of ion channel modulation, pyridine nucleotide sensitivity, particularly differential sensitivity for the oxidized (NAD[P]$^+$) versus reduced (NAD[P]H) states, has been proposed as a mechanism to link the metabolic status of a cell to its excitability. When subjected to hypoxic or anoxic conditions, aerobic metabolic capacity is diminished, resulting in an accumulation of the reduced pyridine nucleotide NADH generated from glycolysis and the tricarboxylic acid cycle. Without available oxygen, this NADH can not be oxidized back to NAD$^+$ through the electron transport chain enzymes. This shift in pyridine nucleotide redox putatively may serve as a metabolic queue to alter the conductances of various ion channels, integrating metabolic activity with cellular excitability. Multiple channels or channel subunits contain nucleotide binding domains which

80

bind pyridine nucleotides with high affinity, including the calcium-activated K^+ channels Slo1 and Slo2, K_{ATP}, the voltage-gated sodium channel $Na_v1.5$, the cystic fibrosis transport regulator CFTR, the lysosomal two-pore channel TPC2, the transient receptor potential channel TRPM2, the ryanodine receptor RYR, and the voltage-gated K^+ channel subunit Kvβ proteins. [128] These channels regulate many distinct cellular processes involved in cellular metabolism and homeostasis, and as such, their regulation by pyridine nucleotides may be a fundamental role of these molecules outside of their electron carrying ability.

Whereas these nucleotides act as ligands to several structurally distinct ion channels by poorly understood mechanisms (see APPENDIX), the understanding of their molecular interaction with the Kvβ proteins is comparatively well delineated. In an elegant set of experiments by Pan et al., [82] serial mutagenesis of residues in the core domain and N-terminus of Kvβ1 was employed to determine the molecular mechanism by which N-type inactivation is modulated by the redox state of the pyridine nucleotide bound to Kvβ1. Mutants were coexpressed with the delayed rectifier Kv1.1 in *Xenopus* oocytes and giant inside-out patches were pulled; patches were depolarized to +60 mV from a -100 mV holding potential and % inactivation (i.e. peak current – steady state current at 200 ms). Patches were perfused with 4-cyanobenzaldehyde, previously described to be a reducible substrate of the Kvβ proteins.[78] Kvβ catalysis of 4-CY into 4-cyanobenzoic acid requires the oxidation of the Kvβ-bound cofactor and thus this was utilized as a model for assaying the residues involved pyridine nucleotide-dependent modulation of N-type inactivation. These experiments provided the information

81

implicating specific residues in the Kvβ1 core and N-terminal domains responsible for restraining the inactivation domain when a reduced nucleotide is present in the nucleotide binding domain. Furthermore, these experiements mechanistically linked the enzymatic turnover of substrate with rapid inactivation kinetics, elucidating the processes by which both altered availability and redox status of cytosolic nucleotides or the presence of an unknown carbonyl substrate may be utilized to alter Kv channel conductances and thus cellular excitability. Thus, this raises the interesting question of whether the primary mode of Kvβ-dependent Kv channel modulation occurs through shifting cytosolic $NAD(P)H/NAD(P)^+$ ratio or through some unknown substrate to which Kvβ has a high turnover rate, or both. Further experiments are being performed by our group as well as others to uncover the physiological significance of these regulatory axes.

In this project, cardiac myocyte Kv conductances were altered by intracellular dialysis of pipette mixtures containing either high NADH or NAD^+ concentrations. Furthermore, modulation of intracellular pyridine nucleotide redox status by lactate perfusion altered both cardiac myocyte and whole heart repolarization rates. These are compelling evidences that pyridine nucleotides have the ability to modulate cardiac repolarization, but further evidence is required to demonstrate that they are endogenous regulators of ion transport or that physiological or pathological changes in pyridine nucleotide levels have any effect on ion transport. A more thorough understanding of these relationships may require development of new modalities which are capable of simultaneously measuring free nucleotide levels and ion channel conductances either in cells or

tissue/organ preparations in order to delineate how these processes contribute to

in vivo.
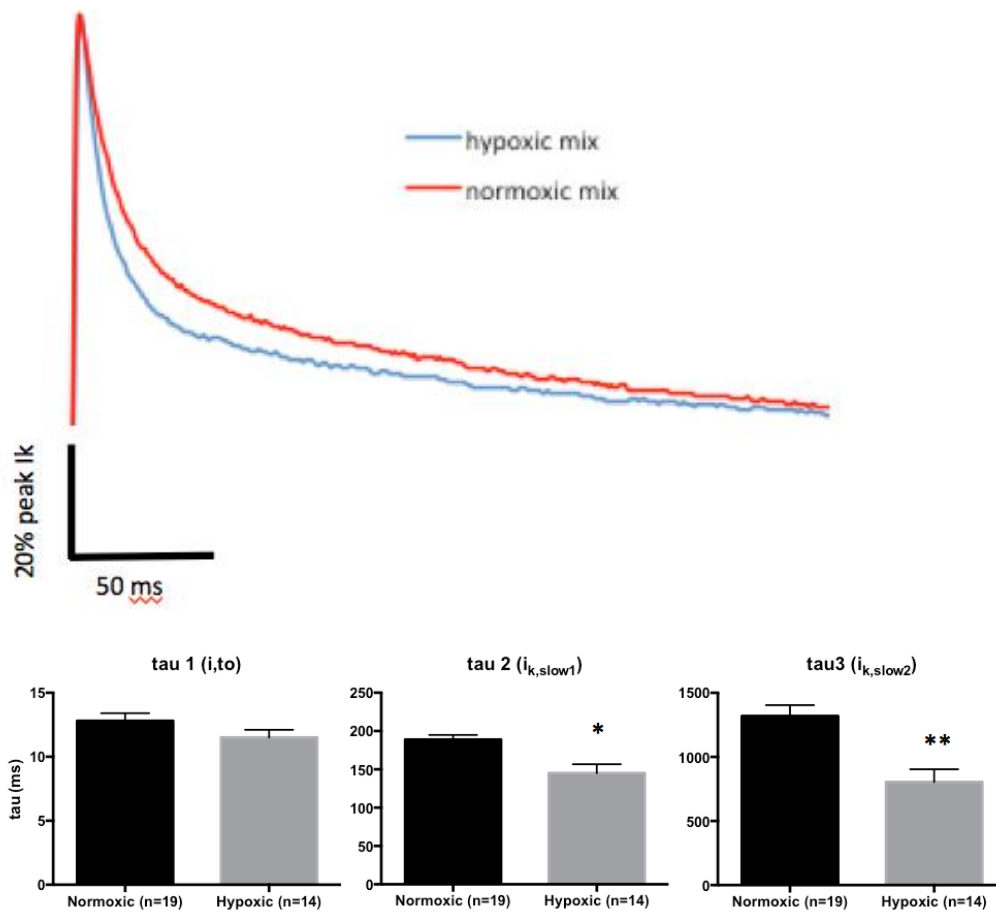
Pipette internal solutions:

	normoxic (uM)	hypoxic (uM)
NADPH	100	80
NADP+	30	50
NADH	50	1000
NAD+	1000	200

Figure 4.1: Cardiac Kv current inactivation.. Whole-cell outward Kv currents were elicited in response to a 5s, +50 mV depolarizing pulse from a holding potential of -80 mV and fit triexponentially. Current inactivation was accelerated under hypoxic pipette conditions. Representative amplitude-normalized Kv currents (A). Inactivation time constants for tau 2 (corresponding to $I_{k,slow1}$) and tau 3 (corresponding to $I_{k,slow2}$) were shorter under hypoxic pipette mix conditions. . Pipette internal solutions contained either normoxic (high NAD+) or hypoxic mixes (high NADH) of pyridine nucleotides. n= 19 cells (normoxic), 14 cells (hypoxic). (*: $p<0.01$, **: $p<0.001$.)

84
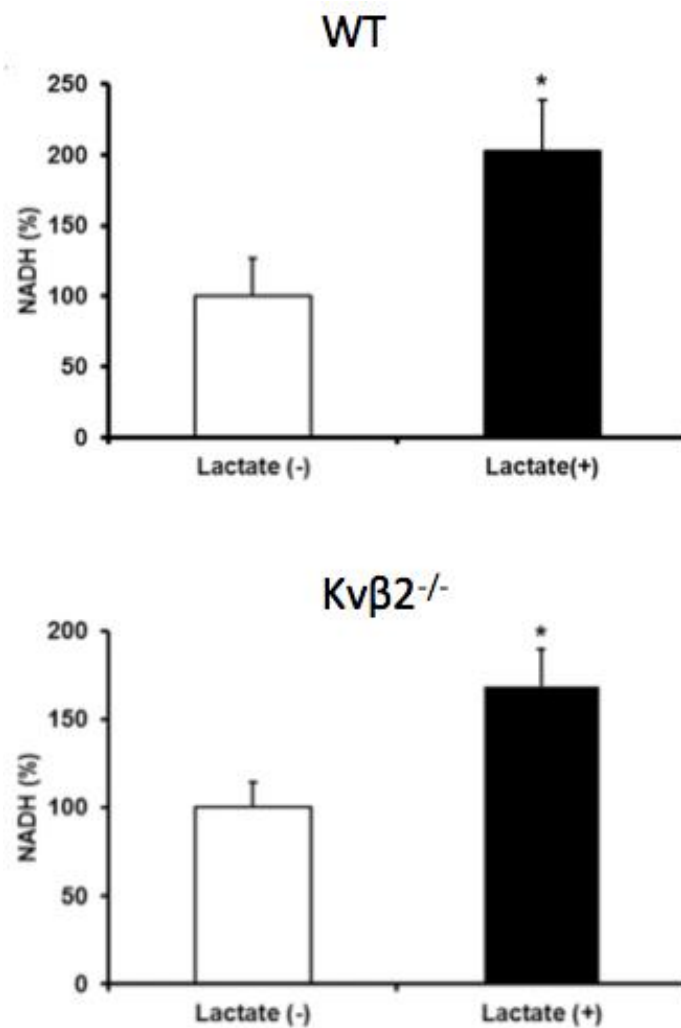
Figure 4.2: Perfusion of hearts in Langendorff mode with lactate.
Hearts were perfused *ex vivo* with lactate 20 mM (Lactate +) for 20 minutes and flash frozen for later measurement of pyridine nucleotides. Cellular NADH concentration increased significantly in both WT (top) and Kvβ2$^{-/-}$ compared to controls perfused with standard Tyrode's buffer (Lactate -). n= 3 hearts WT and 3 hearts Kvβ2$^{-/-}$ for each treatment. *: $p<0.05$. These experiments were performed in collaboration with Dr. Srinivas Tipparaju and Dr. Kalyan Chapalamadugu at the University of South Florida Department of Pharmaceutical Sciences.
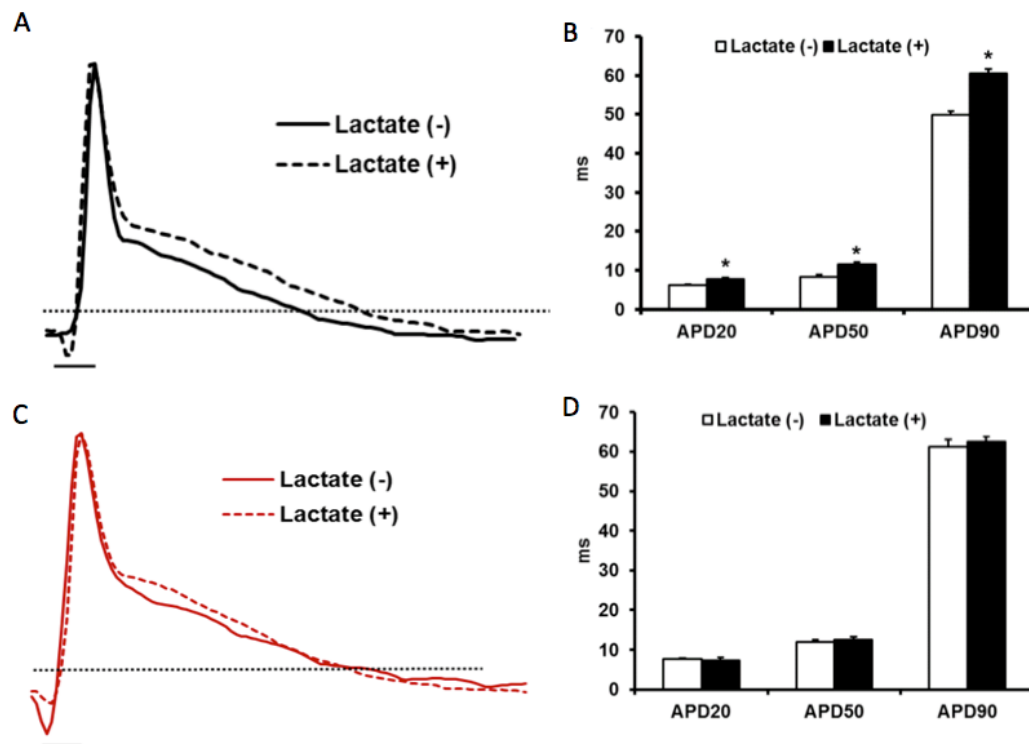
Figure 4.3: Lactate perfusion causes action potential prolongation in WT but not Kvβ2-/- hearts. Monophasic action potentials were recorded from Langendorff perfused hearts during control (Lactate -) and following lactate 20 mM perfusion for 15 minutes (Lactate +). A. WT hearts displayed prolonged action potential durations (APD). B. Action potential duration at 20, 50, and 90 % repolarization was increased. C. Kvβ2-/- repolarization was not sensitive to lactate. D. Action potential durations in Kvβ2-/- were not changed from control. n=5 hearts WT and 5 hearts Kvβ2-/- *:$p<0.05$. These experiments were performed in collaboration with Dr. Srinivas Tipparaju and Dr. Kalyan Chapalamadugu at the University of South Florida Department of Pharmaceutical Sciences.

86
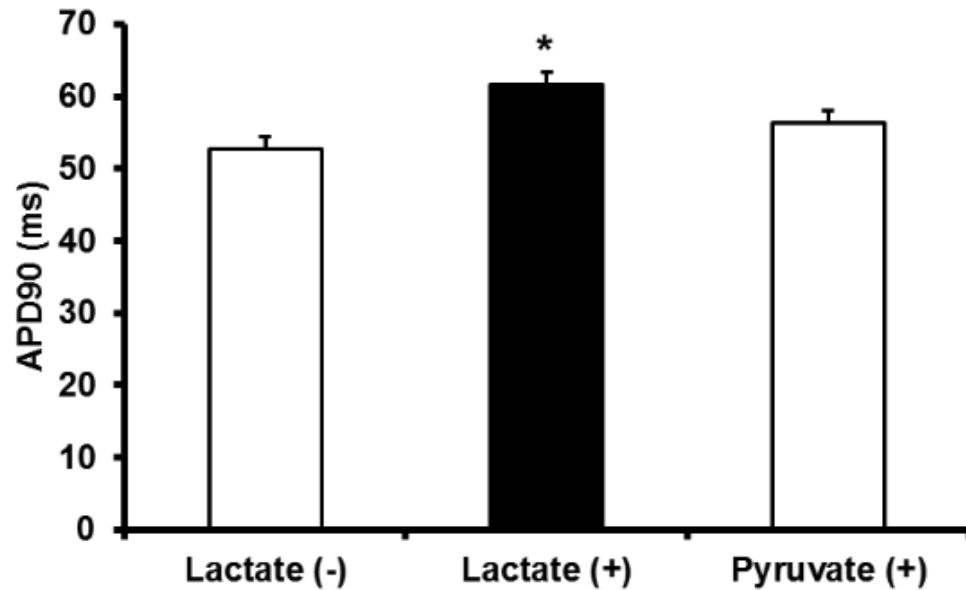
Figure 4.4: Action potential prolongation caused by lactate is rescued by perfusion with pyruvate. Monophasic action potentials were recorded on hearts as they were perfused with control Tyrode's (Lactate -) for 15 min, followed by 20 mM lactate (Lactate +) for 20 minutes followed by 20 mM pyruvate (Pyruvate +) for 20 minutes. Pyruvate perfusion shortened APD90 back to control values. n=5 hearts. *: p<0.05. These experiments were performed in collaboration with Dr. Srinivas Tipparaju and Dr. Kalyan Chapalamadugu at the University of South Florida Department of Pharmaceutical Sciences.
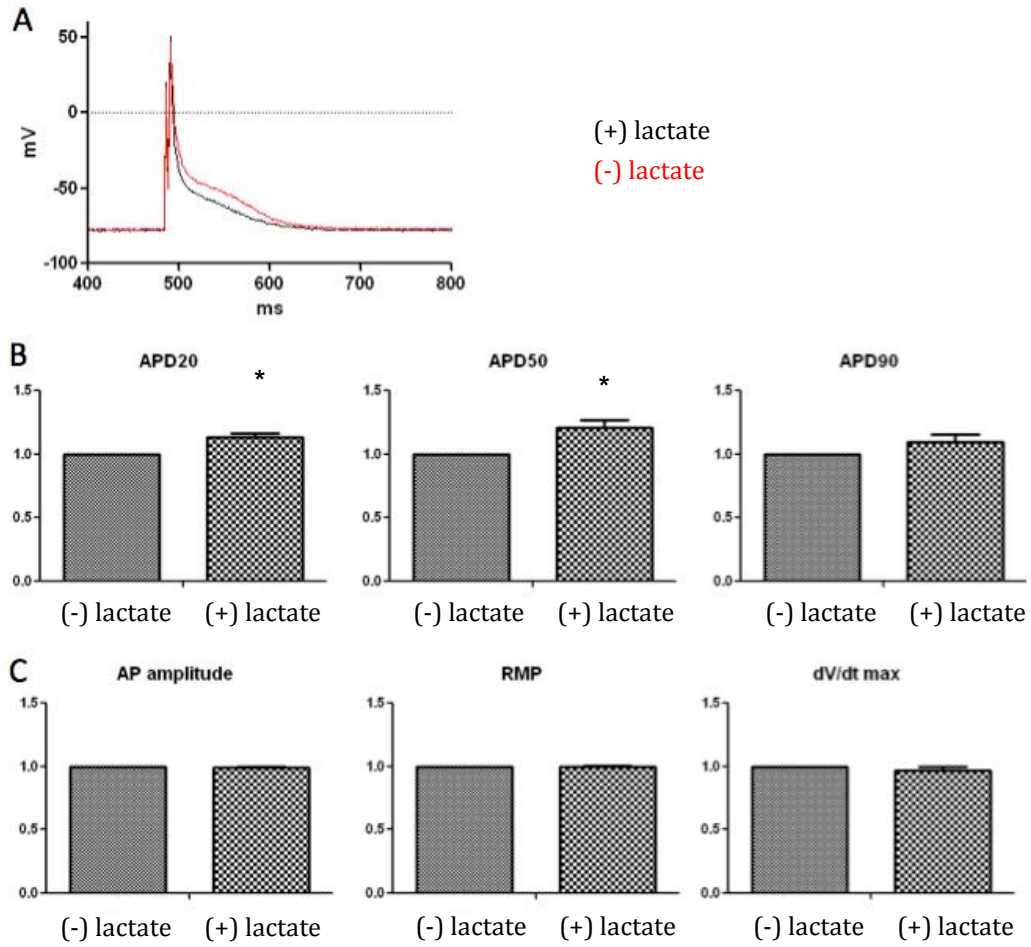
Figure 4.5: Cardiac myocyte action potentials are prolonged by lactate superfusion. Single cell action potentials were recorded in WT cardiac myocytes (n=6) in the perforated patch configuration to allow intracellular NADH accumulation during lactate perfusion. A. Representative traces recorded during control (black) and following 8 min 10 mM lactate superfusion. B. Action potential duration at 50% repolarization was significantly prolonged. C. Action potential amplitude, resting membrane potential and upstroke velocity was not different from control. n=6 cells. *: $p < 0.05$.
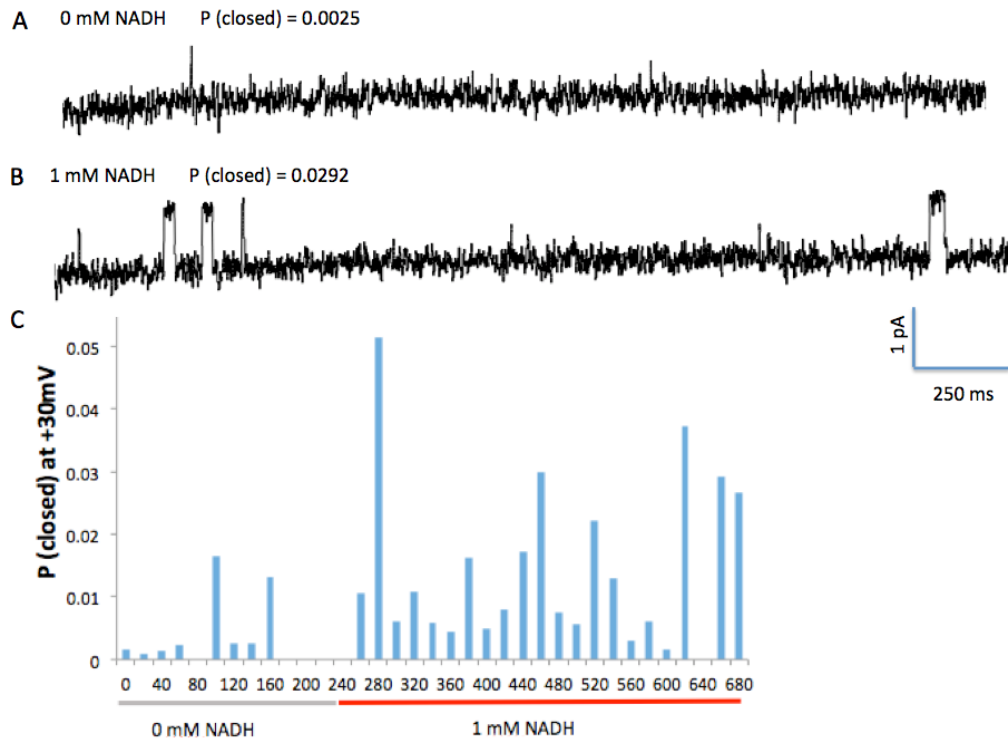
Figure 4.6: Single channel Kv activity in cardiac myocyte inside-out patches is increased by NADH. A. Single channel activity was recorded from excised patches pulled from cardiac myocytes perfused with control buffer. B. When 1 mM NADH was added to the perfusate, single channel event activity increased approximately 10-fold (percentage of time the channel spend in the closed state.) C. P(closed) was calculated for each 5 second sweep during 4 minutes of control and 6 minutes of 1 mM NADH perfusion.
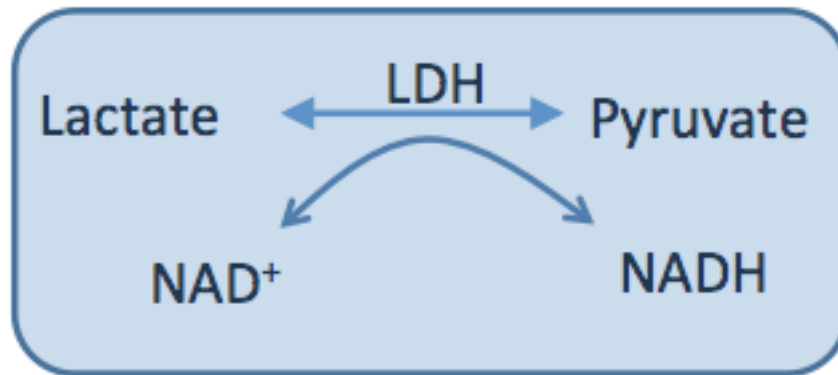
Scheme 4.1: Lactate dehydrogenase reaction. Langendorff-perfused hearts and cardiomyocytes in perforated patch configuration were perfused with 10 mM or 20 mM sodium lactate in order to drive the LDH reaction to produce elevated cytoplasmic NADH. Langendorff perfused hearts

Table 2: Effect of pyridine nucleotide redox ratio on Kv currents

Treatment	I_{to} (pA/pF)	τ (ms)	$I_{k, slow1}$ (pA/pF)	τ (ms)	$I_{k,slow2}$ (pA/pF)	τ (ms)	I_{ss}(pA/pF)
Normoxic (n=19)	43.3 ± 4.0	12.8 ± 0.6	22.3 ± 3.4	188.8 ± 6.1	12.3 ± 1.4	1319.3 ± 85.3	10.5 ± 0.8
Hypoxic (n=13)	39.6 ± 5.9	11.5 ± 0.6	20.8 ± 4.2	145.2 ± 11.6	16.3 ± 2.5	804.9 ± 99.1	13.2 ± 1.6
p<	ns	ns	ns	0.01	ns	0.001	ns

T=33-35°C

REFERENCES

1.   Mulkidjanian AY, Bychkov AY, Dibrova DV, Galperin MY, Koonin EV. Origin of first cells at terrestrial, anoxic geothermal fields. *Proceedings of the National Academy of Sciences of the United States of America*. 2012;109:E821-830

2.   Anbar AD. Oceans. Elements and evolution. *Science*. 2008;322:1481-1483

3.   Schmidt TA, Kjeldsen K. Human myocardial na,k-atpase--quantification, regulation and relation to ca. *Cardiovascular research*. 1998;37:335-345

4.   Silver IA, Erecinska M. Energetic demands of the na+/k+ atpase in mammalian astrocytes. *Glia*. 1997;21:35-45

5.   Clausen T, Van Hardeveld C, Everts ME. Significance of cation transport in control of energy metabolism and thermogenesis. *Physiological reviews*. 1991;71:733-774

6.   Bers DM. Cardiac excitation-contraction coupling. *Nature*. 2002;415:198-205

7.   Kerr PM, Clement-Chomienne O, Thorneloe KS, Chen TT, Ishii K, Sontag DP, Walsh MP, Cole WC. Heteromultimeric kv1.2-kv1.5 channels underlie 4-aminopyridine-sensitive delayed rectifier k(+) current of rabbit vascular myocytes. *Circulation research*. 2001;89:1038-1044

8.   Vicente R, Villalonga N, Calvo M, Escalada A, Solsona C, Soler C, Tamkun MM, Felipe A. Kv1.5 association modifies kv1.3 traffic and membrane localization. *The Journal of biological chemistry*. 2008;283:8756-8764

9.   Pongs O. Molecular biology of voltage-dependent potassium channels. *Physiological reviews*. 1992;72:S69-88

10.   Pongs O, Schwarz JR. Ancillary subunits associated with voltage-dependent k+ channels. *Physiological reviews.* 2010;90:755-796

11.   Browne DL, Gancher ST, Nutt JG, Brunt ER, Smith EA, Kramer P, Litt M. Episodic ataxia/myokymia syndrome is associated with point mutations in the human potassium channel gene, kcna1. *Nature genetics.* 1994;8:136-140

12.   Smart SL, Lopantsev V, Zhang CL, Robbins CA, Wang H, Chiu SY, Schwartzkroin PA, Messing A, Tempel BL. Deletion of the k(v)1.1 potassium channel causes epilepsy in mice. *Neuron.* 1998;20:809-819

13.   Van Wagoner DR, Pond AL, McCarthy PM, Trimmer JS, Nerbonne JM. Outward k+ current densities and kv1.5 expression are reduced in chronic human atrial fibrillation. *Circulation research.* 1997;80:772-781

14.   Olson TM, Alekseev AE, Liu XK, Park S, Zingman LV, Bienengraeber M, Sattiraju S, Ballew JD, Jahangir A, Terzic A. Kv1.5 channelopathy due to kcna5 loss-of-function mutation causes human atrial fibrillation. *Human molecular genetics.* 2006;15:2185-2191

15.   Christophersen IE, Olesen MS, Liang B, Andersen MN, Larsen AP, Nielsen JB, Haunso S, Olesen SP, Tveit A, Svendsen JH, Schmitt N. Genetic variation in kcna5: Impact on the atrial-specific potassium current ikur in patients with lone atrial fibrillation. *European heart journal.* 2013;34:1517-1525

16.   Fadool DA, Tucker K, Perkins R, Fasciani G, Thompson RN, Parsons AD, Overton JM, Koni PA, Flavell RA, Kaczmarek LK. Kv1.3 channel gene-targeted deletion produces "super-smeller mice" with altered glomeruli, interacting scaffolding proteins, and biophysics. *Neuron.* 2004;41:389-404

17.   Arnett DK, Li N, Tang W, Rao DC, Devereux RB, Claas SA, Kraemer R, Broeckel U. Genome-wide association study identifies single-nucleotide polymorphism in kcnb1 associated with left ventricular mass in humans: The hypergen study. *BMC medical genetics.* 2009;10:43

18.   Torkamani A, Bersell K, Jorge BS, Bjork RL, Jr., Friedman JR, Bloss CS, Cohen J, Gupta S, Naidu S, Vanoye CG, George AL, Jr., Kearney JA. De novo kcnb1 mutations in epileptic encephalopathy. *Annals of neurology.* 2014;76:529-540

19.   Waters MF, Minassian NA, Stevanin G, Figueroa KP, Bannister JP, Nolte D, Mock AF, Evidente VG, Fee DB, Muller U, Durr A, Brice A, Papazian DM, Pulst SM. Mutations in voltage-gated potassium channel kcnc3 cause degenerative and developmental central nervous system phenotypes. *Nature genetics*. 2006;38:447-451

20.   Sesti F, Abbott GW, Wei J, Murray KT, Saksena S, Schwartz PJ, Priori SG, Roden DM, George AL, Jr., Goldstein SA. A common polymorphism associated with antibiotic-induced cardiac arrhythmia. *Proceedings of the National Academy of Sciences of the United States of America*. 2000;97:10613-10618

21.   Singh B, Ogiwara I, Kaneda M, Tokonami N, Mazaki E, Baba K, Matsuda K, Inoue Y, Yamakawa K. A kv4.2 truncation mutation in a patient with temporal lobe epilepsy. *Neurobiology of disease*. 2006;24:245-253

22.   Long SB, Campbell EB, Mackinnon R. Crystal structure of a mammalian voltage-dependent shaker family k+ channel. *Science*. 2005;309:897-903

23.   Doyle DA, Morais Cabral J, Pfuetzner RA, Kuo A, Gulbis JM, Cohen SL, Chait BT, MacKinnon R. The structure of the potassium channel: Molecular basis of k+ conduction and selectivity. *Science*. 1998;280:69-77

24.   Jiang Y, Ruta V, Chen J, Lee A, MacKinnon R. The principle of gating charge movement in a voltage-dependent k+ channel. *Nature*. 2003;423:42-48

25.   Long SB, Campbell EB, Mackinnon R. Voltage sensor of kv1.2: Structural basis of electromechanical coupling. *Science*. 2005;309:903-908

26.   Liu Y, Jurman ME, Yellen G. Dynamic rearrangement of the outer mouth of a k+ channel during gating. *Neuron*. 1996;16:859-867

27.   Rasmusson RL, Morales MJ, Wang S, Liu S, Campbell DL, Brahmajothi MV, Strauss HC. Inactivation of voltage-gated cardiac k+ channels. *Circulation research*. 1998;82:739-750

28.   Kukuljan M, Labarca P, Latorre R. Molecular determinants of ion conduction and inactivation in k+ channels. *The American journal of physiology*. 1995;268:C535-556

29.   Demo SD, Yellen G. The inactivation gate of the shaker k+ channel behaves like an open-channel blocker. *Neuron*. 1991;7:743-753

30.   Labro AJ, Priest MF, Lacroix JJ, Snyders DJ, Bezanilla F. Kv3.1 uses a timely resurgent k(+) current to secure action potential repolarization. *Nature communications*. 2015;6:10173

31.   Litovsky SH, Antzelevitch C. Rate dependence of action potential duration and refractoriness in canine ventricular endocardium differs from that of epicardium: Role of the transient outward current. *Journal of the American College of Cardiology*. 1989;14:1053-1066

32.   Roeper J, Lorra C, Pongs O. Frequency-dependent inactivation of mammalian a-type k+ channel kv1.4 regulated by ca2+/calmodulin-dependent protein kinase. *The Journal of neuroscience : the official journal of the Society for Neuroscience*. 1997;17:3379-3391

33.   Bahring R, Boland LM, Varghese A, Gebauer M, Pongs O. Kinetic analysis of open- and closed-state inactivation transitions in human kv4.2 a-type potassium channels. *The Journal of physiology*. 2001;535:65-81

34.   Rosati B, Pan Z, Lypen S, Wang HS, Cohen I, Dixon JE, McKinnon D. Regulation of kchip2 potassium channel beta subunit gene expression underlies the gradient of transient outward current in canine and human ventricle. *The Journal of physiology*. 2001;533:119-125

35.   Teutsch C, Kondo RP, Dederko DA, Chrast J, Chien KR, Giles WR. Spatial distributions of kv4 channels and kchip2 isoforms in the murine heart based on laser capture microdissection. *Cardiovascular research*. 2007;73:739-749

36.   Nerbonne JM, Kass RS. Molecular physiology of cardiac repolarization. *Physiological reviews*. 2005;85:1205-1253

37.   Sheng M, Tsaur ML, Jan YN, Jan LY. Subcellular segregation of two a-type k+ channel proteins in rat central neurons. *Neuron*. 1992;9:271-284

38.   Birnbaum SG, Varga AW, Yuan LL, Anderson AE, Sweatt JD, Schrader LA. Structure and function of kv4-family transient potassium channels. *Physiological reviews*. 2004;84:803-833

39.   Nakamura TY, Nandi S, Pountney DJ, Artman M, Rudy B, Coetzee WA. Different effects of the ca(2+)-binding protein, kchip1, on two kv4 subfamily members, kv4.1 and kv4.2. *FEBS letters.* 2001;499:205-209

40.   An WF, Bowlby MR, Betty M, Cao J, Ling HP, Mendoza G, Hinson JW, Mattsson KI, Strassle BW, Trimmer JS, Rhodes KJ. Modulation of a-type potassium channels by a family of calcium sensors. *Nature.* 2000;403:553-556

41.   Nadal MS, Ozaita A, Amarillo Y, Vega-Saenz de Miera E, Ma Y, Mo W, Goldberg EM, Misumi Y, Ikehara Y, Neubert TA, Rudy B. The cd26-related dipeptidyl aminopeptidase-like protein dppx is a critical component of neuronal a-type k+ channels. *Neuron.* 2003;37:449-461

42.   Radicke S, Cotella D, Graf EM, Ravens U, Wettwer E. Expression and function of dipeptidyl-aminopeptidase-like protein 6 as a putative beta-subunit of human cardiac transient outward current encoded by kv4.3. *The Journal of physiology.* 2005;565:751-756

43.   Pusch M. Increase of the single-channel conductance of kvlqt1 potassium channels induced by the association with mink. *Pflugers Archiv : European journal of physiology.* 1998;437:172-174

44.   McCrossan ZA, Abbott GW. The mink-related peptides. *Neuropharmacology.* 2004;47:787-821

45.   Barhanin J, Lesage F, Guillemare E, Fink M, Lazdunski M, Romey G. K(v)lqt1 and lsk (mink) proteins associate to form the i(ks) cardiac potassium current. *Nature.* 1996;384:78-80

46.   Sanguinetti MC, Curran ME, Zou A, Shen J, Spector PS, Atkinson DL, Keating MT. Coassembly of k(v)lqt1 and mink (isk) proteins to form cardiac i(ks) potassium channel. *Nature.* 1996;384:80-83

47.   Hedley PL, Jorgensen P, Schlamowitz S, Wangari R, Moolman-Smook J, Brink PA, Kanters JK, Corfield VA, Christiansen M. The genetic basis of long qt and short qt syndromes: A mutation update. *Human mutation.* 2009;30:1486-1511

48.   Milnes JT, Crociani O, Arcangeli A, Hancox JC, Witchel HJ. Blockade of herg potassium currents by fluvoxamine: Incomplete attenuation by s6 mutations at f656 or y652. *British journal of pharmacology.* 2003;139:887-898

49.   Rehm H, Lazdunski M. Purification and subunit structure of a putative k+-channel protein identified by its binding properties for dendrotoxin i. *Proceedings of the National Academy of Sciences of the United States of America*. 1988;85:4919-4923

50.   Baumann A, Krah-Jentgens I, Muller R, Muller-Holtkamp F, Seidel R, Kecskemethy N, Casal J, Ferrus A, Pongs O. Molecular organization of the maternal effect region of the shaker complex of drosophila: Characterization of an i(a) channel transcript with homology to vertebrate na channel. *The EMBO journal*. 1987;6:3419-3429

51.   Isom LL, De Jongh KS, Patton DE, Reber BF, Offord J, Charbonneau H, Walsh K, Goldin AL, Catterall WA. Primary structure and functional expression of the beta 1 subunit of the rat brain sodium channel. *Science*. 1992;256:839-842

52.   Catterall WA. Functional subunit structure of voltage-gated calcium channels. *Science*. 1991;253:1499-1500

53.   Jan LY, Jan YN. How might the diversity of potassium channels be generated? *Trends in neurosciences*. 1990;13:415-419

54.   Rettig J, Heinemann SH, Wunder F, Lorra C, Parcej DN, Dolly JO, Pongs O. Inactivation properties of voltage-gated k+ channels altered by presence of beta-subunit. *Nature*. 1994;369:289-294

55.   Heinemann SH, Rettig J, Graack HR, Pongs O. Functional characterization of kv channel beta-subunits from rat brain. *The Journal of physiology*. 1996;493 (Pt 3):625-633

56.   Leicher T, Bahring R, Isbrandt D, Pongs O. Coexpression of the kcna3b gene product with kv1.5 leads to a novel a-type potassium channel. *The Journal of biological chemistry*. 1998;273:35095-35101

57.   Nakahira K, Shi G, Rhodes KJ, Trimmer JS. Selective interaction of voltage-gated k+ channel beta-subunits with alpha-subunits. *The Journal of biological chemistry*. 1996;271:7084-7089

58.   Parcej DN, Dolly JO. Dendrotoxin acceptor from bovine synaptic plasma membranes. Binding properties, purification and subunit composition of a putative

constituent of certain voltage-activated k+ channels. *The Biochemical journal.* 1989;257:899-903

59.   Xu J, Yu W, Jan YN, Jan LY, Li M. Assembly of voltage-gated potassium channels. Conserved hydrophilic motifs determine subfamily-specific interactions between the alpha-subunits. *The Journal of biological chemistry.* 1995;270:24761-24768

60.   Sewing S, Roeper J, Pongs O. Kv beta 1 subunit binding specific for shaker-related potassium channel alpha subunits. *Neuron.* 1996;16:455-463

61.   Yu W, Xu J, Li M. Nab domain is essential for the subunit assembly of both alpha-alpha and alpha-beta complexes of shaker-like potassium channels. *Neuron.* 1996;16:441-453

62.   Drewe JA, Verma S, Frech G, Joho RH. Distinct spatial and temporal expression patterns of k+ channel mrnas from different subfamilies. *The Journal of neuroscience : the official journal of the Society for Neuroscience.* 1992;12:538-548

63.   Yang EK, Alvira MR, Levitan ES, Takimoto K. Kvbeta subunits increase expression of kv4.3 channels by interacting with their c termini. *The Journal of biological chemistry.* 2001;276:4839-4844

64.   Scott VE, Rettig J, Parcej DN, Keen JN, Findlay JB, Pongs O, Dolly JO. Primary structure of a beta subunit of alpha-dendrotoxin-sensitive k+ channels from bovine brain. *Proceedings of the National Academy of Sciences of the United States of America.* 1994;91:1637-1641

65.   Kwak YG, Hu N, Wei J, George AL, Jr., Grobaski TD, Tamkun MM, Murray KT. Protein kinase a phosphorylation alters kvbeta1.3 subunit-mediated inactivation of the kv1.5 potassium channel. *The Journal of biological chemistry.* 1999;274:13928-13932

66.   Williams CP, Hu N, Shen W, Mashburn AB, Murray KT. Modulation of the human kv1.5 channel by protein kinase c activation: Role of the kvbeta1.2 subunit. *The Journal of pharmacology and experimental therapeutics.* 2002;302:545-550

67.   Vacher H, Trimmer JS. Diverse roles for auxiliary subunits in phosphorylation-dependent regulation of mammalian brain voltage-gated

potassium channels. *Pflugers Archiv : European journal of physiology*. 2011;462:631-643

68.   Shi G, Nakahira K, Hammond S, Rhodes KJ, Schechter LE, Trimmer JS. Beta subunits promote k+ channel surface expression through effects early in biosynthesis. *Neuron*. 1996;16:843-852

69.   Nagaya N, Papazian DM. Potassium channel alpha and beta subunits assemble in the endoplasmic reticulum. *The Journal of biological chemistry*. 1997;272:3022-3027

70.   Yang JW, Vacher H, Park KS, Clark E, Trimmer JS. Trafficking-dependent phosphorylation of kv1.2 regulates voltage-gated potassium channel cell surface expression. *Proceedings of the National Academy of Sciences of the United States of America*. 2007;104:20055-20060

71.   Vacher H, Yang JW, Cerda O, Autillo-Touati A, Dargent B, Trimmer JS. Cdk-mediated phosphorylation of the kvbeta2 auxiliary subunit regulates kv1 channel axonal targeting. *The Journal of cell biology*. 2011;192:813-824

72.   Gong J, Xu J, Bezanilla M, van Huizen R, Derin R, Li M. Differential stimulation of pkc phosphorylation of potassium channels by zip1 and zip2. *Science*. 1999;285:1565-1569

73.   Moral-Sanz J, Gonzalez T, Menendez C, David M, Moreno L, Macias A, Cortijo J, Valenzuela C, Perez-Vizcaino F, Cogolludo A. Ceramide inhibits kv currents and contributes to tp-receptor-induced vasoconstriction in rat and human pulmonary arteries. *American journal of physiology. Cell physiology*. 2011;301:C186-194

74.   McCormack T, McCormack K. Shaker k+ channel beta subunits belong to an nad(p)h-dependent oxidoreductase superfamily. *Cell*. 1994;79:1133-1135

75.   Gulbis JM, Mann S, MacKinnon R. Structure of a voltage-dependent k+ channel beta subunit. *Cell*. 1999;97:943-952

76.   Liu SQ, Jin H, Zacarias A, Srivastava S, Bhatnagar A. Binding of pyridine nucleotide coenzymes to the beta-subunit of the voltage-sensitive k+ channel. *The Journal of biological chemistry*. 2001;276:11812-11820

77.   Tipparaju SM, Saxena N, Liu SQ, Kumar R, Bhatnagar A. Differential regulation of voltage-gated k+ channels by oxidized and reduced pyridine nucleotide coenzymes. *American journal of physiology. Cell physiology*. 2005;288:C366-376

.78.   Pan Y, Weng J, Cao Y, Bhosle RC, Zhou M. Functional coupling between the kv1.1 channel and aldoketoreductase kvbeta1. *The Journal of biological chemistry*. 2008;283:8634-8642

79.   Tipparaju SM, Li XP, Kilfoil PJ, Xue B, Uversky VN, Bhatnagar A, Barski OA. Interactions between the c-terminus of kv1.5 and kvbeta regulate pyridine nucleotide-dependent changes in channel gating. *Pflugers Archiv : European journal of physiology*. 2012;463:799-818

80.   Weng J, Cao Y, Moss N, Zhou M. Modulation of voltage-dependent shaker family potassium channels by an aldo-keto reductase. *The Journal of biological chemistry*. 2006;281:15194-15200

81.   Tipparaju SM, Liu SQ, Barski OA, Bhatnagar A. Nadph binding to beta-subunit regulates inactivation of voltage-gated k(+) channels. *Biochemical and biophysical research communications*. 2007;359:269-276

82.   Pan Y, Weng J, Levin EJ, Zhou M. Oxidation of nadph on kvbeta1 inhibits ball-and-chain type inactivation by restraining the chain. *Proceedings of the National Academy of Sciences of the United States of America*. 2011;108:5885-5890

83.   Xu H, Guo W, Nerbonne JM. Four kinetically distinct depolarization-activated k+ currents in adult mouse ventricular myocytes. *The Journal of general physiology*. 1999;113:661-678

84.   Zhou J, Kodirov S, Murata M, Buckett PD, Nerbonne JM, Koren G. Regional upregulation of kv2.1-encoded current, ik,slow2, in kv1dn mice is abolished by crossbreeding with kv2dn mice. *American journal of physiology. Heart and circulatory physiology*. 2003;284:H491-500

85.   Tseng-Crank JC, Tseng GN, Schwartz A, Tanouye MA. Molecular cloning and functional expression of a potassium channel cdna isolated from a rat cardiac library. *FEBS letters*. 1990;268:63-68

86.   Roberds SL, Tamkun MM. Cloning and tissue-specific expression of five voltage-gated potassium channel cdnas expressed in rat heart. *Proceedings of the National Academy of Sciences of the United States of America*. 1991;88:1798-1802

87.   Baldwin TJ, Tsaur ML, Lopez GA, Jan YN, Jan LY. Characterization of a mammalian cdna for an inactivating voltage-sensitive k+ channel. *Neuron*. 1991;7:471-483

88.   Blair TA, Roberds SL, Tamkun MM, Hartshorne RP. Functional characterization of rk5, a voltage-gated k+ channel cloned from the rat cardiovascular system. *FEBS letters*. 1991;295:211-213

89.   Wickenden AD, Jegla TJ, Kaprielian R, Backx PH. Regional contributions of kv1.4, kv4.2, and kv4.3 to transient outward k+ current in rat ventricle. *The American journal of physiology*. 1999;276:H1599-1607

90.   Costantini DL, Arruda EP, Agarwal P, Kim KH, Zhu Y, Zhu W, Lebel M, Cheng CW, Park CY, Pierce SA, Guerchicoff A, Pollevick GD, Chan TY, Kabir MG, Cheng SH, Husain M, Antzelevitch C, Srivastava D, Gross GJ, Hui CC, Backx PH, Bruneau BG. The homeodomain transcription factor irx5 establishes the mouse cardiac ventricular repolarization gradient. *Cell*. 2005;123:347-358

91.   Guo W, Xu H, London B, Nerbonne JM. Molecular basis of transient outward k+ current diversity in mouse ventricular myocytes. *The Journal of physiology*. 1999;521 Pt 3:587-599

92.   Johns DC, Nuss HB, Marban E. Suppression of neuronal and cardiac transient outward currents by viral gene transfer of dominant-negative kv4.2 constructs. *The Journal of biological chemistry*. 1997;272:31598-31603

93.   Dixon JE, Shi W, Wang HS, McDonald C, Yu H, Wymore RS, Cohen IS, McKinnon D. Role of the kv4.3 k+ channel in ventricular muscle. A molecular correlate for the transient outward current. *Circulation research*. 1996;79:659-668

94.   Nerbonne JM. Molecular basis of functional voltage-gated k+ channel diversity in the mammalian myocardium. *The Journal of physiology*. 2000;525 Pt 2:285-298

95.   Bertaso F, Sharpe CC, Hendry BM, James AF. Expression of voltage-gated k+ channels in human atrium. *Basic research in cardiology*. 2002;97:424-433

96.   Tomaselli GF, Marban E. Electrophysiological remodeling in hypertrophy and heart failure. *Cardiovascular research*. 1999;42:270-283

97.   Kaab S, Dixon J, Duc J, Ashen D, Nabauer M, Beuckelmann DJ, Steinbeck G, McKinnon D, Tomaselli GF. Molecular basis of transient outward potassium current downregulation in human heart failure: A decrease in kv4.3 mrna correlates with a reduction in current density. *Circulation*. 1998;98:1383-1393

98.   Nishiyama A, Ishii DN, Backx PH, Pulford BE, Birks BR, Tamkun MM. Altered k(+) channel gene expression in diabetic rat ventricle: Isoform switching between kv4.2 and kv1.4. *American journal of physiology. Heart and circulatory physiology*. 2001;281:H1800-1807

99.   Lengyel C, Virag L, Biro T, Jost N, Magyar J, Biliczki P, Kocsis E, Skoumal R, Nanasi PP, Toth M, Kecskemeti V, Papp JG, Varro A. Diabetes mellitus attenuates the repolarization reserve in mammalian heart. *Cardiovascular research*. 2007;73:512-520

100.   Gallego M, Alday A, Urrutia J, Casis O. Transient outward potassium channel regulation in healthy and diabetic hearts. *Canadian journal of physiology and pharmacology*. 2009;87:77-83

101.   Pandit SV, Giles WR, Demir SS. A mathematical model of the electrophysiological alterations in rat ventricular myocytes in type-i diabetes. *Biophysical journal*. 2003;84:832-841

102.   London B, Guo W, Pan X, Lee JS, Shusterman V, Rocco CJ, Logothetis DA, Nerbonne JM, Hill JA. Targeted replacement of kv1.5 in the mouse leads to loss of the 4-aminopyridine-sensitive component of i(k,slow) and resistance to drug-induced qt prolongation. *Circulation research*. 2001;88:940-946

103.   Xu H, Barry DM, Li H, Brunet S, Guo W, Nerbonne JM. Attenuation of the slow component of delayed rectification, action potential prolongation, and triggered activity in mice expressing a dominant-negative kv2 alpha subunit. *Circulation research*. 1999;85:623-633

104.   Fiset C, Clark RB, Larsen TS, Giles WR. A rapidly activating sustained k+ current modulates repolarization and excitation-contraction coupling in adult mouse ventricle. *The Journal of physiology*. 1997;504 (Pt 3):557-563

105.   Zhou J, Jeron A, London B, Han X, Koren G. Characterization of a slowly inactivating outward current in adult mouse ventricular myocytes. *Circulation research*. 1998;83:806-814

106.   Tamargo J, Caballero R, Gomez R, Delpon E. I(kur)/kv1.5 channel blockers for the treatment of atrial fibrillation. *Expert opinion on investigational drugs*. 2009;18:399-416

107.   Ravens U, Wettwer E. Ultra-rapid delayed rectifier channels: Molecular basis and therapeutic implications. *Cardiovascular research*. 2011;89:776-785

108.   Ravens U. Antiarrhythmic therapy in atrial fibrillation. *Pharmacology & therapeutics*. 2010;128:129-145

109.   Brandt MC, Priebe L, Bohle T, Sudkamp M, Beuckelmann DJ. The ultrarapid and the transient outward k(+) current in human atrial fibrillation. Their possible role in postoperative atrial fibrillation. *Journal of molecular and cellular cardiology*. 2000;32:1885-1896

110.   Panama BK, Latour-Villamil D, Farman GP, Zhao D, Bolz SS, Kirshenbaum LA, Backx PH. Nuclear factor kappab downregulates the transient outward potassium current i(to,f) through control of kchip2 expression. *Circulation research*. 2011;108:537-543

111.   Isenberg G, Klockner U. Calcium tolerant ventricular myocytes prepared by preincubation in a "kb medium". *Pflugers Archiv : European journal of physiology*. 1982;395:6-18

112.   Rodrigo GC, Chapman RA. The calcium paradox in isolated guinea-pig ventricular myocytes: Effects of membrane potential and intracellular sodium. *The Journal of physiology*. 1991;434:627-645

113.   Tiffany AM, Manganas LN, Kim E, Hsueh YP, Sheng M, Trimmer JS. Psd-95 and sap97 exhibit distinct mechanisms for regulating k(+) channel surface expression and clustering. *The Journal of cell biology*. 2000;148:147-158

114.   Gu C, Zhou W, Puthenveedu MA, Xu M, Jan YN, Jan LY. The microtubule plus-end tracking protein eb1 is required for kv1 voltage-gated k+ channel axonal targeting. *Neuron*. 2006;52:803-816

115.   Accili EA, Kiehn J, Yang Q, Wang Z, Brown AM, Wible BA. Separable kvbeta subunit domains alter expression and gating of potassium channels. *The Journal of biological chemistry*. 1997;272:25824-25831

116.   McIntosh P, Southan AP, Akhtar S, Sidera C, Ushkaryov Y, Dolly JO, Robertson B. Modification of rat brain kv1.4 channel gating by association with accessory kvbeta1.1 and beta2.1 subunits. *Pflugers Archiv : European journal of physiology*. 1997;435:43-54

117.   Aimond F, Kwak SP, Rhodes KJ, Nerbonne JM. Accessory kvbeta1 subunits differentially modulate the functional expression of voltage-gated k+ channels in mouse ventricular myocytes. *Circulation research*. 2005;96:451-458

118.   Lazaroff MA, Taylor AD, Ribera AB. In vivo analysis of kvbeta2 function in xenopus embryonic myocytes. *The Journal of physiology*. 2002;541:673-683

119.   McCormack K, Connor JX, Zhou L, Ho LL, Ganetzky B, Chiu SY, Messing A. Genetic analysis of the mammalian k+ channel beta subunit kvbeta 2 (kcnab2). *The Journal of biological chemistry*. 2002;277:13219-13228

120.   Perez-Garcia MT, Lopez-Lopez JR, Gonzalez C. Kvbeta1.2 subunit coexpression in hek293 cells confers o2 sensitivity to kv4.2 but not to shaker channels. *The Journal of general physiology*. 1999;113:897-907

121.   Rhodes KJ, Strassle BW, Monaghan MM, Bekele-Arcuri Z, Matos MF, Trimmer JS. Association and colocalization of the kvbeta1 and kvbeta2 beta-subunits with kv1 alpha-subunits in mammalian brain k+ channel complexes. *The Journal of neuroscience : the official journal of the Society for Neuroscience*. 1997;17:8246-8258

122.   McCormack T, McCormack K, Nadal MS, Vieira E, Ozaita A, Rudy B. The effects of shaker beta-subunits on the human lymphocyte k+ channel kv1.3. *The Journal of biological chemistry*. 1999;274:20123-20126

123.	Kim SJ, Ao Z, Warnock G, McIntosh CH. Incretin-stimulated interaction between beta-cell kv1.5 and kvbeta2 channel proteins involves acetylation/deacetylation by cbp/sirt1. *The Biochemical journal*. 2013;451:227-234

124.	Yang KT, Chang WL, Yang PC, Chien CL, Lai MS, Su MJ, Wu ML. Activation of the transient receptor potential m2 channel and poly(adp-ribose) polymerase is involved in oxidative stress-induced cardiomyocyte death. *Cell death and differentiation*. 2006;13:1815-1826

125.	Liu J, Kim KH, London B, Morales MJ, Backx PH. Dissection of the voltage-activated potassium outward currents in adult mouse ventricular myocytes: I(to,f), i(to,s), i(k,slow1), i(k,slow2), and i(ss). *Basic research in cardiology*. 2011;106:189-204

126.	Ussher JR, Jaswal JS, Lopaschuk GD. Pyridine nucleotide regulation of cardiac intermediary metabolism. *Circulation research*. 2012;111:628-641

127.	Neely JR, Grotyohann LW. Role of glycolytic products in damage to ischemic myocardium. Dissociation of adenosine triphosphate levels and recovery of function of reperfused ischemic hearts. *Circulation research*. 1984;55:816-824

128.	Kilfoil PJ, Tipparaju SM, Barski OA, Bhatnagar A. Regulation of ion channels by pyridine nucleotides. *Circulation research*. 2013;112:721-741

129.	Tipparaju SM, Barski OA, Srivastava S, Bhatnagar A. Catalytic mechanism and substrate specificity of the beta-subunit of the voltage-gated potassium channel. *Biochemistry*. 2008;47:8840-8854

130.	Alka K, Ryan BJ, Dolly JO, Henehan GT. Substrate profiling and aldehyde dismutase activity of the kvbeta2 subunit of the mammalian kv1 potassium channel. *The international journal of biochemistry & cell biology*. 2010;42:2012-2018

131.	Liu M, Sanyal S, Gao G, Gurung IS, Zhu X, Gaconnet G, Kerchner LJ, Shang LL, Huang CL, Grace A, London B, Dudley SC, Jr. Cardiac na+ current regulation by pyridine nucleotides. *Circulation research*. 2009;105:737-745

132.	Oka S, Hsu CP, Sadoshima J. Regulation of cell survival and death by pyridine nucleotides. *Circulation research*. 2012;111:611-627

133. Abdellatif M. Sirtuins and pyridine nucleotides. *Circulation research*. 2012;111:642-656

134. Roosild TP, Miller S, Booth IR, Choe S. A mechanism of regulating transmembrane potassium flux through a ligand-mediated conformational switch. *Cell*. 2002;109:781-791

135. Durell SR, Hao Y, Nakamura T, Bakker EP, Guy HR. Evolutionary relationship between k(+) channels and symporters. *Biophysical journal*. 1999;77:775-788

136. Schlosser A, Hamann A, Bossemeyer D, Schneider E, Bakker EP. Nad+ binding to the escherichia coli k(+)-uptake protein trka and sequence similarity between trka and domains of a family of dehydrogenases suggest a role for nad+ in bacterial transport. *Molecular microbiology*. 1993;9:533-543

137. Roosild TP, Castronovo S, Healy J, Miller S, Pliotas C, Rasmussen T, Bartlett W, Conway SJ, Booth IR. Mechanism of ligand-gated potassium efflux in bacterial pathogens. *Proceedings of the National Academy of Sciences of the United States of America*. 2010;107:19784-19789

138. Fujisawa M, Ito M, Krulwich TA. Three two-component transporters with channel-like properties have monovalent cation/proton antiport activity. *Proceedings of the National Academy of Sciences of the United States of America*. 2007;104:13289-13294

139. Miller S, Ness LS, Wood CM, Fox BC, Booth IR. Identification of an ancillary protein, yabf, required for activity of the kefc glutathione-gated potassium efflux system in escherichia coli. *Journal of bacteriology*. 2000;182:6536-6540

140. Roosild TP, Castronovo S, Miller S, Li C, Rasmussen T, Bartlett W, Gunasekera B, Choe S, Booth IR. Ktn (rck) domains regulate k+ channels and transporters by controlling the dimer-hinge conformation. *Structure*. 2009;17:893-903

141. Lyngberg L, Healy J, Bartlett W, Miller S, Conway SJ, Booth IR, Rasmussen T. Keff, the regulatory subunit of the potassium efflux system kefc, shows quinone oxidoreductase activity. *Journal of bacteriology*. 2011;193:4925-4932

142.   Tamsett TJ, Picchione KE, Bhattacharjee A. Nad+ activates kna channels in dorsal root ganglion neurons. *The Journal of neuroscience : the official journal of the Society for Neuroscience.* 2009;29:5127-5134

143.   Salkoff L, Butler A, Ferreira G, Santi C, Wei A. High-conductance potassium channels of the slo family. *Nature reviews. Neuroscience.* 2006;7:921-931

144.   Yuan A, Santi CM, Wei A, Wang ZW, Pollak K, Nonet M, Kaczmarek L, Crowder CM, Salkoff L. The sodium-activated potassium channel is encoded by a member of the slo gene family. *Neuron.* 2003;37:765-773

145.   Bhattacharjee A, Joiner WJ, Wu M, Yang Y, Sigworth FJ, Kaczmarek LK. Slick (slo2.1), a rapidly-gating sodium-activated potassium channel inhibited by atp. *The Journal of neuroscience : the official journal of the Society for Neuroscience.* 2003;23:11681-11691

146.   Egan TM, Dagan D, Kupper J, Levitan IB. Properties and rundown of sodium-activated potassium channels in rat olfactory bulb neurons. *The Journal of neuroscience : the official journal of the Society for Neuroscience.* 1992;12:1964-1976

147.   Mitani A, Shattock MJ. Role of na-activated k channel, na-k-cl cotransport, and na-k pump in [k]e changes during ischemia in rat heart. *The American journal of physiology.* 1992;263:H333-340

148.   Lawrence CL, Rodrigo GC. The na+-activated k+ channel contributes to k+ efflux in na+-loaded guinea-pig but not rat ventricular myocytes. *Pflugers Archiv : European journal of physiology.* 2001;442:595-602

149.   Wojtovich AP, Sherman TA, Nadtochiy SM, Urciuoli WR, Brookes PS, Nehrke K. Slo-2 is cytoprotective and contributes to mitochondrial potassium transport. *PloS one.* 2011;6:e28287

150.   Yuan P, Leonetti MD, Pico AR, Hsiung Y, MacKinnon R. Structure of the human bk channel ca2+-activation apparatus at 3.0 a resolution. *Science.* 2010;329:182-186

151.   Lee S, Park M, So I, Earm YE. Nadh and nad modulates ca(2+)-activated k+ channels in small pulmonary arterial smooth muscle cells of the rabbit. *Pflugers Archiv : European journal of physiology.* 1994;427:378-380

152. Thuringer D, Findlay I. Contrasting effects of intracellular redox couples on the regulation of maxi-k channels in isolated myocytes from rabbit pulmonary artery. *The Journal of physiology*. 1997;500 (Pt 3):583-592

153. MacDonald PE, Salapatek AM, Wheeler MB. Temperature and redox state dependence of native kv2.1 currents in rat pancreatic beta-cells. *The Journal of physiology*. 2003;546:647-653

154. Yoshida M, Dezaki K, Yamato S, Aoki A, Sugawara H, Toyoshima H, Ishikawa SE, Kawakami M, Nakata M, Yada T, Kakei M. Regulation of voltage-gated k+ channels by glucose metabolism in pancreatic beta-cells. *FEBS letters*. 2009;583:2225-2230

155. Ravier MA, Cheng-Xue R, Palmer AE, Henquin JC, Gilon P. Subplasmalemmal ca(2+) measurements in mouse pancreatic beta cells support the existence of an amplifying effect of glucose on insulin secretion. *Diabetologia*. 2010;53:1947-1957

156. Ivarsson R, Quintens R, Dejonghe S, Tsukamoto K, in 't Veld P, Renstrom E, Schuit FC. Redox control of exocytosis: Regulatory role of nadph, thioredoxin, and glutaredoxin. *Diabetes*. 2005;54:2132-2142

157. MacDonald PE. Signal integration at the level of ion channel and exocytotic function in pancreatic beta-cells. *American journal of physiology. Endocrinology and metabolism*. 2011;301:E1065-1069

158. Wilde AA, Brugada R. Phenotypical manifestations of mutations in the genes encoding subunits of the cardiac sodium channel. *Circulation research*. 2011;108:884-897

159. London B, Michalec M, Mehdi H, Zhu X, Kerchner L, Sanyal S, Viswanathan PC, Pfahnl AE, Shang LL, Madhusudanan M, Baty CJ, Lagana S, Aleong R, Gutmann R, Ackerman MJ, McNamara DM, Weiss R, Dudley SC, Jr. Mutation in glycerol-3-phosphate dehydrogenase 1 like gene (gpd1-l) decreases cardiac na+ current and causes inherited arrhythmias. *Circulation*. 2007;116:2260-2268

160. Van Norstrand DW, Valdivia CR, Tester DJ, Ueda K, London B, Makielski JC, Ackerman MJ. Molecular and functional characterization of novel glycerol-3-phosphate dehydrogenase 1 like gene (gpd1-l) mutations in sudden infant death syndrome. *Circulation*. 2007;116:2253-2259

161.	Westaway SK, Reinier K, Huertas-Vazquez A, Evanado A, Teodorescu C, Navarro J, Sinner MF, Gunson K, Jui J, Spooner P, Kaab S, Chugh SS. Common variants in casq2, gpd1l, and nos1ap are significantly associated with risk of sudden death in patients with coronary artery disease. *Circulation. Cardiovascular genetics*. 2011;4:397-402

162.	Valdivia CR, Ueda K, Ackerman MJ, Makielski JC. Gpd1l links redox state to cardiac excitability by pkc-dependent phosphorylation of the sodium channel scn5a. *American journal of physiology. Heart and circulatory physiology*. 2009;297:H1446-1452

163.	Kelly TJ, Souza AL, Clish CB, Puigserver P. A hypoxia-induced positive feedback loop promotes hypoxia-inducible factor 1alpha stability through mir-210 suppression of glycerol-3-phosphate dehydrogenase 1-like. *Molecular and cellular biology*. 2011;31:2696-2706

164.	Campomanes CR, Carroll KI, Manganas LN, Hershberger ME, Gong B, Antonucci DE, Rhodes KJ, Trimmer JS. Kv beta subunit oxidoreductase activity and kv1 potassium channel trafficking. *The Journal of biological chemistry*. 2002;277:8298-8305

165.	Liu M, Liu H, Dudley SC, Jr. Reactive oxygen species originating from mitochondria regulate the cardiac sodium channel. *Circulation research*. 2010;107:967-974

166.	Bhatnagar A, Srivastava SK, Szabo G. Oxidative stress alters specific membrane currents in isolated cardiac myocytes. *Circulation research*. 1990;67:535-549

167.	Bhatnagar A. Electrophysiological effects of 4-hydroxynonenal, an aldehydic product of lipid peroxidation, on isolated rat ventricular myocytes. *Circulation research*. 1995;76:293-304

168.	Wagner S, Ruff HM, Weber SL, Bellmann S, Sowa T, Schulte T, Anderson ME, Grandi E, Bers DM, Backs J, Belardinelli L, Maier LS. Reactive oxygen species-activated ca/calmodulin kinase iidelta is required for late i(na) augmentation leading to cellular na and ca overload. *Circulation research*. 2011;108:555-565

169.	Hallaq H, Wang DW, Kunic JD, George AL, Jr., Wells KS, Murray KT. Activation of protein kinase c alters the intracellular distribution and mobility of

cardiac na+ channels. *American journal of physiology. Heart and circulatory physiology*. 2012;302:H782-789

170.   Dunne MJ, Findlay I, Petersen OH. Effects of pyridine nucleotides on the gating of atp-sensitive potassium channels in insulin-secreting cells. *The Journal of membrane biology*. 1988;102:205-216

171.   Flagg TP, Enkvetchakul D, Koster JC, Nichols CG. Muscle katp channels: Recent insights to energy sensing and myoprotection. *Physiological reviews*. 2010;90:799-829

172.   Burke MA, Mutharasan RK, Ardehali H. The sulfonylurea receptor, an atypical atp-binding cassette protein, and its regulation of the katp channel. *Circulation research*. 2008;102:164-176

173.   Inoue I, Nagase H, Kishi K, Higuti T. Atp-sensitive k+ channel in the mitochondrial inner membrane. *Nature*. 1991;352:244-247

174.   O'Rourke B. Myocardial k(atp) channels in preconditioning. *Circulation research*. 2000;87:845-855

175.   Foster DB, Ho AS, Rucker J, Garlid AO, Chen L, Sidor A, Garlid KD, O'Rourke B. Mitochondrial romk channel is a molecular component of mitok(atp). *Circulation research*. 2012;111:446-454

176.   Dabrowski M, Trapp S, Ashcroft FM. Pyridine nucleotide regulation of the katp channel kir6.2/sur1 expressed in xenopus oocytes. *The Journal of physiology*. 2003;550:357-363

177.   Queliconi BB, Wojtovich AP, Nadtochiy SM, Kowaltowski AJ, Brookes PS. Redox regulation of the mitochondrial k(atp) channel in cardioprotection. *Biochimica et biophysica acta*. 2011;1813:1309-1315

178.   Stutts MJ, Gabriel SE, Price EM, Sarkadi B, Olsen JC, Boucher RC. Pyridine nucleotide redox potential modulates cystic fibrosis transmembrane conductance regulator cl- conductance. *The Journal of biological chemistry*. 1994;269:8667-8674

179.   Ramsey IS, Delling M, Clapham DE. An introduction to trp channels. *Annual review of physiology*. 2006;68:619-647

180.   Shen BW, Perraud AL, Scharenberg A, Stoddard BL. The crystal structure and mutational analysis of human nudt9. *Journal of molecular biology*. 2003;332:385-398

181.   Du J, Xie J, Yue L. Intracellular calcium activates trpm2 and its alternative spliced isoforms. *Proceedings of the National Academy of Sciences of the United States of America*. 2009;106:7239-7244

182.   Perraud AL, Fleig A, Dunn CA, Bagley LA, Launay P, Schmitz C, Stokes AJ, Zhu Q, Bessman MJ, Penner R, Kinet JP, Scharenberg AM. Adp-ribose gating of the calcium-permeable ltrpc2 channel revealed by nudix motif homology. *Nature*. 2001;411:595-599

183.   Massullo P, Sumoza-Toledo A, Bhagat H, Partida-Sanchez S. Trpm channels, calcium and redox sensors during innate immune responses. *Seminars in cell & developmental biology*. 2006;17:654-666

184.   Togashi K, Hara Y, Tominaga T, Higashi T, Konishi Y, Mori Y, Tominaga M. Trpm2 activation by cyclic adp-ribose at body temperature is involved in insulin secretion. *The EMBO journal*. 2006;25:1804-1815

185.   Lange I, Yamamoto S, Partida-Sanchez S, Mori Y, Fleig A, Penner R. Trpm2 functions as a lysosomal ca2+-release channel in beta cells. *Science signaling*. 2009;2:ra23

186.   Yamamoto S, Shimizu S, Kiyonaka S, Takahashi N, Wajima T, Hara Y, Negoro T, Hiroi T, Kiuchi Y, Okada T, Kaneko S, Lange I, Fleig A, Penner R, Nishi M, Takeshima H, Mori Y. Trpm2-mediated ca2+influx induces chemokine production in monocytes that aggravates inflammatory neutrophil infiltration. *Nature medicine*. 2008;14:738-747

187.   Hara Y, Wakamori M, Ishii M, Maeno E, Nishida M, Yoshida T, Yamada H, Shimizu S, Mori E, Kudoh J, Shimizu N, Kurose H, Okada Y, Imoto K, Mori Y. Ltrpc2 ca2+-permeable channel activated by changes in redox status confers susceptibility to cell death. *Molecular cell*. 2002;9:163-173

188.   Sano Y, Inamura K, Miyake A, Mochizuki S, Yokoi H, Matsushime H, Furuichi K. Immunocyte ca2+ influx system mediated by ltrpc2. *Science*. 2001;293:1327-1330

189.   Kolisek M, Beck A, Fleig A, Penner R. Cyclic adp-ribose and hydrogen peroxide synergize with adp-ribose in the activation of trpm2 channels. *Molecular cell*. 2005;18:61-69

190.   Kuhn FJ, Luckhoff A. Sites of the nudt9-h domain critical for adp-ribose activation of the cation channel trpm2. *The Journal of biological chemistry*. 2004;279:46431-46437

191.   Smith MA, Herson PS, Lee K, Pinnock RD, Ashford ML. Hydrogen-peroxide-induced toxicity of rat striatal neurones involves activation of a non-selective cation channel. *The Journal of physiology*. 2003;547:417-425

192.   Herson PS, Dulock KA, Ashford ML. Characterization of a nicotinamide-adenine dinucleotide-dependent cation channel in the cri-g1 rat insulinoma cell line. *The Journal of physiology*. 1997;505 (Pt 1):65-76

193.   Heiner I, Eisfeld J, Luckhoff A. Role and regulation of trp channels in neutrophil granulocytes. *Cell calcium*. 2003;33:533-540

194.   Baker ML, Serysheva, II, Sencer S, Wu Y, Ludtke SJ, Jiang W, Hamilton SL, Chiu W. The skeletal muscle ca2+ release channel has an oxidoreductase-like domain. *Proceedings of the National Academy of Sciences of the United States of America*. 2002;99:12155-12160

195.   Zima AV, Copello JA, Blatter LA. Effects of cytosolic nadh/nad(+) levels on sarcoplasmic reticulum ca(2+) release in permeabilized rat ventricular myocytes. *The Journal of physiology*. 2004;555:727-741

196.   Cherednichenko G, Zima AV, Feng W, Schaefer S, Blatter LA, Pessah IN. Nadh oxidase activity of rat cardiac sarcoplasmic reticulum regulates calcium-induced calcium release. *Circulation research*. 2004;94:478-486

197.   Sitsapesan R, McGarry SJ, Williams AJ. Cyclic adp-ribose competes with atp for the adenine nucleotide binding site on the cardiac ryanodine receptor ca(2+)-release channel. *Circulation research*. 1994;75:596-600

198.   Sitsapesan R, Williams AJ. Cyclic adp-ribose and related compounds activate sheep skeletal sarcoplasmic reticulum ca2+ release channel. *The American journal of physiology*. 1995;268:C1235-1240

199.   Lee HC. Nicotinic acid adenine dinucleotide phosphate (naadp)-mediated calcium signaling. *The Journal of biological chemistry*. 2005;280:33693-33696

200.   Kim BJ, Park KH, Yim CY, Takasawa S, Okamoto H, Im MJ, Kim UH. Generation of nicotinic acid adenine dinucleotide phosphate and cyclic adp-ribose by glucagon-like peptide-1 evokes ca2+ signal that is essential for insulin secretion in mouse pancreatic islets. *Diabetes*. 2008;57:868-878

201.   Tugba Durlu-Kandilci N, Ruas M, Chuang KT, Brading A, Parrington J, Galione A. Tpc2 proteins mediate nicotinic acid adenine dinucleotide phosphate (naadp)- and agonist-evoked contractions of smooth muscle. *The Journal of biological chemistry*. 2010;285:24925-24932

202.   Macgregor A, Yamasaki M, Rakovic S, Sanders L, Parkesh R, Churchill GC, Galione A, Terrar DA. Naadp controls cross-talk between distinct ca2+ stores in the heart. *The Journal of biological chemistry*. 2007;282:15302-15311

203.   Esposito B, Gambara G, Lewis AM, Palombi F, D'Alessio A, Taylor LX, Genazzani AA, Ziparo E, Galione A, Churchill GC, Filippini A. Naadp links histamine h1 receptors to secretion of von willebrand factor in human endothelial cells. *Blood*. 2011;117:4968-4977

204.   Brailoiu GC, Gurzu B, Gao X, Parkesh R, Aley PK, Trifa DI, Galione A, Dun NJ, Madesh M, Patel S, Churchill GC, Brailoiu E. Acidic naadp-sensitive calcium stores in the endothelium: Agonist-specific recruitment and role in regulating blood pressure. *The Journal of biological chemistry*. 2010;285:37133-37137

205.   Aarhus R, Graeff RM, Dickey DM, Walseth TF, Lee HC. Adp-ribosyl cyclase and cd38 catalyze the synthesis of a calcium-mobilizing metabolite from nadp. *The Journal of biological chemistry*. 1995;270:30327-30333

206.   Soares S, Thompson M, White T, Isbell A, Yamasaki M, Prakash Y, Lund FE, Galione A, Chini EN. Naadp as a second messenger: Neither cd38 nor base-exchange reaction are necessary for in vivo generation of naadp in myometrial cells. *American journal of physiology. Cell physiology*. 2007;292:C227-239

207. Cosker F, Cheviron N, Yamasaki M, Menteyne A, Lund FE, Moutin MJ, Galione A, Cancela JM. The ecto-enzyme cd38 is a nicotinic acid adenine dinucleotide phosphate (naadp) synthase that couples receptor activation to ca2+ mobilization from lysosomes in pancreatic acinar cells. *The Journal of biological chemistry*. 2010;285:38251-38259

208. Zhu MX, Ma J, Parrington J, Calcraft PJ, Galione A, Evans AM. Calcium signaling via two-pore channels: Local or global, that is the question. *American journal of physiology. Cell physiology*. 2010;298:C430-441

209. Brailoiu E, Churamani D, Cai X, Schrlau MG, Brailoiu GC, Gao X, Hooper R, Boulware MJ, Dun NJ, Marchant JS, Patel S. Essential requirement for two-pore channel 1 in naadp-mediated calcium signaling. *The Journal of cell biology*. 2009;186:201-209

210. Calcraft PJ, Ruas M, Pan Z, Cheng X, Arredouani A, Hao X, Tang J, Rietdorf K, Teboul L, Chuang KT, Lin P, Xiao R, Wang C, Zhu Y, Lin Y, Wyatt CN, Parrington J, Ma J, Evans AM, Galione A, Zhu MX. Naadp mobilizes calcium from acidic organelles through two-pore channels. *Nature*. 2009;459:596-600

211. Dammermann W, Guse AH. Functional ryanodine receptor expression is required for naadp-mediated local ca2+ signaling in t-lymphocytes. *The Journal of biological chemistry*. 2005;280:21394-21399

212. Zhang F, Xu M, Han WQ, Li PL. Reconstitution of lysosomal naadp-trp-ml1 signaling pathway and its function in trp-ml1(-/-) cells. *American journal of physiology. Cell physiology*. 2011;301:C421-430

213. Sumoza-Toledo A, Penner R. Trpm2: A multifunctional ion channel for calcium signalling. *The Journal of physiology*. 2011;589:1515-1525

214. Lin-Moshier Y, Walseth TF, Churamani D, Davidson SM, Slama JT, Hooper R, Brailoiu E, Patel S, Marchant JS. Photoaffinity labeling of nicotinic acid adenine dinucleotide phosphate (naadp) targets in mammalian cells. *The Journal of biological chemistry*. 2012;287:2296-2307

215. Billington RA, Thuring JW, Conway SJ, Packman L, Holmes AB, Genazzani AA. Production and characterization of reduced naadp (nicotinic acid-adenine dinucleotide phosphate). *The Biochemical journal*. 2004;378:275-280

216.   Schomer B, Epel D. Redox changes during fertilization and maturation of marine invertebrate eggs. *Developmental biology*. 1998;203:1-11

217.   Wang TA, Yu YV, Govindaiah G, Ye X, Artinian L, Coleman TP, Sweedler JV, Cox CL, Gillette MU. Circadian rhythm of redox state regulates excitability in suprachiasmatic nucleus neurons. *Science*. 2012;337:839-842

APPENDIX

OTHER ION CHANNELS MODULATED BY PYRIDINE NUCLEOTIDES[128]

Bacterial Potassium Transporters

It is currently believed that life originated in an aqueous environment in which negatively charged biomolecules, such as proteins and nucleic acids, were trapped in a semipermeable membrane. The high osmotic pressure exerted by charged biomolecules was counterbalanced by a high concentration of positively charged K^+ ions within the membrane-delimited cell. This intracellular accumulation of K^+ and exclusion of the more abundant seawater cation, Na^+ was probably used to energize the cell membrane. As a result, all living cells tightly regulate K^+ transport and use K^+ as the major solute to control osmolarity. The regulation of K^+ transport is critically important not only for survival and growth but also for maintaining cytosolic pH and for transmitting information from the extracellular to the intracellular environment. Although it is unknown how archaic cells regulated K^+ transport, modern bacteria, such as *Escherichia coli*, maintain separate systems for K^+ uptake and efflux. Transport systems, such as Trk, Ktr, and T2M channels, mediate active uptake of K^+ ions, whereas K^+ efflux is effected

by the Kef system. Remarkably, all 4 of these transport systems possess a nucleotide-binding potassium transport nucleotide–binding domain (KTNBD).[134, 135] In uptake systems, this domain is in the cytosolic subunits (TrKA or KtrA) that assemble with the membrane-spanning subunits (TrkG/H or KtrB/D), whereas in systems mediating K^+ efflux (KefC/B), the KTNBD is covalently linked to the cytosolic C-terminus of the ion transporter. In both instances, the cytosolic location of the NBD suggests a sensing mechanism in which ligand binding to the intracellular domains of the transporter could alter K^+ flux through the ion-conducting pore. This possibility is reinforced by the invariant proximity of the KTNBDs to the base of the innermost pore-forming helices[134], suggesting that conformational changes in the KTNBD could readily alter the ion transport properties of the pore. The KTNBDs of bacteria form a well-conserved Rossmann fold, which is a stable NAD^+-binding motif composed of 6 parallel β strands linked to 2 pairs of α-helices. This fold is commonly found in several bacterial and eukaryotic dehydrogenases. The Rossmann fold of KtrA binds to both NAD^+ and NADH. Binding of these ligands is essential for the maintenance of the tetrameric state of KTNBD and ligand-mediated changes. This could impart conformational changes in the ion-transporting subunit to alter its conducting properties,[134] although this has not been directly demonstrated.

Like KtrA, the K^+ uptake proteins TrkG/H also interact with subunits (TrkA) containing the KTNBD. The TrkA subunit of TrkG/H has 2 distinct dinucleotide-binding sites in each of 2 similar subdomains and, in addition to TrkG/H, TrkA also interacts with several other proteins, such as TrkE, to form functional channels.

Each half of the protein sequence of TrkA aligns with NAD^+-dependent dehydrogenases, such as lactate, malate, and alanine dehydrogenase, and purified TrkA binds NAD^+ and NADH with much higher affinity than ATP.[136] Because TrkA lacks the C-terminal catalytic domain of dehydrogenases, it is considered unlikely that the protein has enzyme activity. Nevertheless, it has been proposed that binding of NAD(H) to TrkA regulates the transport activity of the TrkG and the TrkH systems,[134] but the functional regulation of Trk transporters by NAD(H) has not been directly demonstrated to date. However, the presence of a pyridine NBD in TrkA suggests potential coupling between energy expensive import of K^+ ions and active metabolism. This coupling might be particularly important during cell growth. A high $NADH:NAD^+$ ratio is a prerequisite for cell growth, and activation of K^+ import by pyridine nucleotides may be required to maintain cytoplasmic K^+ levels and turgor pressure during cell expansion.[134]

In contrast to the K^+ uptake systems, which associate with nucleotide-binding proteins, the K^+-efflux system, KefC, has a KTNBD that is covalently linked to its ion-transporting subunits. The KefC transport system is inactivated by reduced glutathione, and it is activated by glutathione-S-conjugates.[137] Activation of this transport by glutathione conjugates leads to acidification of the cytosol. Because thiol reactivity is decreased at low pH, this might be a strategy for preventing the modification of cytosolic protein thiols, and thereby for protecting the bacteria from electrophilic stress. The C-terminal KTNBD of KefC is similar in structure to the Rossmann fold of dihydrofolate reductase and it binds glutathione.

Inhibition of KefC by glutathione is enhanced by NADH, but not NAD^+, indicating that $NADH:NAD^+$ ratio could regulate the antiporter activity of KefC.[138]

In addition to glutathione and NADH, the KTNBD of KefC also binds to the auxiliary subunits, KefF and KefG, which are required for the full activation of KefB/C.[139] The primary sequences of KefC and KefG show striking resemblance to human quinone reductases and in the crystal structure of KefF, FMN is bound to the KTNBD of the protein.[140] Recently, it has been shown that the KefF is a bonafide oxidoreductase in which NADH and NADPH act as electron donors and quinones and ferricyanide act as acceptors.[141] Although enzyme activity was not found to be required for KefC activation, it was suggested that by catalyzing the reduction of quinones, KefF protects KefC from the toxicity of electrophilic quinones.[141]

As discussed, the link between K^+ channels and nucleotide-binding proteins in bacteria is conserved in eukaryotic K^+ channels. Like the bacteria efflux systems (Kef), some of the eukaryotic channels, such as the Slo channels, possess a nucleotide-binding site in their cytosolic domain, whereas others, such as Kv channels, associate with auxiliary subunits that bind pyridine nucleotides in a manner reminiscent of the bacterial K^+ uptake systems (Trk/Ktr). Moreover, like bacterial channels, the mammalian K^+ channels also are regulated by pyridine nucleotides. It is likely that this mode of regulation is conserved during evolution because it plays a critical, nonredundant role in linking K^+ transport to the metabolic state of the cell, thereby enabling the cell to sense and respond to changes in the external environment.

Slo K+ Channels

The Slo family comprises high-to-intermediate conductance channels with a C-terminal domain that bears close resemblance to TrkA and other NAD^+-binding prokaryotic K^+ transporters.[142] These channels are widely distributed across Linnaean borders and are expressed in many types of cells, including cardiac myocytes and smooth muscle cells. The 4 mammalian Slo genes, Slo1 (BKCa), Slo2.1 (Slick), Slo2.2 (Slack), and Slo3, encode proteins that form K^+-selective homotetrameric channels.[143] The core region of these channels resembles the canonical Kv channels, but their cytoplasmic domain shows unusually high structural diversity. Variations in the cytosolic domain enable these channels to respond to a wide range of intracellular ions and metabolites. The cytosolic region of Slo1 binds to calcium via the calcium bowl located at the distal end of its hydrophilic tail; therefore, these channels are sensitive to changes in both membrane potential and $[Ca^{2+}]_i$. The Slo2.1 channel is regulated by Cl^-, but it contains an ATP-binding domain as well. The Slo2.2 channel is insensitive to Cl^- and it does not bind ATP. Nevertheless, both Slo2 channels respond to elevated $[Na^+]_i$ levels, giving rise to the K_{Na} current.[144]

Initial work showed that the K_{Na} channels are sensitive to sodium only at supraphysiological levels (50–80 mmol/L), making it doubtful whether they could be regulated by physiological changes in $[Na^+]_i$ that usually vary between 5 and 15 mmol/L.[145] Channel run-down after initial excision also was frequently observed. These discrepancies remained unresolved until Tamsett et al[142] found that the

cytoplasmic domain of both Slo2.1 and Slo2.2 contains NBDs similar to TrkA. This site includes a canonical NAD^+-binding $\beta\alpha\beta\alpha\beta$ motif that was required for nucleotide binding. They also found that application of physiological levels of NAD^+ to inside-out patches of rat dorsal root ganglion neurons led to a 2- to 2.5-fold increase in the open probability of K_{Na} channels and a decrease in EC50 of Na^+ from 50 to 20 mmol/L. The specificity of this interaction was reinforced by the finding that other cytosolic factors (cAMP, cGMP, and ATP) were without effect.[146] NAD^+, but not NADH, was effective in altering the gating properties of the channel, but only in the presence of Na^+. Moreover, like native K_{Na} channels, the current generated by Slack channels also was increased by NAD^+ or $NADP^+$. Site-directed mutations at the NAD^+-binding site of the Slo2 channel abolished this response, suggesting that direct nucleotide binding to the cytosolic region of the channel is required for these channels to respond to changes in pyridine nucleotide levels.

The regulation of K_{Na}/Slo2 channels by $NAD(P)^+$ suggests that the activity of these channels may be coupled to the metabolic state of the cell. This mode of regulation may be particularly important during ischemia–reperfusion and other conditions in which accumulation of $NAD(P)^+$ could increase K^+ efflux via these channels. High levels of intracellular $NAD(P)^+$ also would increase the sensitivity of these channels to intracellular sodium. Indeed, it has been suggested that in ischemic cardiac myocytes, elevated $[Na^+]_i$ levels activate K_{Na}, and an increase in this current shortens the action potential duration and induces calcium overload.[147,148] Therefore, regulation by pyridine nucleotides would allow these channels to adapt simultaneously to both the metabolic and the ionic conditions prevalent in

the ischemic heart. Interestingly, even though the evidence is indirect, it has been proposed that the Slo2 channels are present in cardiac mitochondria.[149] If present, the regulation of these channels by pyridine nucleotides might represent conservation of the link between metabolism and ion transport in modern mitochondria and their prokaryotic ancestors.

The NAD^+-binding site of Slo2 resembles the calcium binding site of the cytoplasmic domain of Slo1 channels, which contain 2 regulators of potassium conductance domains.[143] The regulator of potassium conductance domain is similar to the KTNBD of bacterial channels[134] found in 6-transmembrane K^+ channels, except that in the KTNBD the nucleotide binding Rossmann fold is not conserved. The N-terminus of the regulator of potassium conductance domain of Slo1 forms a Rossmann fold, which is similar to that seen in the structure of the cytoplasmic region of Slo2.2[150]; however, amino acid replacements in this domain during evolution have recruited the structure to bind calcium ions in case of Slo1 and sodium in case of Slo2.2. Although no direct pyridine nucleotide binding to the regulator of potassium conductance domain of Slo1 channels has been demonstrated, Lee et al[151] have reported that application of 2 mmol/L NAD^+ to the internal face of excised patches from small (<300 µm) pulmonary arteries reduces the open probability of BKCa channels, whereas NADH has the opposite effect. However, pyridine nucleotides had no effect on steady-state BKCa conductance in ear arterial smooth muscle cells[151] or in large (>300 µm) intralobar pulmonary arteries,[152] although in large arteries, application of NADH did lead to a voltage-dependent block of the channel. Although these observations are intriguing,

further studies are required to understand how intracellular changes in pyridine nucleotides regulate the activity and the physiological role of Slo channels.

Kv2.1 Channels

Like members of the Kv1 and Kv4 family, the Kv2.1 channels also have been shown to be sensitive to the redox ratio of pyridine nucleotides. MacDonald et al[153] have reported that in whole-cell recordings of Kv2.1 from pancreatic β-cells, increasing the NADPH:NADP$^+$ ratio in the patch pipette from 1:10 to 10:1 increased the contribution of fast inactivation to total inactivation from 40% to 60%. The effects, however, were modest and could not be duplicated by Yoshida et al.[154] Moreover, it is unclear how Kv2.1 is regulated by NADP(H). The Kv2.1 protein does not associate with pyridine-binding subunit, such as Kvβ, and direct binding of pyridine nucleotide to Kv2.1 has not been demonstrated. Although it is possible that changes in NADPH/NADP$^+$ levels could also affect Kv2.1 currents indirectly by changing cell metabolism or kinase activation, there is no evidence to support this possibility. Moreover, the physiological significance of the redox sensitivity of Kv2.1 in insulin secretion is unclear, because it has been reported that changes in Kv2.1 channels do not affect the levels of the critical pool of subplasma membrane calcium that regulates exocytosis.[155] Because NADPH facilitates insulin exocytosis,[156] it has been speculated that the binding of NADPH increases the association of Kv2.1 with SNARE proteins, which facilitates granule docking or priming.[157] Although this is an interesting possibility, additional investigations are required to fully elucidate the relationship between NADP(H) and Kv2.1 and to

assess its importance in regulating insulin secretion or other physiological phenomena.

Voltage-gated Sodium Channel

The voltage-gated sodium channel (Nav) conducts the fast inward sodium current that gives rise to the upstroke of the action potential and regulates the action potential duration. Therefore, small changes in sodium current profoundly impact myocardial excitability and conductance and such changes attributable to genetic mutations increase myocardial susceptibility to arrhythmias. Several gain-of-function and loss-of-function mutations in the cardiac channel (SCN5A) and its auxiliary subunits (Nav β1–β4 subunits) have been linked to arrhythmic syndromes, such as the long Q-T (LQTS type 3), the Brugada, the sick sinus, and the sudden infant death syndromes.[158] In a large multigenerational family of Italian descent with Brugada syndrome[159] and in several cases of sudden infant death syndrome,[160] the pathogenic cause has been identified to mutations in the glycerol-3-phosphate dehydrogenase-1-like protein (GPD1-L), which decrease surface trafficking of SCN5A and the peak sodium current. The importance of GPD1-L is further underscored by recent evidence showing that common variations in or near GPD1-L are associated with increased risk of sudden cardiac death in patients with coronary artery disease.[161]

GPD1-L is a 40-kDa protein that shares 84% sequence homology with GPD, an oxidoreductase that converts dihydroxyacetone phosphate to glycerol-3-phosphate. Because glycerol-3-phosphate is required for lipid synthesis, the

activity of GPD connects carbohydrate metabolism to lipid synthesis. GPD also contributes electrons to the mitochondrial electron transport system and maintains the redox status of the pyridine nucleotide levels in the mitochondria by participating in glycerol phosphate shuttle. GPD1-L displays glycerol phosphate dehydrogenase activity, although its catalytic activity is slower than that of GPD.[162, 163] Results of GST pull-down assays in a heterologous expression system suggest that GPD1-L is directly or closely associated with the pore-forming α-subunit of SCN5A.[162] GPDL-1 mutations that have been linked to Brugada syndrome (A280V) and sudden infant death syndrome (E83K) decrease GPDL-1 activity, but do not alter its association with SCN5A.[162] However, these mutations decrease the surface expression of SCN5A, thereby reducing total INa.[159, 162] This phenomenon is reminiscent of the behavior of Kvβ, which is also an oxidoreductase that regulates the surface expression of its pore-forming partner (Kv1). As seen with GPDL-1, loss-of-function mutations also decrease the effects of Kvβ on Kv1 trafficking.[164]

The close association between Nav and GPD1-L suggests that the sodium current may be sensitive to redox chemistry. Patch-clamp experiments of Dudley et al[165] show that in rat neonatal cardiac myocytes and in HEK cells expressing SCN5A, intracellular dialysis with 20 to 100 µmol/L NADH directly inhibits and that this is antagonized by incubating the cells with NAD$^+$. This inhibition of I$_{Na}$ was linked to NADH-dependent protein kinase C (PKC) activation or mitochondrial superoxide generation.[165] However, the processes by which NADH could stimulate PKC have not been identified and it was unclear how activated PKC could increase

mitochondrial reactive oxygen species production. Moreover, NADH-mediated I_{Na} suppression was not accompanied by changes in the inactivation of the channel or the induction of window current or a late sodium current, usually seen in cardiac myocytes exposed to oxidants.[166-168] Valdivia et al [162] suggest that at least some of the effects of NADH on sodium current may be attributable to changes in GPD1-L activity, because they were completely abolished by inhibiting PKC, indicating that NADH has no direct effects on Nav. They link PKC activation to GPD1-L activity, suggesting that NADH increased the production of glycerol-3-phosphate by GPD1-L, which increases diacylglycerol formation. This increase in diacylglycerol stimulates PKC activity and results in greater SCN5A phosphorylation. Moreover, they found that PKC activation acutely decreases the surface expression of SCN5A and this effect is prevented by the NADPH oxidase inhibitor apocynin, suggesting that both channel phosphorylation and reactive oxygen species production are required for PKC-mediated regulation of SCN5A trafficking.[162, 169] ENREF 153 However, these signaling pathways have been delineated mostly in heterologous systems and, therefore, additional experiments are required to determine endogenous regulation of I_{Na} by pyridine nucleotide in cardiac myocytes (or neurons) and to determine whether GPD1-L and pyridine nucleotide–dependent changes in PKC activation and reactive oxygen species generation affect only sodium channels or other ion transport mechanisms as well.

ATP-regulated K+ Channels

The ATP-regulated K^+ channels represent another class of K^+ channels that are regulated by nucleotides. Although these channels are primary regulated by ATP, they also have been found to be sensitive to pyridine nucleotides as well. The effects of pyridine nucleotides on the K_{ATP} channels were first described by Dunne et al,[170] who reported that in excised patches of insulin-secreting cells low (100 µmol/L) concentrations of $NAD(P)^+$ and NAD(P)H promoted channel opening, whereas high concentrations (500 µmol/L) led to channel closure. These effects were modified by ATP and ADP, indicating that pyridine coenzymes compete with adenine nucleotides for the NBD of the channel.

The K_{ATP} currents are generated by a large conductance channel present in the plasma membrane of several tissues, including the heart, smooth muscle, and pancreatic β-cells.[171, 172] An ATP-dependent potassium conductance has also been identified in the mitochondria,[173, 174] which has recently been found to be attributable to a channel related to the ROMK (Kir1.1) channel of the renal outer medulla.[175] The sarcolemmal KATP channels open when the cellular concentrations of ATP are low and are blocked at high ATP levels. These channels are formed by the 4 pore-forming Kir6.2 subunits and 4 regulatory sulfonylurea receptor (SUR2A) subunits. The current is inhibited by the binding of adenine nucleotides to Kir6.2. Moreover, the NBD of SUR interacts specifically with Mg–nucleotide complexes, resulting in channel opening.[171] Therefore, in any given metabolic state, the activity of the channel is a balance between the stimulatory and inhibitory effects of adenine nucleotide binding. Experiments with Kir6.2/SUR1 expressed in *Xenopus* oocytes have shown that inhibition of these currents by

NAD$^+$ and NADP$^+$ is mediated via binding to the Kir6.2 NBD, but not to the SUR1 NBD. The affinity of Kir6.2 for NADP(H) is markedly enhanced on interaction with SUR1, perhaps because modification of the nucleotide-binding pocket of Kir6.2 by SUR1 facilitates the attachment of molecules bulkier than adenine mononucleotides, such as NADP(H).[176] Nevertheless, the physiological significance of this interaction has not been assessed, and it is not clear whether the cardiac SUR2A isoform responds similarly. Because pyridine nucleotides are much less potent in inhibiting IK$_{ATP}$, it is likely that these nucleotides make only a small contribution to inhibition of the channel. Moreover, because the Kir6.2 displays no specificity for oxidized or reduced species but responds only to bulk nucleotide concentrations, it cannot participate in modulation of membrane potential by the redox state of pyridine nucleotides. Additionally, the ability of low concentrations of pyridine nucleotides to increase the activity of native K$_{ATP}$ channels in pancreatic cells[170] was not observed in oocytes expressing Kir6.2/SUR1.[176] Clearly, additional work is required to elucidate the mechanism of binding of low levels of pyridine nucleotides and to assess the significance of binding to physiological levels of NADP(H). Nevertheless, because pyridine nucleotides levels change under conditions that affect ATP levels, it is likely that native K$_{ATP}$ channels are sensitive to both adenine and pyridine nucleotides.

Like the sarcolemmal K$_{ATP}$ channel, the mitochondrial K$_{ATP}$ currents also respond to pyridine nucleotides. Measurements of mitochondrial K$_{ATP}$ activation by osmotic swelling indicate that the channel activity could be inhibited by NADPH.[177] The inhibition of the channel could not be related to reduction of mitochondrial

thiols and, therefore, was ascribed to direct regulation of the channel activity by NADPH. These observations suggest that the regulation of mitoK$_{ATP}$ channels by NADPH may be a physiological mechanism for sensing changes in energy metabolism and the redox status of mitochondria, but extensive work will be required to determine whether pyridine nucleotides are endogenous regulators of mitochondrial K$^+$ transport.

Cystic Fibrosis Transmembrane Conductance Regulator

The cystic fibrosis transmembrane conductance regulator is an ATP-binding cassette ion exchanger responsible for moving chloride and thiocyanate ions across epithelial cell membranes. Mutations in this gene create a nonfunctional protein that does not transport chloride and water in and out of cells that line the lungs, the pancreas, the liver, and the reproductive and digestive tracts. This disruption of osmotic gradients results in the production of abnormally viscous mucous, causing the obstruction of the respiratory tract characteristic of cystic fibrosis, as well as chronic dysfunction of other affected organs. The cystic fibrosis transmembrane conductance regulator acts as a cAMP-activated ATP-gated ion channel that allows Cl$^-$ ions to flow down their electrochemical gradient and exit the cell. It has been reported that pyridine nucleotides can interact with the NBD of cystic fibrosis transmembrane conductance regulator and that the redox potential of pyridine nucleotides regulates the Cl$^-$ conductance of the channel.[178] It was found that when ATP levels were clamped, there was a marked increase in Cl$^-$ conductance on dialysis of the cell with NADP$^+$. In contrast, dialysis

with NADPH inhibited Cl⁻ conductance. Although these studies point to an intriguing link between the redox state of pyridine nucleotides and Cl⁻ conductance, no studies seem to have followed-up on these initial findings.

Transient Receptor Potential (TRP) M2 Channel

Pyridine nucleotides and their metabolites also regulate calcium transport and homeostasis. Although the effects of pyridine nucleotides on the voltage-dependent calcium channels have not been reported, recent work has shown that NAD⁺ regulates calcium homeostasis by modifying the activity of TRPM2 channel (TRPM2). The transient receptor potential (TRP) M2 channel belongs to a large TRP superfamily which comprises several 6 transmembrane cation channels involved in a variety of processes ranging from sensation of touch, smell, taste, pain, temperature, osmotic pressure, and apoptosis.[179] A distinguishing feature of the TRPM2 channel is the presence of a cytosolic nudix hydrolase domain in the C-terminus of the channel that is highly homologous to the ADP pyrophosphatase NUDT9 and is therefore named the NUDT9-homologous domain (NUDT9-H). The NUDT9 domain of ADP pyrophosphatase displays 39% sequence identity with TRPM2 and is a member of the Nudix family of proteins, such as 8-oxo-dGTP hydrolase (MutT) and diadenosine tetraphosphate pyrophosphatase (AP4A hydrolase).[180] TRPM2 is highly abundant in the brain, but it is also expressed in other tissues, including, spleen, liver, lung, heart, and myeloid cells.[181] The channel is nonselective for cations and displays a nearly linear current–voltage relationship with a reversal potential near 0 mV.[182] The physiological functions of

TRPM2 have not been completely elucidated, but there is evidence showing that the channel is involved in monocyte chemotaxis[183], insulin secretion by pancreatic β-cells[184], and lysosomal calcium release.[185]   Studies with TRPM2-null mice suggest that the channel controls the production of chemokines in monocytes and the infiltration of neutrophils during inflammation.[186]   Because TRPM2 is highly responsive to oxidative stress, it is likely that this channel could function as a redox sensor[187] by directly binding to NAD^+ or its metabolite, ADPR.

Data from whole-cell patch-clamp experiments show that intracellular dialysis with NAD^+ [188] evokes a large inward current in cells expressing TRPM2 channels. In excised patches, application of NAD^+ lead to instantaneous activation of the channel, suggesting that NAD^+ directly activates the channel without the involvement of cytoplasmic or membrane components. However, regulation of the channel by NAD^+ remains controversial. Some investigators suggest that stimulation of the channel by NAD^+ may be attributable to contamination of the commercially available NAD^+ preparations that contain trace levels of ADPR, which is the natural ligand of the channel.[189]   Nevertheless, direct binding of ^{32}P-NAD^+ to a GST fusion protein of the C-terminal domain of TRPM2[184, 187] suggests that the channel protein interacts with NAD^+, presumably as it does with ADPR. Moreover, even though trace contamination by ADPR could account for the effects of 1 mmol/L NAD^+, channel activation at higher temperature also has been observed at 300 µmol/L NAD^+ [184] and only minimal channel activation was observed with 10 µmol/L ADPR[188] (EC50 ≈100 µmol/L),[182] suggesting that

contamination with >10% ADPR would be required to fully account for pronounced channel activation by commercial NAD$^+$ preparations.

The binding of ^{32}P-NAD$^+$ to the C-terminus of TRPM2 channels indicates that NAD$^+$ interacts with ADPR binding site of the Nudix domain. The importance of this domain has been confirmed by experiments showing that deletion of the C-terminus abolishes the activation of the channel by both ADPR and NAD$^+$.[187, 190] Hara et al[187] have suggested that H$_2$O$_2$ activates TRPM2 by increasing the intracellular NAD$^+$, which precipitates cell death by inducing calcium and sodium overload. A similar NAD$^+$-activated conductance, reminiscent of the TRPM2 activity, also has been implicated in rat striatal neuron cell death induced by cell depolarization and calcium influx.[191] Additionally, it has been reported that a similar NAD$^+$-gated nonselective cation channel is activated in CRI-G1 rat insulinoma cells treated with H$_2$O$_2$.[192] The findings of these studies suggest that stimulation of TRPM2 by NAD$^+$ could activate cation influx and trigger cell death. Similarly, in cardiac myocytes, activation of TRPM2 and the resultant sodium and calcium overload have been proposed to be obligatory steps in H$_2$O$_2$-mediated apoptosis.[124] Nonetheless, it remains unclear whether myocardial oxidative injury in vivo during ischemia–reperfusion could be attributed to TRPM2 activation and whether this is mediated by NAD$^+$ binding to the channel. Further experiments with TRPM2-null mice are warranted to rigorously delineate the role of TRPM2 in myocardial ischemic injury and heart failure and to determine whether the activity of the myocardial channel is regulated by NAD$^+$.

In addition to its direct effects on the channel, NAD$^+$ could affect the regulation of TRPM2 by its endogenous ligand, ADPR, or inhibit the catalytic activity of the C-terminal domain of the channel. It is currently believed that TRPM2 is activated by ADPR generated from the cleavage of NAD$^+$ by CD38.[193] Thus, NAD$^+$ levels could indirectly affect TRPM2 activity by regulating the supply of ADPR. NAD$^+$ also could compete with ADPR binding and catalysis. The NUDT9 domain of the channel has low levels of ADPR pyrophosphatase activity[182] which could be inhibited by NAD$^+$ and other pyridine nucleotides and their metabolites, although this possibility has not been directly tested. Regardless, the presence of a catalytic domain within the channel is fascinating because it indicates that as seen with the bacterial Kef system, the TRPM2 channels belong to a distinct class of channel proteins that possess catalytic activity. Even though the enzymatic activity of NUDT9 is considerably lower than in the ADPR pyrophosphatases, this may be an evolutionary adaptation to increase the dwell time of ADPR at the channel.[190] Moreover, mutations of the catalytic domain that increase enzymatic activity of NUDT9-H decreased channel activity, suggesting that nucleotide binding, not catalysis, activates the channel. Notably, the interesting possibility that channel gating or ion flow modulates the catalytic activity of NUDT9-H has not been tested.

Ryanodine Receptor (RyR) Calcium Release Channel

The RyRs represent another class of ion channels that may be regulated by pyridine nucleotides. Sequence analysis and homology modeling studies show

that the RyR of the skeletal muscle (RyR1) contains several dehydrogenase and NAD$^+$/NADH oxidoreductase domains.[194] This region is located near the N-terminus of the RyR1 and it shows significant structural homology to isocitrate dehydrogenase and isopropylmalate dehydrogenase. It also contains additional motifs related to the alcohol dehydrogenase. Notably, several of the residues that participate in NADP$^+$ binding in isocitrate dehydrogenase are conserved in RyR1, suggesting that the channel may be capable of binding to pyridine nucleotides. Indeed, equilibrium-binding studies indicate low-affinity binding of [^{3}H] NAD$^+$ to the sarcoplasmic reticulum membrane (Kd=10 µmol/L), although kinetic studies indicate a much higher affinity (Kd=50 nmol/L). On the basis of these studies, it has been estimated that nearly 10 molecules of NAD$^+$ bind to each subunit of RyR1.[194] Sequence alignment demonstrates that the the cardiac RyR2 protein shares ≈82% homology with RyR1 between amino acids 41 and 1200, and that this region of the protein contains multiple nucleotide-binding sites with significant structural and sequence homology to phosphorylated isocitrate dehydrogenase. The same region also encompasses both catalytic and binding sequences common to dehydrogenases and oxidoreductases.

The results of structural and biochemical studies are consistent with functional measurements. In permeabilized ventricular myocytes, addition of NADH decreases the frequency of calcium sparks,[195] and this inhibitory effect of NADH is partially reversed by NAD$^+$, although NAD$^+$ by itself has no effect on calcium spark frequency. These findings suggest that an increase in NADH/NAD$^+$ (eg, during ischemia) could inhibit spontaneous sarcoplasmic reticulum calcium

release. Nevertheless, the biochemical basis and the physiological significance of these findings are yet to be established. Particularly, it is unclear whether these effects are because of direct binding of NAD$^+$ to RyR or because of some other indirect NAD$^+$-dependent changes, such as increased superoxide generation by NADH oxidase.[196]

Although NAD$^+$ does not activate calcium sparks in permeabilized myocytes, addition of 1 μmol/L NAD$^+$ increases the open probability of single RyR2 cardiac calcium release channels incorporated into planar phospholipid bilayers.[197] A similar increase has been reported for skeletal muscle RyR1 channels; in which case, addition of 1 to 10 μmol/L NAD$^+$ led to a 7- to 80-fold increase in open probability.[198] These observations suggest that NAD$^+$ can directly activate calcium release channels; however, additional investigations are required to fully assess the role of pyridine nucleotides in regulating the calcium release channels, to determine whether the oxidoreductase domains of the RyR are catalytically active, and whether this catalysis regulates calcium release by the channel.

Regulation of Calcium Signaling by NAADP$^+$

In addition to directly regulating ion transport, pyridine nucleotides also generate specialized metabolites that regulate cell signaling, particularly calcium fluxes. The most potent of these metabolites is nicotinic acid adenine dinucleotide phosphate (NAADP$^+$), which stimulates calcium release in different cell types at concentrations as low as 5 to 10 nmol/L. Activation of calcium release by NAADP$^+$ has been found to regulate several physiological processes, including fertilization,

134

neurite outgrowth, synaptic function,[199] and insulin secretion.[200] NAADP$^+$ also mobilizes calcium stores in smooth muscle cells[201] and cardiac myocytes.[202] In endothelial cells, NAADP$^+$ has been recognized as an essential mediator of histamine-induced secretion of von Willebrand factor[203] and a regulator of nitric oxide production.[204] On the basis of the observation that intravenous administration of a cell permanent NAADP-ester lowers blood pressure in rats, it has been suggested that NAADP$^+$ regulates systemic blood pressure.[204]

NAADP$^+$ is an NADP$^+$ derivative in which the nicotinamide ring is replaced by nictonic acid. This structural difference may be sufficient in preventing NAADP$^+$ binding to most NADP$^+$-binding proteins, and in promoting specific recognition of NAADP$^+$ by its cognate receptors. The biochemical processes involved in NAADP$^+$ synthesis have not been completely identified. In vitro NAADP$^+$ is synthesized from NADP$^+$ by both ADP-ribosyl cyclases and CD38,[205] but it is not clear whether these enzymes synthesize NAADP$^+$ in vivo. Measurements of basal NAADP$^+$ levels in several tissues show that CD38-null mice maintain normal NAADP$^+$ levels.[206] Moreover, increases in NAADP$^+$ levels in histamine-stimulated myometrial cells[206] and in glucose-stimulated islet cells[200] are preserved in the absence of CD38, although NAADP$^+$ generation in response to CCK stimulation in pancreatic acinar cells[207] is attenuated. Thus, at least in some cells, NAADP$^+$ synthesis seems to be CD38-independent and it is likely that there are additional enzyme(s) involved in generating basal and agonist-evoked NAADP$^+$.

Agonist-stimulated increase in NAADP[+] levels is associated with release of calcium from intracellular stores that are different from those mobilized by IP3 or cyclic ADPR.[208] It is currently believed that NAADP[+] targets lysosome-related stores as some of its effects are inhibited by depletion of acidic calcium stores, but not by inhibitors of sarco/plasmic or endoplasmic reticulum Ca^{2+}-ATPase. The ability of NAADP[+] to release calcium from lysosomes has been related to the activation of 2-pore channels (TPCs).[209, 210] These channels contain 2 putative pore-forming repeats and their transmembrane regions are similar to that of other channels, such as the Nav or TRP channels however, instead of the plasma membrane, these channels are located in the endolysosomes and lysosomes or the ER. To date, 3 genes encoding TPCs (TPCN1-3) have been identified, of which TPCN2 is the predominant form expressed in primates and humans. Cells expressing TPC2 show a marked increase in calcium release on intracellular dialysis with 10 nmol/L NAADP[+]. Conversely, genetic knockdown of these channels abolishes NAADP[+]-induced calcium release, indicating that TPCs are endogenous targets of NAADP[+].[208] However, in addition to TPCs, NAADP[+] also activates RyR[211] and TRP subtype mucolipin 1 (TRP-ML1)[212] and, at high concentrations, the TRPM2[213] channels. The role of each of these channels in shaping the overall calcium response to NAADP[+] is not clear, but it has been suggested that responses of multiple NAADP[+] targets are integrated such that the small localized release of calcium by NAADP[+] via TPCs is amplified by neighboring receptors to generate well-orchestrated calcium oscillations.

The molecular mechanisms by which NAADP$^+$ regulates TPCs remain to be fully elucidated. Data from HEK-293 cells show that relative to wild-type cells, cells stably overexpressing TPC2 display increased [^{32}P] NAADP$^+$ binding at high-affinity (K_d=5 nmol/L) and low-affinity (K_d=10 μmol/L) sites.[210] However, the results of photoaffinity studies using radioactive 5-azido NAADP$^+$ show no direct binding to the TPC protein. These studies, however, did show that some unknown low-molecular-weight proteins were labeled by [^{32}P] NAADP$^+$ and that the labeling of these proteins was preserved in TPC-null cells.[214] These observations suggest that similar to what has been observed with other pyridine coenzyme–regulated channels (eg, Kv channels), there might be ancillary proteins within the larger TPC complex, which impart NAADP$^+$ sensitivity to TPCs.

Because NAADP$^+$ is synthesized from NADP$^+$, it is possible that this synthesis is sensitive to prevailing intracellular levels of pyridine nucleotide as well as cellular redox state. However, CD38-ribose and ADP-ribose cyclase-dependent NAADP$^+$ synthesis requires nicotinic acid, which binds to these enzyme with low affinity (half maximal effective concentration, 5 mmol/L).[205] Therefore, under most conditions, the availability of nicotinic acid, rather than NADP$^+$, is likely to be the limiting factor. NAADP$^+$ signaling could, however, be coupled to the cellular redox state by enzymatic reduction of NAADP$^+$ to NAADPH. NAADP$^+$ is structurally related to NADP$^+$ and it binds to NADP$^+$-linked enzymes, such as glucose-6-phosphate dehydrogenase and 6-phospho gluconate dehydrogenase.[215] The reduction of NAADP$^+$ by glucose-6-phosphate dehydrogenase generates NAADPH, which

does not induce calcium release. Hence, it is possible that enzymatic reduction is an off signal that limits the actions of NAADP$^+$, and that this reductive process couples NAADP$^+$ signaling to the overall redox state of the cell. In this regard, it is interesting to point out that several processes that involve NAADP$^+$ signaling, for example, fertilization,[216] are also associated with dramatic changes in the redox state; therefore, the redox sensitivity of NAADP$^+$ may be the missing link between calcium-mediated signaling and cell metabolism.

Summary and Perspective

In classical biochemistry, pyridine nucleotides are most frequently viewed as soluble electron carriers. As coenzymes, they are known to support oxidation–reduction reactions and to control cell metabolism. However, recent research suggests that pyridine nucleotides can also regulate cell signaling, gene transcription, and ion transport by acting as electron donors, enzyme substrates, or ligands of specific receptors. Unlike most signaling molecules, pyridine nucleotides also impart redox sensitivity to regulatory processes. By doing so, these nucleotides control a large network of reactions, and therefore they can effectively integrate metabolism, cell signaling, gene transcription, proliferation, and cell death. Many of these processes depend on ion transport and homeostasis and, thus, the ability to regulate ion channels may be a fundamental feature of the biological role of pyridine nucleotides.

Although research in this area is still maturing, several ion-transporting proteins have been shown to either contain NBD motifs or assemble with auxiliary

subunits that bind pyridine nucleotides. The association between nucleotides and ion transport has been conserved during evolution, and NBD-containing ion transport systems have been found in organisms ranging from bacterium to human. Although during evolution, some of these domains have been recruited to provide structural stability to proteins or to bind other ligands, most are still capable of high-affinity pyridine nucleotide binding. In addition, recent studies have shown that some NBD motifs of ion transport proteins are functional and that the activity of several ion transporters is modified by exogenous addition of pyridine nucleotides. There is also evidence to suggest that pyridine nucleotides regulate ion fluxes by binding directly to ion transport proteins or their ancillary subunits. Yet, there is little direct evidence showing that pyridine nucleotides are endogenous regulators of ion transport or that physiological or pathological changes in pyridine nucleotide levels have any significant effect on ion transport. Additional research therefore is needed to establish cause-and-effect relationships between pyridine nucleotides and ion transport. To delineate these relationships, it may be necessary to develop new methods for simultaneously measuring free nucleotide levels and ion transport in living cells and to determine how pyridine nucleotides regulate ion transport in vivo.

As discussed, recent research has uncovered several potential mechanisms by which pyridine nucleotides can regulate ion fluxes. In bacterial K$^+$ transporters, such as KtrA, for example, nucleotide binding induces specific changes in channel conformation—changes that could possibly alter the ion-conducting properties of the channel pore.[134] Similarly, in eukaryotic channels,

such as the Slo K$^+$ channels, the binding of pyridine nucleotides to the cytosolic domain of the channel alters channel gating, whereas in Kv1 complex nucleotide binding to Kvβ affects inactivation of the current. In addition, as shown for Kv1[164] and SCN5A[162] channels, NBD proteins could also facilitate channel trafficking and localization. Moreover, as in the bacterial KefC channels, catalytically active NBD proteins could help protect channel proteins from oxidative injury. Such proteins could also provide the channel privileged access to metabolites that regulate channel activity—as in case of the Nav-associated protein GPD1-L, which regulates selective PKC phosphorylation of the channel. Although the general applicability of this function is unclear, other channel proteins, like Kvβ, are also constitutively associated with PKC,[72] suggesting that association with other signaling proteins may be required to support local channel-specific regulation. In most cases described in the literature, however, the speculated roles of pyridine nucleotides in regulating ion fluxes remain unsubstantiated. Additional research is required to delineate the specific roles of pyridine nucleotides and their metabolites in the regulation of channel activity, localization, and posttranslational modification.

Additional research also is required to evaluate the physiological and the pathological implications of this regulatory axis. For instance, even though circumstantial evidence suggests that pyridine nucleotides play an important role in the regulation of HPV, insulin secretion, oxygen sensing, or even circadian rhythms,[217] there is no clear evidence to actually implicate pyridine nucleotides in these phenomena. It is similarly unclear whether the ischemic dysfunction of myocardial ion conductances is related to changes in pyridine nucleotide signaling.

Finally, the exciting possibility that, in addition to being regulated by NBD proteins, ion transport proteins in turn can regulate the activity of pyridine nucleotide–dependent proteins has yet to be tested. As mentioned, several channel-associated proteins, such as KefF, Kvβ, GPD1-L, and NUDT9-H, are catalytically active; therefore, changes in membrane potential could affect the activities of these enzymes. Further exploration of this possibility could reveal new mechanisms by which membrane potential regulates cell chemistry and metabolism. In the brain, such processes might be the basic molecular units of memory and learning; in non-neuronal cells, this mechanism could, perhaps, impart metabolic memory or contribute to the epigenetic regulation of gene expression. To understand these and other complex relationships between ion transport and pyridine nucleotides, however, we would first need to identify and characterize specific components of the individual ions channels that are regulated by pyridine nucleotides. From these findings, we would have to develop an integrated systemwide view—a view that would detail how exactly different ion transport mechanisms are synchronously regulated to support basic cell function or to mount a well-orchestrated unified response to environmental cues. Thus, further elucidation of this link between pyridine nucleotides and ion transport might provide a new understanding of the mechanisms underlying several physiological processes and disease states.

CURRICULUM VITAE

Peter J. Kilfoil

University of Louisville, School of Medicine
Institute of Molecular Cardiology
580 S Preston St
Louisville, KY 40202
Preferred Phone: 720-985-4372
pjkilf01@louisville.edu
citizenship: United States

Education

Graduate – University of Louisville School of Medicine, Louisville, KY
Biochemistry and Molecular Genetics
Advisor: Dr. Aruni Bhatnagar
08/2011-present
M.S., 04/2014
Ph.D., April 2016, GPA 4.0
Dissertation: MODULATION OF CARDIAC Kv CURRENTS BY Kvβ2 AND PYRIDINE NUCLEOTIDES

Graduate - University of Kentucky, Lexington, KY
Biomedical Engineering
08/2003 - 8/2005
M.S., 2007, GPA 3.91

Undergraduate – Vanderbilt University, Nashville, TN
Biomedical Engineering
08/1997 - 05/2001
B.E., 2001, GPA 3.20

Summary of expertise and research experience

My overall career goal is to identify mechanisms responsible for arrhythmogenesis and to further understanding of cardiac electrophysiology. To date, my research has focused on how subunits of the voltage-gated K^+ channels modulate the repolarization phase of the cardiac action potential. Utilizing mice lacking genes for the Kvβ1 and Kvβ2 proteins, I have examined the physiological

roles of these subunits with an approach utilizing patch-clamp electrophysiology, biotelemetry, immunofluorescence, confocal microscopy, intracardiac pacing and molecular biology techniques. Using these approaches, I have uncovered a cardiac phenotype in mice lacking Kvβ2. I have also spearheaded a side project in which I am investigating a role of the same protein in pancreatic islet excitation-secretion coupling and glucose homeostasis. While the above projects described are mine, I also have a track record of successful collaboration, contributing my electrophysiological expertise to other projects in our center. Recently, I collaborated on a project in which I examined the effects of a reactive aldehyde on voltage-gated sodium currents in isolated cardiomyocytes. As a whole, I believe this training has prepared me well to identify and investigate various cardiac pathologies as a postdoctoral researcher and ultimately an independent investigator.

08/2010 - current
University of Louisville, Dept. of Molecular Cardiology
Examining the role of voltage-gated ion channels in cardiomyocyte electrophysiology. .

08/2010 – current
University of Louisville, Diabetes and Obesity Research Center
Examining the role of voltage-gated potassium channel subunit Kvβ2 in pancreatic β-cell repolarization and insulin secretion.

0/2003- 08/2005
University of Kentucky, Wenner Gren Center for Biomedical Engineering
In completion of Masters' degree, investigated the effects of endurance training on lower-limb vascular properties as pertaining to orthostatic hypotension following spaceflight. Research techniques used include: ECG analysis, human instrumentation, signal processing, MATLAB coding and analysis.

Publications

Kilfoil PJ, Chapalamadugu KC, Raucci FJ, Tur J, Brittian KR, BrittBhatnagar A, Tipparaju SM. The ancillary subunit Kvβ2 alters Kv1 trafficking and modulates the electrophysiological properties of ventricular cardiac myocytes. *Manuscript in preparation*

Kilfoil PJ, Barski OA, Bhatnagar A. Modulation of Pancreatic Islet Electrophysiology and Insulin Release by Potassium Channel Subunit Kvbeta2. *Manuscript in preparation*

Dassanayaka S, Brainard RE, Watson LJ, Long BW, Brittian KR, DeMartino AM, Aird AL, **Kilfoil PJ**, Muthusamy S, Hamid T, Prabhu SD, and Jones SP. Cardiomyocyte Ogt limits ventricular

dysfunction in mice following pressure overload without affecting hypertrophy. *In submission, AJP Heart and Circ Phys*

Tur J, Chapalamadugu KC, Padawer T, Badole SL, **Kilfoil PJ**, Bhatnagar A, Tipparaju SM. Deletion of Kvβ1.1 subunit leads to electrical and haemodynamic changes causing cardiac hypertrophy in female murine hearts. *Exp Physiol.* 2016 Apr 1;101(4):494-508.

Conklin DJ, Guo Y, Jagatheesan G, **Kilfoil PJ**, Haberzettl P, Hill BJ, Baba SP, Guo L, Wetzelberger K, Obal D, Rokosh DG, Prough RP, Prabhu SD, Velayutham M, Zweier JL, Hoetker D, Riggs DW, Srivastava S, Bolli R, and Bhatnagar A. Genetic Deficiency of Glutathione S-Transferase P Increases Myocardial Sensitivity to Ischemia-Reperfusion Injury. *Circulation Research.* 2015 Aug 14; 117(5):437-49.

Kilfoil PJ, Tipparaju SM, Barski OA, and Bhatnagar A. Regulation of Ion Channels by Pyridine Nucleotides. *Circulation Research* 2013 Feb 15;112(4):721-41.

Tipparaju SM, Li XP, **Kilfoil PJ**, Xue B, Uversky VN, Bhatnagar A, Barski OA. Interactions between the C-terminus of Kv1.5 and Kvβ regulate pyridine nucleotide-dependent changes in channel gating. *Pflugers Archive* 2012;463:799-818.

Wang R, Lacour-Gayet FG, Lanning CJ, Rech BA, **Kilfoil PJ**, Hertzberg J, Shandas R. Initial experience with the development and numerical and in vitro studies of a novel low-pressure artificial right ventricle for pediatric Fontan patients. *ASAIO J.* 2006 Nov-Dec;52(6):682-92.

Presentations and Abstracts

Kilfoil PJ, Barski OA, Bhatnagar A. Modulation of Pancreatic Islet Electrophysiology and Insulin Release by Potassium Channel Subunit Kvbeta2. *Biophysical Journal*, vol. 108, issue 2, p. 278a

Panguluri SK, **Kilfoil PJ**, Chapalamadugu KC, Tur J, Bhatnagar A, Tipparaju SM. Genetic Ablation of Voltage-Gated Potassium Channel Beta-subunit 2 Causes Distinct Physiological and Cardiac Alterations in Mice. *Circulation.* 2013;128:A18907

Kilfoil PJ, Barski OA, Brittain K, Prabhu SD, Bhatnagar A, Tipparaju SM. Genetic Ablation of Potassium Channel Subunit Kvβ2 Slows Repolarization in the Cardiac Septum and Leads to Cardiac Remodeling. *Circulation.* 2011; 124: A14194

Kilfoil PJ, Barski OA, Brittain KR, Prabhu SD, Bhatnagar A, Tipparaju SM. Physiological characteristics of mouse with genetic ablation of Kvbeta2. Gordon Research Conference-Ion Channels. July 2010, Tilton, NH.

Evans JM, **Kilfoil PJ**, Wang S, Mohney L, Knapp CJ. Cardiovascular Responses to Standing and Walking in Earth and Simulated Moon and Mars Gravities. *FASEB J.* April 2010 24 (Meeting Abstract Supplement) 616.1

Wang S, Randall DC, Knapp CF, Nelson KR, Patwardhan AR, **Kilfoil PJ**, Evans JM. Autonomic regulation in patients with diabetic neuropathy. *FASEB J.* April 2010 24 (Meeting Abstract Supplement) 1020.14

Wang S, Randall DC, Knapp CF, Patwadhan A, **Kilfoil PJ**, Evans JM. Dysfunction of Autonomic Regulation of Short Term Blood Pressure in Diabetes. Gill Heart Institute Annual Conference. Lexington, KY 2009

Kilfoil PJ. Gender Differences in Artificial Gravity Training. Biomedical Engineering Society National Conference, Philadelphia, PA **2005**

Kilfoil PJ. Active and Passive Artificial Gravity Training Results. Gill Heart Institute Annual Conference. Lexington, KY 2004

Technical Expertise:
- Patch clamp electrophysiology (whole cell, perforated patch, single channel)
- Voltage clamp and action potential recording
- Adult mouse cardiomyocyte isolation
- Adult mouse pancreatic islet isolation
- Confocal microscopy
- ECG telemetry implantation and analysis
- Protein isolation and Western blot analysis
- mRNA isolation and quantitative rt-PCR
- Coimmunoprecipitation
- Cell culture
- Technical training of students and postdocs
- Review of manuscripts for *Toxicology and Applied Pharmacology*
- Assisted in review of manuscripts for *Circulation Research*

Professional Societies

American Heart Association, Council for Basic Cardiovascular Sciences
Biophysical Society
Kentucky Academy of Sciences
The Society for Experimental Biology

References

Aruni Bhatnagar, Ph.D., F.A.H.A.
Director, Diabetes and Obesity Research Center
University of Louisville
580 S Preston St. Louisville, KY 40202
aruni@louisville.edu

Steven P. Jones, Ph.D., F.A.H.A.
Professor of Medicine, Division of Cardiology
University of Louisville
580 S Preston St. Louisville, KY 40202
spjone04@louisville.edu

Daniel J. Conklin, Ph.D.
Professor, Department of Medicine
University of Louisville
580 S Preston St. Louisville, KY 40202
dj.conklin@louisville.edu